THESIS ON NATURAL AND EXACT SCIENCES B243

Electrospinning of a Polymer Membrane Reinforced with Carbon Nanotubes

VIKTORIA VASSILJEVA

TTÜ
PRESS

TALLINN UNIVERSITY OF TECHNOLOGY
School of Engineering
Department of Materials and Environmental Technology
Laboratory of Polymers and Textile Technology

This dissertation was accepted for the defense of the degree of Doctor of Philosophy in Natural and Exact Sciences on 14th of November 2017

Supervisor: Dr. Andres Krumme
Department of Materials and Environmental Technology,
Tallinn University of Technology

Opponents: Dr. Heikki Tenhu
Department of Chemistry, University of Helsinki,
Finland

Dr. Jaan Leis
Skeleton Technologies OÜ, lead scientist
Institute of Chemistry, University of Tartu, Estonia

Defense of the thesis: 13th of December 2017 at 13:00
Lecture hall: U03-103
Tallinn University of Technology, Ehitajate tee 5

Declaration:

I hereby declare that this doctoral thesis, my original investigation and achievement, submitted to Tallinn University of Technology in partial fulfilment of my doctoral degree program, has not been submitted for any academic degree.

/Viktoria Vassiljeva/

European Union
European Regional
Development Fund

Investing
in your future

ISSN 1406-4723
ISBN 978-9949-83-189-0 (publication)
ISBN 978-9949-83-190-6 (PDF)

LOODUS- JA TÄPPISTEADUSED B243

Süsinik nanotorudega tugevdatud polümeerse membraani elektroketrus

VIKTORIA VASSILJEVA

TTÜ
KIRJASTUS

TABLE OF CONTENTS

LIST OF PUBLICATIONS 7

AUTHOR'S CONTRIBUTION 8

INTRODUCTION 9

LIST OF ABBREVIATIONS 10

1. LITERATURE REVIEW 12

1.1. Electrospinning 12

1.1.1. Electrospinning setup 12

1.1.2. Factors affecting electrospinning process and fiber quality 14

1.1.3. Fiber properties and application 17

1.2. CNT as reinforcing and electroconductive components in electrospun fibers and membranes 18

1.2.1. CNTs 18

1.2.2. Methods for CNT dispersion into polymer matrix 20

1.2.3 IL assisted dispersion of the CNTs 21

1.2.4. CNT modification by polymers 22

1.2.5. CNT modification by SAN 22

1.3 Aim and objectives of the study 26

2. EXPERIMENTAL 27

2.1. Materials and chemicals 27

2.2. Preparation of SANm and SANm-g-CNTs 27

2.3. Preparation of electrospinning solutions and electrospinning 29

2.4. Characterization of the SANm-g-CNTs, solutions and electrospun membranes 31

3. RESULTS AND DISCUSSION 33

3.1. Optimization of electrospinning parameters 33

3.1.1. Impact of solvent and solution concentration on electrospinning process and fiber morphology 33

3.1.2. Effect of IL and its concentration on properties of electrospinning solutions, fiber morphology, and electrospinning process 34

3.1.3. Effect of IL and CNTs on properties of electrospinning solutions and fiber morphology 37

3.1.4. Effect of IL and CNTs on properties of electrospun membranes 39

3.2. CNT grafting with SAN for electrospinning applications 44

3.2.1. Characterization of SANm and SANm-g-CNTs 44

3.2.2. Effect of CNT grafting with SANm on properties of electrospinning solutions 47

3.2.3. Effect of CNT grafting with SANm on properties of electrospun membrane 50

CONCLUSIONS 58

ACKNOWLEDGEMENTS 61

ABSTRACT 63

KOKKUVÕTE 64

REFERENCES 66

APPENDIX A 77

APPENDIX B 137

APPENDIX C 139

LIST OF OTHER PUBLICATIONS 147

LIST OF PUBLICATIONS

This thesis is based on the following publications that are referred in the text by Roman numbers I-III:

I. **Gudkova, V.,** Krumme, A., Märtson, T., Rikko, M., Tarasova, E., Viirsalu, M. (2014). The impact of 1-butyl-3-methylimidazolium chloride on electrospinning process of SAN polymer solutions and electrospun fiber morphology. *Journal of Electrostatics*, 72, 433−436. (https://doi.org/10.1016/j.elstat.2014.08.003)

II. **Gudkova, V.,** Krumme, A., Märtson, T., Rikko, M., Tarasova, E., Savest, N., Viirsalu, M. (2015). 1-butyl-3-methylimidazolium chloride assisted electrospinning of SAN/MWCNT conductive reinforced composite membranes. Journal of Electrostatics, 78, 11−16. (https://doi.org/10.1016/j.elstat.2015.09.002)

III. **Vassiljeva, V.,** Kirikal, K.-K., Hietala, S., Kaljuvee, T., Mikli, V., Rähn, M., Tarasova, E., Krasnou, I., Viirsalu, M., Savest, N., Plamus, T., Javed, K., Krumme, A. (2017). One-step carbon nanotubes grafting with styrene-co-acrylonitrile by reactive melt blending for electrospinning of conductive reinforced composite membranes. *Fullerenes, Nanotubes and Carbon Nanostructures* - Manuscript ID FNCN17204.R2 (accepted)

Copies of these articles are included in APPENDIX A.

AUTHOR’S CONTRIBUTION

I. The author prepared the electrospinning solutions, investigated the impact of ionic liquid on solution viscosity, electrical conductivity and fiber morphology with a M.Sc. student. The author analyzed the results and wrote the paper.

II. The author prepared the electrospinning solutions, investigated the impact of ionic liquid and unmodified carbon nanotubes on solution viscosity, electrical conductivity, and fiber morphology and membrane strength properties with the M.Sc. student. The author analyzed the results and wrote the paper.

III. The author developed a method for functionalization of the carbon nanotubes by modified poly(styrene-co-acrylonitrile) for improvement of carbon nanotube dispersions into polymer solutions for electrospinning. The author prepared functionalized carbon nanotubes and electrospinning solutions. The author also investigated the impact of ionic liquid and different types of carbon nanotubes on solution viscosity, electrical conductivity, fiber morphology, and membrane strength properties with the help of the M.Sc. student. The author then analyzed the results and wrote the paper.

INTRODUCTION

Electrospinning is a fascinating method for creation of fibrous structures through an electrically charged jet of the polymer solutions or melts [1]. The advantages, in comparison to other fiber formation methods, are the following: high process speed, low cost, easy application, continuous fibers, sub-micro- and nanoscale of average diameter, and flexibility in process parameters among others. [2]. Electrospun fibrous materials have many extraordinary properties, such as large surface area to volume ratio, flexibility in surface functionalities, and superior mechanical performance (e.g. stiffness and tensile strength) compared with any other known forms of the materials [3]. These outstanding characteristics make the polymer fibers optimal candidates for many important applications, like filter media, nano-sensors, functional clothing, cosmetic skin mask, tissue engineering scaffolds, energy storage and harvesting, *etc.* [2, 3]

Nanotechnology has attracted a great interest during the last 20 years. Nowadays, polymer materials are ideal for forming fibrous materials quickly and easily. However, their mechanical, electrical, thermal, rheological and optical properties need improvement for widespread application. For this reason, polymer/carbon nanotubes (CNTs) composites have gained attention in science's and industry's points of view. CNTs are widely used for the improvement of material strength, electrical and thermal conductivity for special applications. However, the literature review showed, that there are several problems in processing CNTs for electrospinning. For example, application of multi-walled CNTs (MWCNTs) is limited by aggregation and poor dispersion in many polymer matrices [4]. Additionally, the weak interfacial adhesion between CNTs and the polymer matrix causes inefficient load transfer between the matrix polymer and CNTs inside the fibers.

Different approaches can be used for solving the problems in the CNT application above described. Largely they involve different mixing techniques, utilization of functional additives and the functionalization of CNTs. Each approach has a potential for being used in industry, as well as it has both advantages and disadvantages. Unfortunately, until now no comparative study of different approaches has been performed focusing on only one polymer.

The aim of this study is to create reinforced composite polymer fibrous membranes through the utilization of CNTs as functional additives. In this dissertation, there were applied different approaches to disperse MWCNTs into a styrene-co-acrylonitrile (SAN) polymer matrix: ultrasonic mixing, application of ionic liquid (IL) as a functional additive and covalent grafting of CNTs with the modified matrix polymer. A novel “grafting to” reaction to bind CNTs with polymer was developed to achieve effective interfacial adhesion between CNTs and the polymer matrix. In addition, current dissertation gives the answers to the problem above described – the comparison of different dispersion methods of CNTs in frames of the only one polymer.

LIST OF ABBREVIATIONS

1,2-DCE	1,2-dichloroethane
AE	2-aminoethanol
ATRP	atom transfer radical polymerization
[Bmim]Cl	1-butyl-3-methylimidazolium chloride
CNCs	cellulose nanocrystals
CNT	carbon nanotube
CNT-COOH	carboxyl group modified carbon nanotube
CVD	chemical vapor deposition
DMSO	dimethyl sulfoxide
DWCNT	double-walled carbon nanotube
$EmimBF_4$	1-ethyl-3methylimidazolium tetrafluoroborate
FT-IR	Fourier transform infrared spectroscopy
^1H NMR	Nuclear magnetic resonance
HA	hydroxyapatite
HEBB	2-hydroxyethyl bromoisobutyrate
HEBB-g-MWCNT	2-hydroxyethyl bromoisobutyrate grafted multi-walled carbon nanotube
IL	ionic liquid
MWCNT	multiwalled carbon nanotube
MWCNT-COCl	acyl chloride modified multi-walled carbon nanotube
MWCNT-COOH	carboxyl group modified multi-walled carbon nanotube
PLA	polylactic acid
PTFE	polytetrafluoroethylene
SAN	styrene-co-acrylonitrile
SANm	oxazoline modified poly(styrene-co-acrylonitrile)

SANm-g-CNT	oxazoline modified poly(styrene-co-acrylonitrile) grafted carbon nanotube
SEM	scanning electron microscope
SWCNT	single-walled carbon nanotube
TEM	transmission electron microscopy
TGA	thermogravimetric analyses
THF	tetrahydrofuran
wt%	weight concentration

1. LITERATURE REVIEW

Since the current research is about the dispersion of the CNTs into a polymer matrix and electrospinning of membranes, the main literature overview is presented in the following topics: electrospinning technology and influence of different parameters on fiber properties, dispersion of the CNTs into the polymer matrixes by different approaches, application of electrospun fibers and polymer/CNT composites.

1.1. Electrospinning

Electrospinning is a widely used method for the electrostatic formation of polymer fibers with diameters ranging from six nm [5] to several micrometers utilizing polymer solutions of both natural and synthetic polymers [6] or melts. Electrospinning technology was first described as a fabrication technique for the production of the finest fibers by electrostatic forces in 1887 by C.V.Boys [7]. The method was first patented in 1902 by J. F. Cooley [8] and W. J. Morton [9] separately. This electrospinning method was then developed for industrialization and it was well described in series of patents by A. Formhals in 1934-1944. But the real popularity in science has not been achieved until around the year of 2000 and still the interest for electrospinning is growing exponentially up to 3280 scientific papers per year in 2016 [10]. The figure 1.1 represents main application fields of electrospinning.

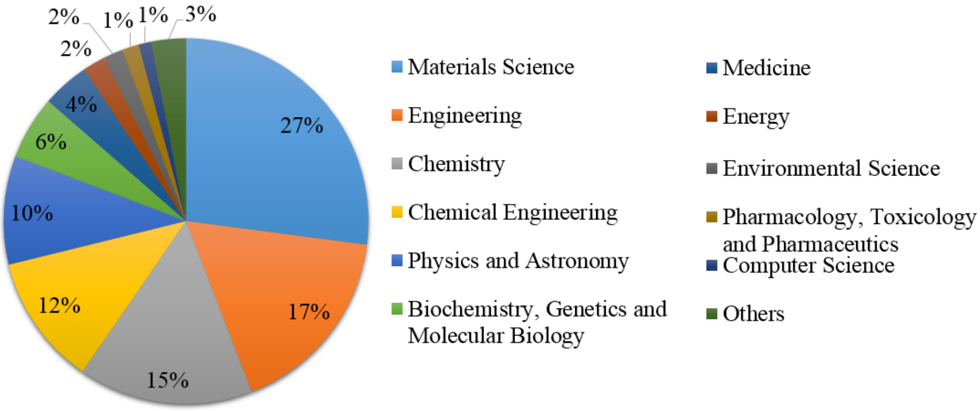

Figure 1.1. Statistics on the scientific literature published about electrospinning from 2000 to 2016 (Search made through www.scopus.com database on 23.08.2017 [10]).

1.1.1. Electrospinning setup

Electrospinning is the cheapest, quickest and an extremely simple way of fiber production in nano- and submicron range compared to other fiber-spinning technologies as drawing, template synthesis, phase separation and self-assembly [2]. For a single-needle electrospinning setup, (see Fig. 1.2) the polymer solution is first supplied through a syringe by an electrical pump to the tip of the needle. When a high voltage is applied to the solution, a Taylor cone forms with a droplet collected at the tip of the needle. At a critical voltage, the repulsive force of induced charges within the solution overcomes the surface tension of electrospinning solution and jet forwards to the area of lower potential, which is usually a grounded collector [11]. Near the tip of the needle and Taylor cone [12], the electrospinning jet is stable but moving forward to the collector it enters an instability stage. Further stretching under the electrostatic force and solvent evaporation results in the deposition of dry fibers on the collector forming an unstructured mesh or structured membrane depending on the collector type.

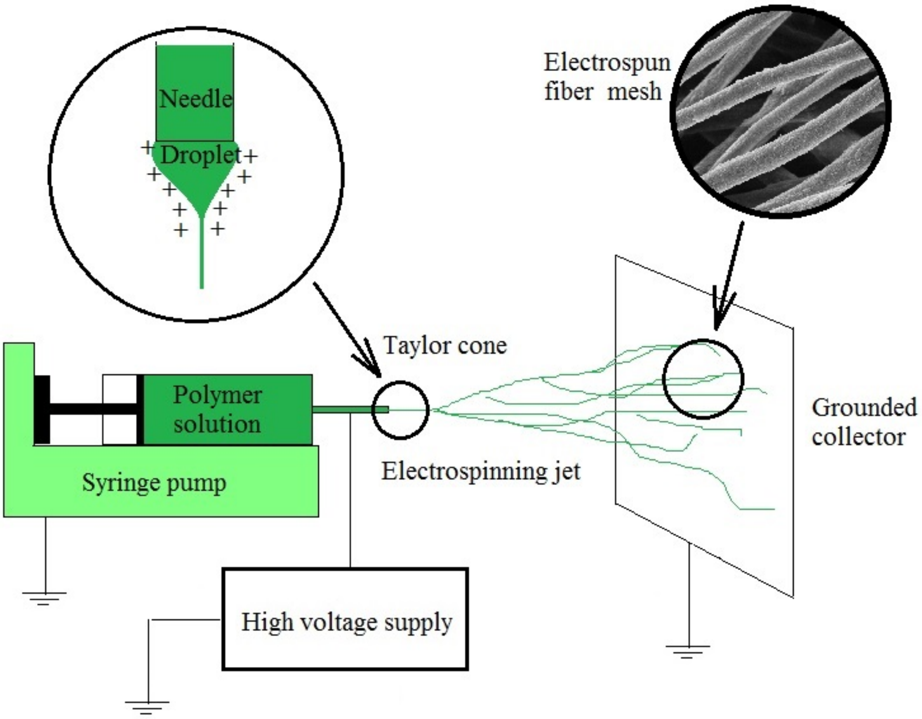

Figure 1.2. Scheme of typical electrospinning setup.

The unstructured mesh can be deposited to a flat stationery collector. The primary disadvantage of the mesh is the limited number of application fields due to the unstructured orientation of the fibers. However, different opportunities can be achieved for increasing the number of application of electrospun fibrous materials with the alignment of the fibers during the electrospinning. This alignment of the fibers can be achieved by utilizing different collector types [3]. A cylinder collector with high rotating speed allows the fibers to be deposited in parallel. An uniaxially aligned polymer nanofiber yarns can be collected with a thin wheel with a sharp edge [13]. A parallel frame collector can be used to obtain individual fibers. Gridded frames can be used to place fibers into a controlled 3D structure to some extent. In addition, a liquid bath filled with an appropriate non-solvent can be used for deposition of fibers.

1.1.2. Factors affecting electrospinning process and fiber quality

Production of fibers by electrospinning is based on the stretching of the viscoelastic liquid by an electrostatic force. To understand the process of electrospinning and formation various fiber structures, the basic principles of the method and influence of electrospinning parameters should be considered. Basic factors influencing the electrospinning process and morphology of the obtained fibers can be divided into solution, process, and ambient parameters. Solution parameters are the most significant followed by the process and then ambient parameters. The most important variables and their influence are presented in the Table 3.1.

Properties of polymer solutions such as viscosity, electrical conductivity, surface tension, solvent evaporation rate and dielectric properties play a significant role in electrospinning process, obtained fiber morphology and the material's properties as a consequence [14, 2].

Table 1.1. Important parameters in electrospinning.

Parameter:	**Explanation**
Solution properties	
Polymer molecular weight, concentration and solution viscosity: Impacts process stability, fiber average diameter and formation of the beads.	Minimal viscosity, concentration and appropriate molecular weight of the polymer are needed to produce continuous electrospinning fiber. Continuous fibers can be produced due to the entanglement of polymer molecules inside the polymer solution. There are two opportunities to affect solution's viscosity: change the polymer concentration or molecular weight of polymer [15]. At low viscosity values, the beaded thin fibers are produced. With an increase of the solution's viscosity, a fiber average diameter also increases. As a result, less-beaded, more uniformed fibers are produced. At the increased solution concentrations, the viscosity inside the electrospinning jet also increases and thus preventing the jet bending instability near the Taylor cone. As a result, bending instability starts further from the tip of the needle [2]. Due to this, the jet path to the collector and the deposition area are reduced. Alternatively, a shorter path to the collector means the decreased stretching of the electrospinning jet resulting in greater fiber diameter. Too high solution viscosity can obstruct the solution pumping through the system; it will also dry faster on the tip of the needle. No continuous fiber can be obtained from the above critical solution viscosity [16].

Table 1.1 (continued)

Surface tension: Has a key role in the bead formation process during electrospinning.	At the initiation of the electrospinning process, the total surface charge on the droplet surface at the tip of the needle must exceed solution surface tension to start the electrospinning process [17]. In fact, at lower viscosity values, more free solvent molecules are present in the solution. In this case, the surface tension of the solvent will play a dominant role; solvent molecules will gather and adopt a spherical shape (see Fig. 1.3). The gradual increase of viscosity will cause changing the shape from spherical to cylindrical until perfectly smooth bead-free fibers are produced. The interaction between the polymer and solvent molecules is greater at higher viscosity values and therefore the solvent molecules are more uniformly distributed throughout the chain [18].
Solvent evaporation rate: Influences dryness of the final membrane and process stability.	Separate fibers can be obtained only if most of the solvent evaporates while the electrospinning jets forward to the collector. Otherwise, the residual solvent will dissolve the fibers into a thin film on the surface of the collector [19]. Again, the needle might clog [20] at too high evaporation rate. The evaporation rate of a solvent is dependent on many factors: vapor pressure, boiling point, specific heat, enthalpy and heat of vaporization of the solvent, rate of heat supply, interaction between solvent molecules and between solvent and solute molecules, surface tension of the liquid, and air movement above the liquid surface [2].
Solution electrical conductivity: Influences the fiber average diameter.	Pulling of the electrospinning solution to the collector is caused by the repulsion of the charges on the surface of the droplet. At zero conductivity, no fibers can be formed. At higher conductivity, jets can carry more charges and the stretching force towards the collector increases as well. Due to that, the greater bending instability will occur and the deposition area increases as well. Finally, more uniform fibers are formed [2, 16]. A small amount of salts, conductive additives, and metal ions can be added to increase the electrical conductivity of the solutions.
Dielectric effect of solvent: Influences formation of the beads.	An increase of bending instability of the electrospinning jet appears with the utilization of the solvents with higher dielectric constants. As a result, the deposition area and the jet path increase, resulting in the formation of the fibers with more uniform shapes and lower average diameters [2]. In opposite, if the polymer does not dissolve effectively in the solvent, fibers with more and larger beads are obtained.

Table 1.1 (continued)

Solution temperature: Impacts solvent evaporation rate and fiber average diameter.	Heating of the solution has two effects: it increases the evaporation rate of the solvent and reduces the viscosity of the solution. At higher temperatures, the mobility of the polymer molecules in the solution increases. Due to this, the solution resists less to pulling by the same Columbic forces, resulting in a decrease of the fiber diameter [21].
Process and ambient parameters	
Applied voltage: Affects fiber average diameter and polymer crystallinity inside fibers.	It is known, that both positive and negative voltages can create Taylor cone [22]. Only a minimal voltage is needed to overcome the surface tension of the solution. Increasing the voltage causes greater stretching of the jet because of the increase of the number of charges. Generally, this causes a decrease in the obtained fiber's diameter. Nevertheless, in some cases, high voltages can cause bead formation. Continuous increasing of the voltage changes their shape from cylindrical to spherical. At too high voltage, the Taylor cone withdraws to the needle, the instability of the jet increases, and this, in turn, increases the frequency of bead formation. However, in a weaker electrical field, acceleration of the jet decreases and the time it takes the polymer to get to the collector of the jet increase. This enables the jet to stretch more during electrospinning and thus thinner fibers are obtained [20]. Also at the weaker stretching, longer deposition time allows polymer molecules to relocate inside the fibers and to increase crystallinity [2].
Solution pumping rate: Affects the stability of Taylor cone and the morphology of the obtained fibers.	The average diameter of fibers increases at a higher than optimum pumping rate. In this case, at a constant voltage, a greater amount of solution collects on the needle tip, which decreases the evaporation rate of the solvent. This can result in pulsing electrospinning. Additionally, if the solvent does not evaporate quickly enough, then the result may be a fused fiber network [23]. Optimal pumping rate is needed for the production of continuous uniform fibers.
Inner diameter of needle: Influences fiber average diameter, needle clogging and applied voltage.	The needle can become clogged if the diameter is not large enough. The wider the needle, the lower voltage is needed for electrospinning and thus thicker fibers are produced. With a smaller inner diameter, the droplet size on its tip decreases. As a result, the surface tension increases and greater electrostatic force is required to erupt a solution jet. Consequently, acceleration and drawing of the jet increase and as the pulling force is stronger, the smaller diameter fibers are formed [17].

Table 1.1 (continued)

Distance between tip of the needle and the collector: Affects deposition time and strength of the electrical field [16].	Thin uniform fibers can be produced at the longer distance. When other parameters are constant, the electrical field is weaker at the longer distance. This increases the flight time and the deposition area. Therefore, the diameter of the obtained fibers and bending instability can be reduced. Finally, thinner fibers of uniform morphology are obtained. No fiber will occur if the distance is too long because the electrical field will be too weak to overcome the viscosity of the solution. Alternatively, at shorter distances, the electrical field strength is increased. This increases the acceleration of the jet to the collector and fiber diameter as well as it decreases the deposition area. Finally, there is not enough time for the solvent evaporation and membranes need additional drying [2].
Humidity: Affects porosity of fibers and packaging density of the membrane.	Condensed water on the fiber surface slows the evaporation of the solvent, which usually leads to pore formation in the fiber structure. The higher the humidity, the wider and deeper the pores that are formed. However, above a certain humidity, the diameter, depth, and number of the pores will be satiated. From another point of view, condensed water reduces the concentration of electrostatic charges on the collector, thus increasing packaging density of the membrane [24].

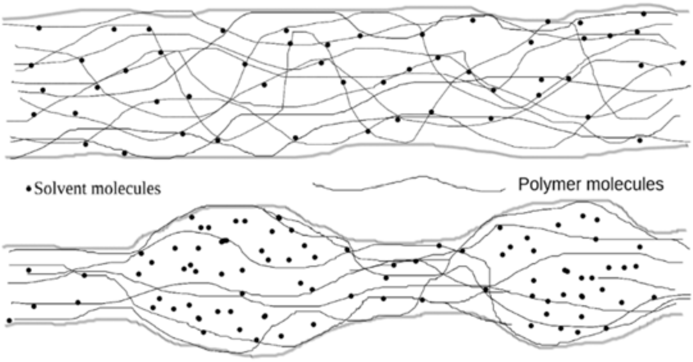

Figure 1.3. At the higher solution viscosity, solvent molecules are distributed along the polymer chains (top fiber). At the lower solution viscosity, solvent molecules have a tendency to accumulate and form spherical shapes due to surface tension (bottom fiber).

1.1.3. Fiber properties and application

Electrospun fibers have an extremely high surface to weight ratios in comparison to conventional nonwovens (nanofibers with ~100 nm diameter have a specific surface of ~1000 m^2/g). Electrospun fibers exhibit special properties such as remarkable high porosity, excellent structural mechanical properties, and high axial strength combined with extreme flexibility, low basis weight, and costeffectiveness, among others [25]. Properties of polymeric fibers offer numerous fields for their application (see Fig. 1.5).

Despite the fact that polymers are ideal for electrospinning of membranes, the mechanical, electrical, thermal, rheological and optical properties need improvement for special applications. Depending on the application, different fillers can be used for this purpose. For example, ceramic nanoparticles such as barium titanate ($BaTiO_3$), aluminum oxide (Al_2O_3) or silicon dioxide (SiO_2) are used to enhance ionic conductivity and the electrochemical stability window of nanocomposite polymer electrolytes (NCPEs) [26]. Calcium carbonate ($CaCO_3$) or hydroxyapatite (HA) can be used for the improvement of the mechanical strength of bone-scaffolding materials [27]. For enhancing the biodegradability of polylactic acid (PLA), fibrous membranes like cellulose nanocrystals (CNCs) can be used as a filler [28]. However, among the wide variety of different fillers, there is one, which can improve many properties of the polymer matrix at once; this is carbon nanotubes. CNTs are widely used for the improvement of mechanical, thermal and electrical properties of fibrous membranes.

1.2. CNT as reinforcing and electroconductive components in electrospun fibers and membranes

1.2.1. CNTs

Since 1991 when Iijima [29] reported the preparation of MWCNTs, a lot of work has been done with CNTs because of their outstanding properties. For example, CNTs have high flexibility, low mass density, large nanotube aspect ratio, high mechanical strength, electrical and thermal conductivity. They exhibit extraordinary stiffness-to-weight and strength-to-weight ratios [30]. The most important properties of CNTs are presented in a Table 1.2.

Table 1.2. Properties of CNTs [31 – 34].

Property	**Value**	**Additional information**
Young’s modulus	Up to 1 TPa	10 times stronger than titanium
Tensile strength	10-63 GPa	50 higher than steel
Thermal conductivity	>3000 W/(m·K)	~2 times higher than diamond
Electrical conductivity	$10^6 – 10^7$ S/m	the same as copper
Strain at break	10%	~4 times higher than Kevlar

CNTs are long and thin tube-shaped materials of rolled graphene sheets (see Fig. 1.4). The diameter ranges from 1 to 50 nm and the length between a few hundred nm up to 50 cm [35]. Sheets of hexagonal-shaped carbon atoms are rolled up into cylinders and are closed by pentagonal-shaped carbon atoms. There are three types of CNTs: single-walled CNTs (SWCNTs), double-walled CNTs (DWCNTs) and MWCNTs [29, 36].

CNTs already have application fields on the industrial scale. For example, CNT powders mixed with polymers or precursor resins can increase stiffness, strength, and toughness of final composite in load-bearing applications [45]. Coatings and films are second large area of CNTs application. As an example: transparent conductive materials made of CNT films can be formed [46]. In addition, CNTs are used in microelectronics, for transistors [47] and Li-ion batteries. Figure 1.5 gives an overview of the main application fields of CNTs, adjacent fields of CNTs and polymeric fibers where both are used. The figure also presents perspectives of utilization of CNTs in other applications with polymeric fibers.

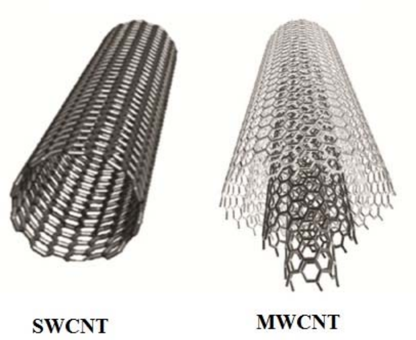

Figure 1.4. Schematic structure of SWCNT and MWCNT [43].

CNTs are widely used nowadays and the interest for their applications in new fields is growing rapidly every year even though there are some difficulties in the application of CNTs (see Fig. 1.5). The enhancement of the final product properties largely depends on the CNTs' purity, quality, surface chemistry, diameter, aspect ratio, alignment, dispersion, and interfacial interaction with the matrix [4]. In polymer/CNT composites, CNTs cannot be used in its bulk bundled form due to insolubility, poor dispersion and incompatibility with the polymer matrix. The problem to be solved is the following: how to break up entanglements, bundles or agglomerates of the CNTs and then uniformly disperse and align them within a polymer matrix. In addition, there is a need for improving the transfer of properties from CNTs to the polymer matrix. The next sections give an overview of the different CNT dispersion methods into polymer matrices.

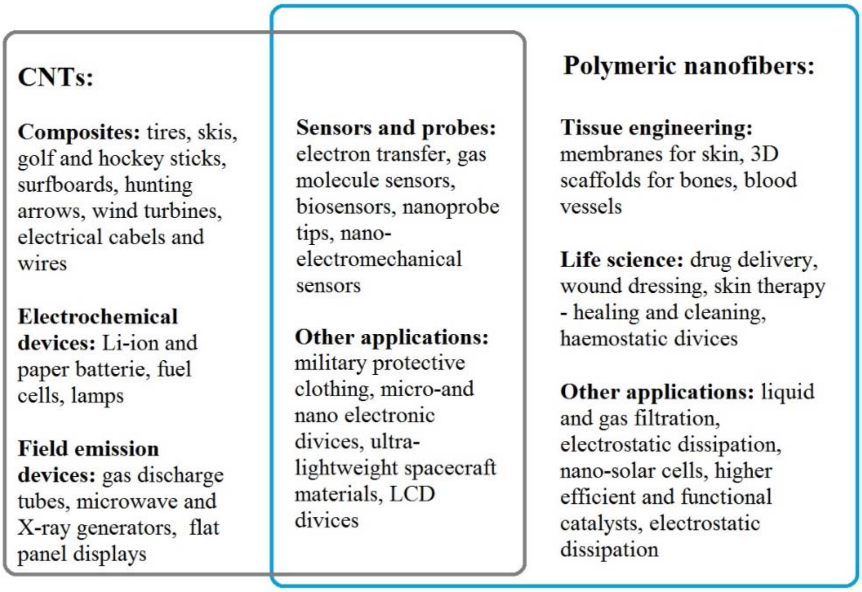

Figure 1.5. Application of CNTs [44], polymeric fibers [3] and adjacent fields.

1.2.2. Methods for CNT dispersion into polymer matrix

Many methods have been developed for better dispersion and compatibility of CNTs with polymer matrices during the last two decades. These methods in principle can be divided into two major sections, those that utilize physical and chemical approach.

Methods with the physical approach can be applied mainly for the dispersion of unmodified CNTs into polymer solutions and melts. In addition to a mechanical stirring of solutions, ultrasonication can be used to achieve a good dispersion of CNTs [48]. For polymer melts, the extrusion method is used for the same aim [49]. Recently, it was found that simple compounding of polymer, mechanical mixing, of a polymer solution with CNTs does not give a uniform mixture. The reason is in the π-π interactions between the CNTs in agglomerates. A lot of energy should be transferred to the mixture of polymer and CNTs to overcome this force [50].

The chemical approach tends to be more effective for the achievement of good dispersion and compatibility of CNTs with polymers. Chemical methods can be divided into three subcategories: functionalization of the CNT surface with chemical groups, utilization of compatibilizers (surfactants) and modification by polymers.

Incorporation of functional groups on the surface of CNTs usually involves treatment with strong acids at high temperature and pressure. Typical groups to be attached are carboxylic (-COOH), hydroxyl (-OH) [51] or amino (-NH_2) [52]. The reason for their popularity is in their reactivity: a large number of chemical reactions can be performed with these groups after CNTs functionalization. Less popular processes include sidewall functionalization, thiolation, halogenation and hydrogenation [53]. The disadvantage of these methods is in structural defects that might introduce in CNTs sidewall [54].

A simpler and non-destructive method to re-bundle CNTs agglomerates is the addition of surfactants. Typically, after the surfactant has been adsorbed on the CNT surface, the physical treatment may help to re-bundle agglomerates by steric or electrostatic repulsions [55]. For different media, surfactants of opposite nature are preferable: for CNTs/water-soluble solutions – ionic, for organic solvents – nonionic surfactants. However, there are additives, which can be used in both media - ILs. The phenomenon of this type of surfactant is discussed separately in next subsection.

1.2.3. IL assisted dispersion of the CNTs

ILs are usually defined as organic salts with a low melting temperature, below 100℃ [56]. In general, they consist of a large cation and small anion. To characterize the ILs as a class it should be marked, that ILs are environmentally friendly or "green" solvents with many remarkable properties. They are "green" because of extremely negligible vapor pressure, which inhibits evaporation into the air and allows simple recycling and reuse. The interest in the application of ILs is growing rapidly every year because of their high electrical conductivity, wide range of densities and viscosities, variable polarity and solubility, negligible vapor pressure, high thermal and chemical stability, high product recovery, an endless number of different compositions and designable functionality [57].

It is known from the literature, that imidazolium ILs can be used to exfoliate or re-bundle the CNTs agglomerates. S. Bellayer *et al.* showed experimentally, that "cation-π" interaction between imidazolium ions and the large π-electronic surface of the CNTs causes the exfoliation of CNT agglomerates [59]. Molecular dynamic simulations proposed by Shim and Kim [60] showed, that cations and anions of 1-ethyl-3methylimidazolium tetrafluoroborate ($EmimBF_4$) form a cylindrical shell outside the CNT surface. Imidazole rings were mainly parallel to the CNT surface thus producing π-stacking between ions and the CNT surface, therefore, enhancing the dispersion of CNTs. CNTs agglomerate because of π-π interactions between separate tubes. The π-π interaction-shielding model for the dispersion process of CNTs in imidazole ILs was proposed by J. Y. Wang *et al* [58]. By this theory, CNT agglomerates gradually exfoliate by a shearing force into smaller bundles and detached separate CNTs are surrounded by ILs immediately. During this process, the strong π-π interaction of CNTs is shielded due to the large dielectric constant of imidazole ILs thus preventing re-bundled nanotubes and smaller agglomerates from aggregating. Finally, separate CNTs and small agglomerates in dispersion are encapsulated because of van der Waals forces between ILs and CNTs (see Fig. 1.6). This suggests that in CNTs dispersion shielding of π-π interaction between CNTs plays an important role and can be provided by utilization of imidazole ILs. For this current research, 1-buthyl-3-methylimidazolium chloride (BmimCl) was chosen as a functional additive to enhance the dispersion of CNTs.

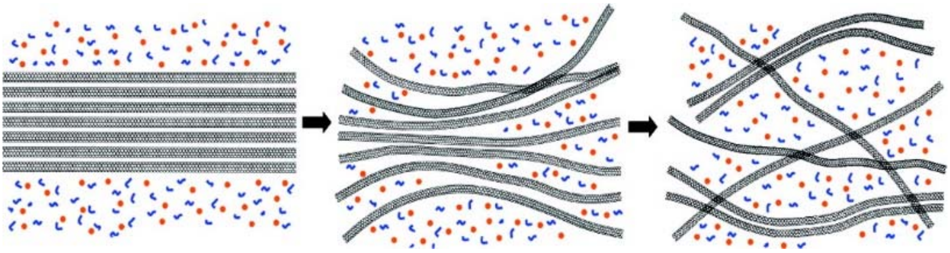

Figure 1.6. Schematic representation of the dispersion process for SWCNTs in ionic liquids [58].

1.2.4. CNT modification by polymers

Despite the variety of methods described, the most attractive method for dispersion of CNTs is covering their surface with an appropriate polymer. This allows for a tailored approach for each polymer/CNT composite system designed to achieve the best transfer of CNTs properties to the matrix polymer and consequently final product. The modification of CNTs by polymers can be broadly divided into two subsections: covalent and non-covalent modification. The non-covalent modification is very modest. It is the polymer wrapping and/or polymer adsorption to CNTs' sidewalls [61]. Mainly, the non-covalent modification is caused by π-π interactions between double bonds of sidewall carbon rings and conjugated polymers or organic polymers with a free electron pair. An advantage of this method is in the holistic structure of CNTs in the final product. The covalent modification is more varied. Broadly, it is divided into "grafting to" and "grafting from". Each direction has numerous variations with the main ones presented in figure 1.7.

1.2.5. CNT modification by SAN

Polymers are very complicated, multiform and unique substances. One polymer can be prepared by different methods, for example, it has different molar mass and 3D structures, and it can be processed by numerous methods to the endless number of products. One can be modified and transformed into another polymer. The same is with SAN.

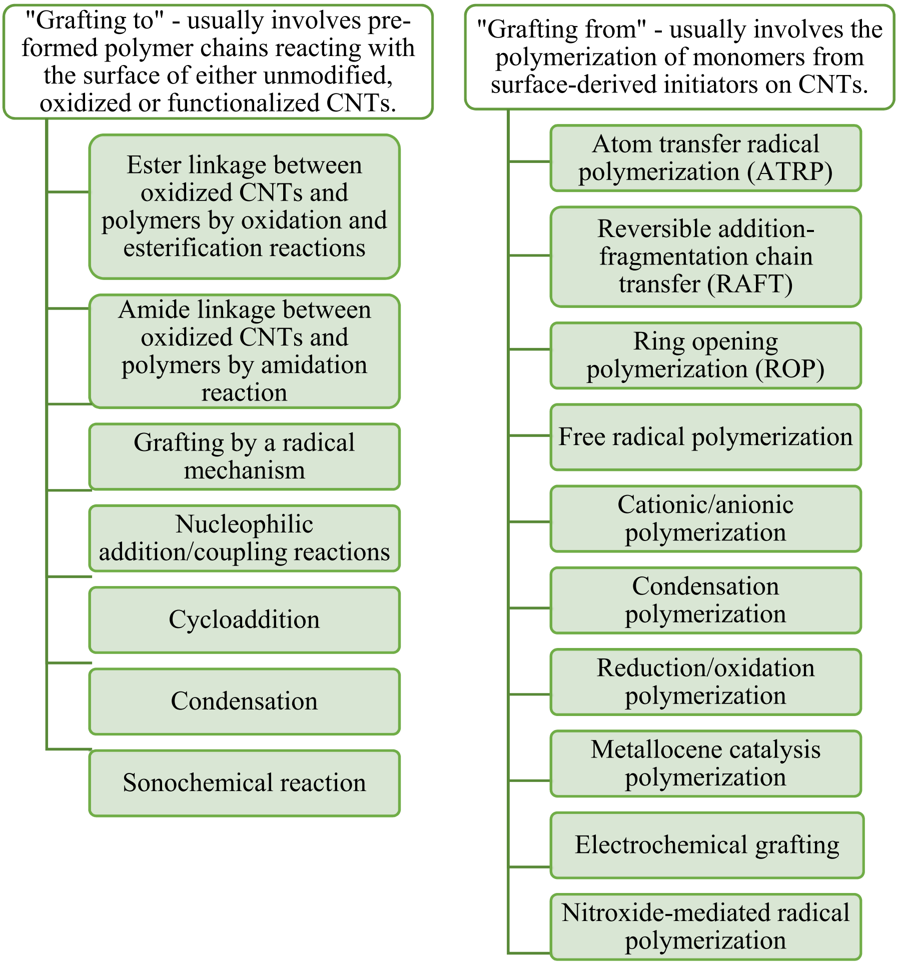

Figure 1.7. CNT modification by "grafting to" [64 - 70] and "grafting from [71 - 80] methods.

SAN has many good properties: excellent transparency, high tensile modulus, good rigidity and hardness, high dimensional stability and accuracy, good heat and high chemical resistance [62]. Chemical resistance, for example, is very important in electrospun filters. It is well known that properties of SAN products strongly depend on the styrene (S) to acrylonitrile (AN) ratio in the polymer chain. With an increase of molecular weight or AN content in the chain, improvements in the following properties of SAN were also observed: strength, stiffness, impact resistance, heat resistance and resistance to stress [63]. For this reason, products with different properties can be made from one polymer, which makes SAN copolymers attractive for future studies. Both S and AN can be modified through chemical reactions for special issues. In CNTs, modification by SAN, for example, can be used in both approaches: "grafting to" and "grafting from".

A. M. Shanmingharaj *et al.* [81] first reported the preparation of SAN-g-CNTs via surface-initiated ATRP. During this “grafting from” procedure, all initiator-grafted MWCNTs were prepared through multistage functionalization. Carboxyl group functionalized MWCNTs (MWCNT-COOHs) were first prepared by refluxing the unmodified MWCNTs in chromic acid for 30 min at 80°C. After washing them with deionized water, filtration and drying *in vacuo,* MWCNT-COOHs were modified to acyl chloride functionalized MWCNTs (MWCNT-COCls) by addition of thionyl chloride ($SOCl_2$) and stirring for 24 h at 65°C. The obtained MWCNT-COCls were washed with anhydrous tetrahydrofuran (THF) and dried *in vacuo* for 30 min at the room temperature. MWCNT-COCls were refluxed with previously synthesized 2-hydroxyethyl bromoisobutyrate (HEBB) in anhydrous THF for 45 min. Obtained HEBB-grafted MWCNTs (HEBB-g-MWCNTs) were washed with THF and ethanol, filtered and dried *in vacuo* for 10 h. Finally, SAN-grafted-MWCNTs (SAN-g-MWCNTs) were prepared via ATRP by mixing of HEBB-g-MWCNTs, S and monomer units in inert nitrogen (N_2) atmosphere with addition of copper bromide (CuBr) and ligand in toluene. The polymerization reaction was maintained at 80°C for 24 h. In the end, the product was purified and dried (see Fig. 1.8). This proposed method has both positive and negative aspects. It is time consuming and complicated. Procedures need careful monitoring on each of the multiple steps. The method is also not environmentally friendly because of the utilization of numerous organic solvents and a copper ligand. Finally, it is very complicated to apply this in the production scale. From another point of view, the ATRP procedure allows controling of properties of the final polymer by reaction time and monomer ratio and creating SAN-g-MWCNTs for specific applications.

J.-H. Shi, *et al.* [82] proposed simpler “grafting to” approach for the production of SAN-g-MWCNTs by reactive melt blending. This procedure was divided into two steps. First, the modified SAN was prepared in a compounder by melt blending. For this purpose, SAN was blended with 2-aminoethanol (AE) and zinc acetate dihydrate ($Zn(Ac)2 \cdot 2H_2O$) for 30 min at 150-200°C in a compounder, extruded, washed with chloroform ($CHCl_3$), filtered and dried *in vacuo* at 70°C for 48 h. In the second step, MWCNTs were oxidized by nitric (HNO_3) and sulfuric acids (H_2SO_4) for 6 h at 50°C to form MWCNT-COOHs. Finally, MWCNT-COOHs and modified SAN were blended to produce SAN-g-MWCNTs for 30 min at 200°C, extruded, washed with THF and dried. J.-H. Shi, *et al.* claim, that the final product is SAN-g-MWCNTs, but actually it is (modified SAN)-g-MWCNTs. Compared to ATRP, reactive melt blending is shorter in time, simpler and it can be adopted by industry. It also allows changing SAN for any AN containing thermoplastic polymer and graft CNTs onto the surface by the same procedure through the addition of an oxazoline functional group to SAN. However, the method is not as flexible as ATPR: it allows using of already synthesized polymer with constant length, monomer ratio and structure.

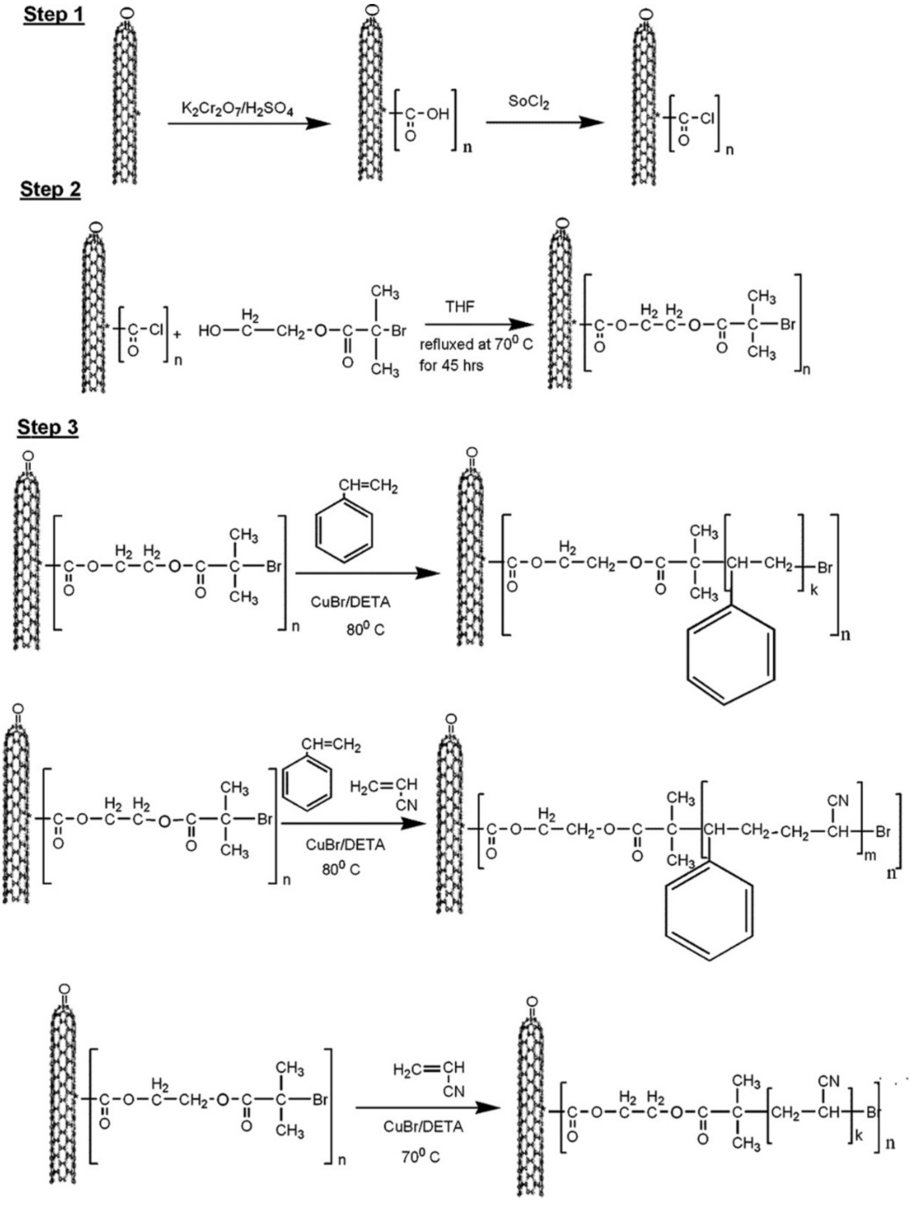

Figure 1.8. Reaction scheme of polymer-grafted CNTs through ATRP [81].

1.3. Aim and objectives of the study

The main aim of the current study was to electrospin reinforced fibrous polymer membranes through the utilization of CNTs as functional additives. Two problems of CNT utilization had to be solved for achieving the aim: the creation of good dispersion of the CNTs into polymer matrix and achievement of effective interfacial adhesion between CNTs and polymer matrix.

First, SAN polymer was chosen from the variety of different polymers. The choice was based on the chemical structure of SAN, which contains acrylonitrile functional groups suitable for further grafting reactions. The polymer-solvent system was chosen for electrospinning based on continuity of the process, solution parameters and fiber morphology.

Different approaches were used for achieving the aim. The ultrasonic treatment and IL were used to improve dispersion of the CNTs into polymer matrix. In the second step, unmodified CNTs were dispersed into a polymer solution by mechanical and ultrasonic mixing while the effect of IL, as a dispersive agent, was evaluated. Finally, a grafting reaction to bind CNTs with modified SAN was developed to create the effective interfacial adhesion between CNTs and polymer matrix.

The additional aim of this study was to evaluate the efficiency of different approaches of CNT dispersion into polymer matrix focusing on the SAN. Solution properties have the biggest influence in electrospinning process on final membrane properties. Therefore, viscosity and electrical conductivity of all solutions were measured and their impact on the final properties was analyzed. After all, the combined method incorporating addition of the IL, application of ultrasonication and covalent bonding of the CNTs with oxazoline modified poly(styrene-co-acrylonitrile) (SANm) was used to disperse the CNTs into the polymer solution.

For electrospun membranes, the effect of ultrasonication, addition of the IL, CNTs grafting and utilization of the combined method on the morphology, mechanical and electrical properties were studied and compared to pure SAN membrane.

2. EXPERIMENTAL

2.1. Materials and chemicals

Two different solvents were used for the preparation of electrospinning solutions of SAN (Polimeri Europa SRL): 1,2-dichloroethane (1,2-DCE, purity ≥ 99.5%) and dimethyl sulfoxide (DMSO, Merck KGaA, purity ≥ 99.9).

1-butyl-3-methylimidazolium chloride ([Bmim]Cl) was synthesized using the procedure reported in the literature [83]. In the standard preparation method, 1.5 moles of chlorobutan (purity ≥ 99%) and 1.0 mole of 1-methylimidazole (Merck Millipore, purity ≥ 99%) were mixed in a round-bottomed flask fitted with a reflux condenser and stirred for 3 days at 80°C under nitrogen (N_2). After the two phases formed, the top phase containing the reagents was removed by washing several times with ethyl acetate (Sigma-Aldrich, purity ≥ 99%). The yellowish IL product of [Bmim]Cl was further heated up to 50°C under vacuum to remove ethyl acetate. Only one IL, [Bmim]Cl, was used in this study and it is referred to as IL in the dissertation.

MWCNTs with an average diameter of 9.5 nm, average length of 1.5 μm and 95wt% purity were purchased from Nanocyl S.A. The carboxyl group modified multiwalled carbon nanotube (MWCNT-COOHs, Cheap Tubes Inc.) have average diameter of 8-15 nm, average length of 0.5-2.0 μm, 2.56wt% content of –COOH functional groups and 95wt% purity. SANm-g-MWCNTs are considered as a special type of MWCNTs in this study. All carbon nanotubes used in this study are MWCNTs and will be considered as CNTs in the dissertation.

For the modification reaction of SAN to SANm, zinc acetate dihydrate ($Zn(Ac)_2 \cdot 2H_2O$, purity ≥ 99%) was purchased from EMSURE® and 2-aminoethanol (AE, purity ≥ 99%) was purchased from Merck Millipore. For washing of oxazoline modified poly(styrene-co-acrylonitrile) grafted carbon nanotubes (SANm-g-CNTs), THF was purchased from Riedel-de Haën (purity ≥ 99.9%). For precipitation of SANm-g-CNTs, methanol was supplied by Riedel-de Haën (purity ≥ 99.8%).

2.2. Preparation of SANm and SANm-g-CNTs

First, for dissolving and achieving better homogenization of $Zn(Ac)_2 \cdot 2H_2O$ in AE, the mixture in a ratio 1:83 was ultrasonically mixed [84] for 10 minutes. SAN was modified using the procedure partially reported by J.-H.Shi in [82]:

1) SAN (4.5 g) was first melted in a HAAKE™ MiniCTW Micro-Conical Twin Screw Compounder using rotational speed 20 rpm at 150°C until it achieved a stable torque (~10 min)

2) a mixture of AE and $Zn(Ac)_2{\cdot}2H_2O$ (455.4 mg) was then quickly added to the SAN and mixed with the polymer at 150°C for 10 min using a rotation speed of 80 rpm

3) next, the temperature was increased up to 200°C and the blending continued for 20 min

4) the oxazoline modified SAN (SANm) was then extruded from the compounder

5) SANm was dissolved in 45 ml of THF by mechanical mixing for 45 min and then precipitated in 1350 ml of methanol. The obtained mixture was filtered with 0.45 µm pore size polytetrafluoroethylene filters (PTFE, Sartonus Stedim Biotech Gmbh, Germany). This process was repeated several times to ensure the complete removal of $Zn(Ac)_2{\cdot}2H_2O$ residue and AE. The resulting SANm was dried in a vacuum oven at the room temperature for 24 h. The yield of this process was 79%. The obtained material was characterized by Fourier transform infrared spectroscopy (FT-IR) and thermogravimetric analyses (TGA).

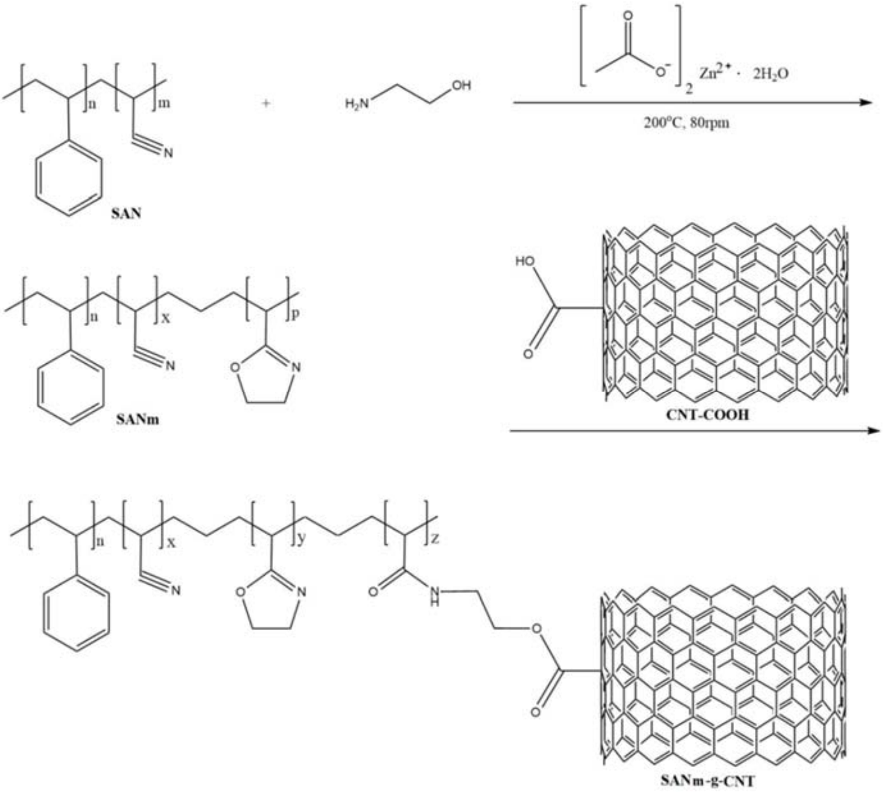

Figure 2.1. Scheme of CNT grafting reaction with SAN (article III).

Steps 1-3 were conducted for nanotube grafting with SANm. Immediately after the step 3, CNT-COOHs with a weight ratio of 1:20 to polymer were added to the compounder, and the melt blended at a rotating speed of 80 rpm at 200°C for another 30 min. Finally, the resulting material was dissolved in THF and centrifuged (EBA 21, Hettich Centrifugen, Germany) at 6000 rpm for 30 min in 50 ml falcon tubes. The washing procedure was repeated several times until transparent centrifugate was obtained to ensure the complete removal of $Zn(Ac)_2 \cdot 2H_2O$ residue, ungrafted SANm and AE. The solid precipitate was dried in a vacuum oven for 24h at 80°C to remove THF. The yield of this process was 55%. The obtained material was characterized by nuclear magnetic resonance (^1H NMR) and TGA. Fig. 2.1 represents the Scheme of the CNT grafting reaction with SAN.

2.3. Preparation of electrospinning solutions and electrospinning

Solutions with IL and different CNTs for the electrospinning experiments were prepared by mechanical and ultrasonic mixing techniques (see Table 2.1). The concentration of IL and CNTs was calculated by the weight of SAN. All concentrations in the current study are presented as the weight to weight concentrations. A Sonoplus HD 2070 (BANDELIN electronic GmbH & Co. KG) ultrasonic device was used for solution preparation.

A typical electrospinning setup is presented in the Fig. 2.2. All solutions were electrospun from a disposable plastic syringe with a medical needle with an inner diameter 0.1 mm. A MK Series power supply (GLASSMAN EUROPE Limited) was used to generate a high voltage up to 20 kV. Fibers were collected on a flat aluminum foil collector or rotating drum of a diameter 7.5 cm covered with aluminum foil. The distance between the tip of the needle and the collector was 10 to 20 cm. A NE-1000 Single Syringe Pump (New Era Pump Systems, Inc.) was used to pump the electrospinning solutions. The pumping rate was from 0.6 to 0.9 ml/h. Mechanical, electrical properties and morphology were investigated for each electrospun membrane.

Figure 2.2. Electrospinning setup.

Table 2.1. Composition and preparation of electrospinning solutions

Solution composition	Preparation technique	Electrospinning variables
Section 3.1 optimization of electrospinning parameters		
10 to 20% SAN in 1,2-DCE	Mechanically mixed at 50ºC using reflux to prevent solvent evaporation.	Voltage: 0 to 20 kV Distance to collector: 10 to 20 cm Syringe: 1 ml Collector: flat aluminum foil 4 x 4 cm
13% SAN in 1,2-DCE + (0.5-20%) IL		
12 to 25% SAN in DMSO	Mechanically mixed at 50ºC for 8h	Voltage: 10 to 20 kV Distance to collector: 10 to 20 cm Syringe: 2.5 ml Collector: rotating drum covered with aluminum foil
20% SAN in DMSO + (0.5-20%) IL		
20% SAN in DMSO + (0-3%) CNTs	First, a solution of SAN in DMSO was mechanically mixed at 50ºC for 8 h. After that, IL and various amounts of CNTs were added and mixed for another 24 h at 50ºC. Before electrospinning, the solutions were ultrasonically treated for 3 h in an ice bath.	
20% SAN in DMSO + 20% IL + (0-3%) CNTs		
Section 3.2 CNTs grafting with SANm for electrospinning		
20% SAN in DMSO	Preparation of mechanically mixed solutions: first a SAN in DMSO solution was mixed by mechanical stirring at 60ºC for 24 h. After that, IL and CNT were added and stirred for another 24 h at 60ºC. Preparation of ultrasonically mixed solutions: first SAN in DMSO solution was mixed by mechanical stirring at 60ºC for 24 h. After that, IL and CNTs were added and stirred for another 24 h at 60ºC. At last solutions were ultrasonically treated for 3 h.	Voltage: 20 kV Distance to collector: 20 cm Syringe: 2.5 ml Collector: rotating drum covered with aluminum foil
20% SAN in DMSO + 1% CNTs		
20% SAN in DMSO + 1% CNT-COOHs		
20% SAN in DMSO + 1% SANm-g-CNTs		
20% SAN in DMSO + 20% IL		
20% SAN in DMSO + 20% IL + 1% CNTs		
20% SAN in DMSO + 20% IL + 1% CNT-COOHs		
20% SAN in DMSO + 20% IL + 1% SANm-g-CNTs		

2.4. Characterization of the SANm-g-CNTs, solutions and electrospun membranes

The transmittance FT-IR spectra was recorded on an Interspec 200-X FTIR spectrometer, with 16 scans averaged at the resolution of 1 cm^{-1} for SAN and SANm.

TGA experiments with a Setaram LabsysEvo 1600 thermoanalyzer were carried out under non-isothermal conditions by heating up to 800ºC at the heating rate of 10°C/min in the argon atmosphere. Standard 0.1 ml alumina crucibles were used, the mass of the samples was 4-5 mg and the gas flow was 60 ml/min.

^{1}H NMR spectrum was recorded with a Bruker Avance III spectrometer operating at 500 MHz. The sample (7 mg/ml) was first dispersed in d6-DMSO by keeping it at 50°C overnight followed by vortex mixing for several minutes. The spectrum was collected at the room temperature with 32 scans averaged.

The viscosity of the electrospinning solutions was measured by a Physica MCR 501 rheometer (Anton Paar, Austria) at the rate 100/s using cone-plate geometry (cone angle 2° and diameter 2.5 cm) and Brookfield Rheometer RVDV II+ (Brookfield eng labs Inc.). Each experiment was performed at a standard temperature 23ºC.

The electrical conductivity of the solutions was measured with a SevenCompact Conductivity S230 electrical conductivity meter (Mettler Toledo, Switzerland) at the room temperature.

The electrical conductance of the electrospun membranes was measured with a High Resistance Meter Model HR2 (AlphaLab, Inc., USA) at the room temperature (2-point method). The thickness of each sample was measured from 3 to 6 different points by digital thickness gauge (INSIZE CO., LTD.) and the average was calculated. After that, each sample was placed into the cell between electrodes and the values were detected. Finally, electrical conductance was calculated into electrical conductivity (σ) considering dimensions of the samples according to the equation (2.1):

$$\sigma = G\,\frac{l}{A}, \qquad (2.1)$$

where G (μS) is the electrical conductance, A (cm^2) is a cross-section area and l (cm) is the sample length.

Mechanical properties of the electrospun membranes were measured at 23°C using an Instron 5866 (Instron Corporation, UK) tensile tester. The samples were cut into a rectangular shape. The thickness of each sample was measured from 3 to 6 different points and the average was calculated. The load cell of maximum capacity 2.5 N was used for tensile testing procedures applying a constant actuator speed of 10 and 20 mm/min. The collected data was analyzed and the tensile stress at maximum load and Young's modulus were calculated using Bluehill^{TM} 2 Version 2.17 software.

The morphology of the electrospun fibers was analyzed using an optical microscope Axiskop 2 (Carl Zeiss Microscopy, LLC), scanning electron microscopes (SEM) Gemini Zeiss Ultra 55 and Hitachi TM1000. Pictures of various magnifications from 10 to 100000 were done for the samples. The average fiber diameter was calculated for each sample. The transmission electron microscopy (TEM) measurements for SANm-g-CNTs were done with FEI Titan Themis 200 working at 80 kV.

3. RESULTS AND DISCUSSION

3.1. Optimization of electrospinning parameters

This section is based on article I and article II. Below is described the optimization of SAN polymer electrospinning process. The main parameters including solution properties and process variables are discussed and evaluated in this part. In the electrospinning process, solution properties are dominant in achieving of continuous fibrous membrane [2]. The SAN concentration in different solvents and its impact on the obtained membrane morphology were analyzed. In addition, the utilization of the IL as a functional additive, its effect on polymer solutions properties, electrospinning process and obtained fiber morphology are discussed. The key point of this research is the utilization of carbon nanotubes as a reinforcing filler. The optimization of effective concentration and creation of good dispersions into polymer solutions is described and analyzed in details.

3.1.1. Impact of solvent and solution concentration on electrospinning process and fiber morphology

To find out the most optimal SAN concentration and electrospinning variables, SAN solutions from 10 to 20% in 1,2-DCE and from 12 to 25% in DMSO were prepared and electrospun. Electrospinning was performed at different variables: distance from 10 to 20 cm and voltage from 10 to 20 kV. The obtained fibers were studied using an optical microscopy and SEM.

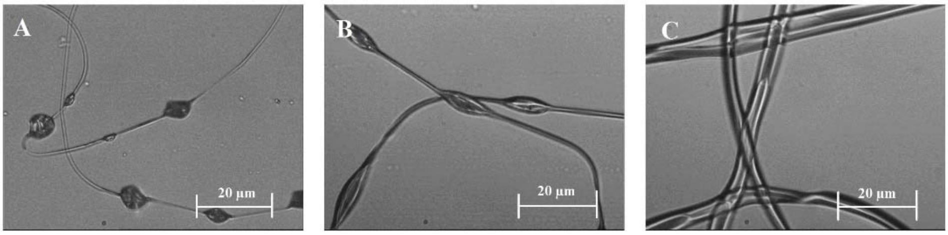

Figure 3.1. SAN fibers, electrospun at 10 kV and 10 cm from the collector with solutions in 1,2-DCE with different polymer concentrations: A - 10%, B - 13%, C - 17% (optical microscope, magnification 50x) (article I).

While analyzing all the electrospun fibers with an optical microscope, it could be seen that at lower solution concentrations beaded fibers of smaller diameter were obtained. The lowest concentration for the formation of continuous fibers was found at 10% for SAN solutions in 1,2-DCE and 12% in DMSO. At a lower concentration, the higher number of solvent molecules and fewer chain entanglements of SAN present in solution. This means that the surface tension of the solvent is higher than the interaction of solvent molecules with polymer chains and is dominant during the electrospinning process [16]. This contributes to bead formation at lower solution concentrations (see Fig. 3.1 A). When the SAN concentration was increased, the formation of fibers with greater diameter was observed. This is caused by the greater resistance of the solution to the stretching force, as the amount of charged particles is decreased [85]. Increasing the solution concentration and viscosity also increases and the competition between viscosity and electrostatic forces appearing in greater fiber diameter. Also at a higher SAN concentration, there is a decrease in the number of beads and a change of shape from spherical to cylindrical was observed (see Fig. 3.1 B and C). At higher polymer concentrations, one can suppose more entanglement of SAN molecules, which prevent the gathering of solvent molecules. Anyway, the concentration cannot be increased infinitely. At SAN concentrations above 20% in 1,2-DCE and 25% in DMSO solutions dry at the tip of the needle before electrospinning can be initiated. This is caused by the viscosity being too high, which cannot be overcome by electrostatic repulsive forces [16]. At the same time, solvent evaporation from the surface of the droplet on the tip of the needle causes needle clogging. Therefore, the solution concentration of 13% for SAN in 1,2-DCE and 20% for SAN in DMSO was chosen as the most optimal for further experiments.

The solutions of 13% SAN in 1,2-DCE and 20% SAN in DMSO were electrospun at 10-20 kV and 10-20 cm in order to find the most optimal electrospinning variables. All other parameters including pumping rate, ambient parameters *etc.* were constant. It was found, that 20 kV and 20 cm should be used for the continuous and stable electrospinning process of SAN. Fibers were less beaded and had a smaller average diameter at a higher voltage and longer distance.

3.1.2 Effect of IL and its concentration on properties of electrospinning solutions, fiber morphology, and electrospinning process

One of the possibilities to eliminate bead formation in fibers is increasing the stretching force of the electrospinning solution [2]. A literature review showed that the addition of charged particles into the electrospinning solution increases the stretching force of the solution to collector due to the increase of the solution electrical conductivity [86]. Therefore, [Bmim]Cl was chosen as a conductive additive for further experiments. To find out the most optimal amount of IL solutions of different [Bmim]Cl concentrations (0.5 to 20% by weight of SAN) were prepared and electrospun at constant variables. First of all, the impact of the IL and its concentration on solution properties including viscosity and electrical conductivity and consequently on fiber morphology was investigated. The diagrams representing the dependences of solution properties on IL concentration are presented in the Fig. 3.3 and in the Fig. 3.4.

The viscosity of pure SAN solution in 1,2-DCE is 0.174 Pa·s and in DMSO is almost 10 times higher, 1.658 Pa·s. The addition of IL reduces the viscosity of both solutions. The same results were reported for gelatin/[C_2OMIM]BF_4 solutions [87]. This is caused by decreases of the intermolecular interactions resulting from [Bmim]Cl dilution in the solvent [88, 89].

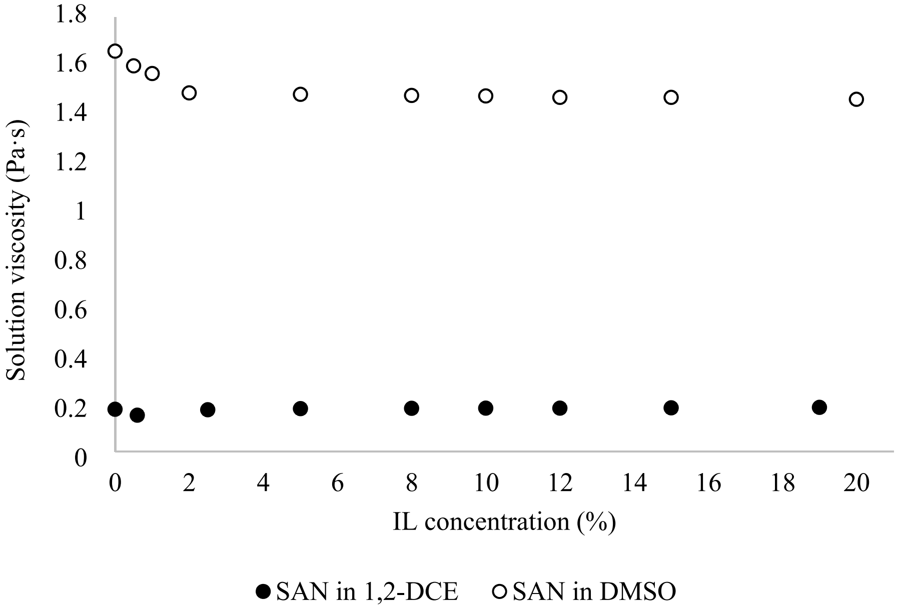

Figure 3.3. Solutions viscosity dependence on the addition of IL (article I and II).

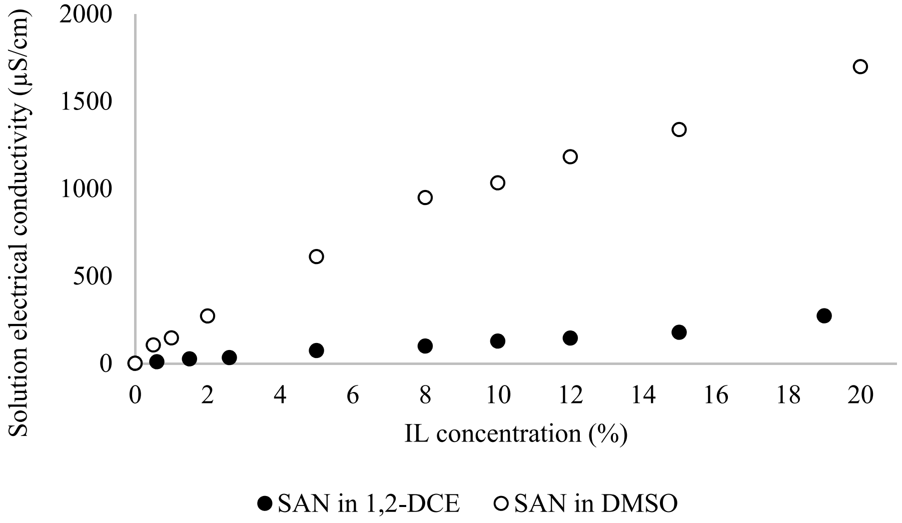

Figure 3.4. Solution electrical conductivity dependence on addition of IL (article I and II).

The results of electrical conductivity measurements of SAN solutions with 0.5 to 20% IL solutions (see Fig. 3.4) show the increase of solution electrical conductivity with an increase of IL concentration. The electrical conductivity of pure liquids was also measured to be 78.3 µS/cm for [Bmim]Cl, for 1,2-DCE it was 0.70 µS/cm and for DMSO it was 0.54 µS/cm. The electrical conductivity of SAN in 1,2-DCE solutions increases from 0.35 µS/cm at 0% up to 272 µS/cm at

19% concentration of the IL. In case of SAN solutions in DMSO the values start at 0.85 µS/cm at 0% and 1698 µS/cm at 20% concentration of IL. The increase of solution electrical conductivity can be explained by the ionic nature of IL. [Bmim]Cl is a salt and consists of a large $[Bmim]^+$ cation and small Cl^- anion. With the addition of [Bmim]Cl into the SAN solutions, the ionic pairs dissociate in solvents, therefore increasing the number of charge carriers.

For both properties, viscosity and electrical conductivity, it was found that solutions of SAN in 1,2-DCE + (0.5-20%) IL have lower values compared to SAN in DMSO + (0.5-20%) IL. This is caused by different chemical and physical properties of the solvents (see APPENDIX B) and as a consequence, by their intermolecular interactions with SAN and the IL.

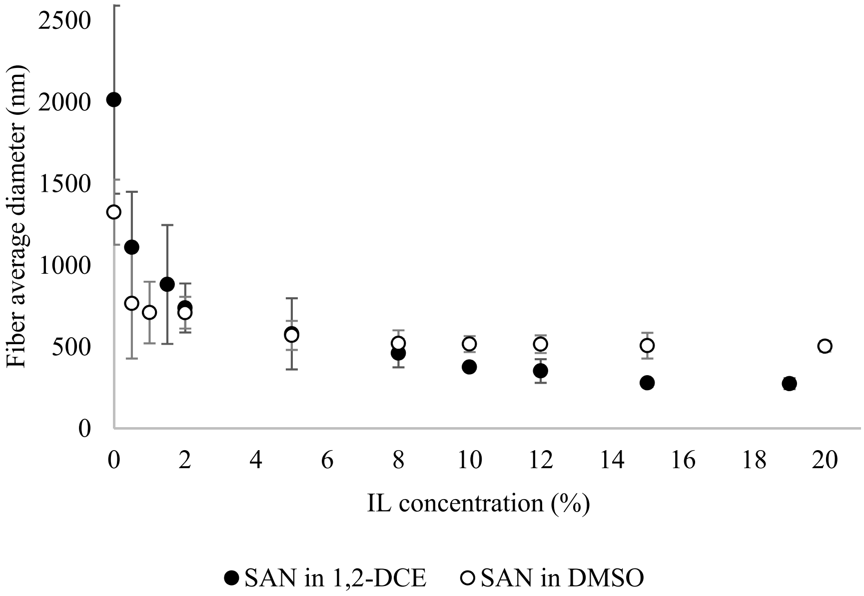

Figure 3.5. Average fiber diameter dependence on addition of IL (article I and II).

After electrospinning, the impact of IL and its concentration on the morphology of the fiber was investigated by SEM and evaluated by calculating the average fiber diameter. One positive impact of IL addition on fiber morphology was the lack of solvent beads. With the addition of at least 1.5% of the IL into the solution of SAN in 1,2-DCE uniform fiber morphology was observed. Secondly, by increasing the IL content, a decrease in the average fiber diameter can be seen in both solvent systems. Finally, with increasing of IL content, fibers are getting more homogeneous in a diameter (see Fig.3.5 and Fig. 3.6). This can be explained by an increase of solution electrical conductivity with an increase of the number of charge carriers (IL ions). This subjects the solution to higher stretching under the electrical field, resulting in the formation of finer fibers with a smoother shape.

In case of solutions with 1,2-DCE, the decrease of the fiber average diameter was 7 times from 2015 nm at 0% down to 275 nm at 19% of IL. For solutions in DMSO, the reduction of the average fiber diameter was only 2.5 times, from 1325 nm at 0% down to 500 nm at 20% of IL. At higher than 20% IL, the process was not stable and safe anymore. Sparks were observed due to the high electrostatic charge and electrical conductivity of the solution. For this reason, the 20% concentration of IL was chosen to be the most optimal for further experiments.

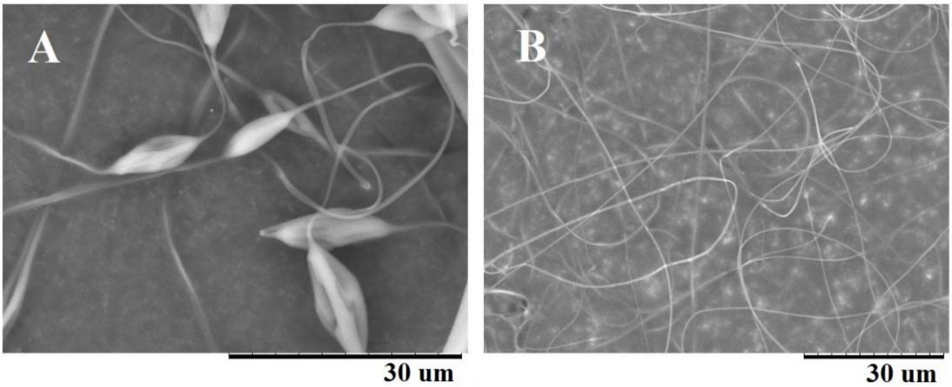

Figure 3.6. SEM micrographs of SAN fibers electrospun from solutions with 1,2-DCE. A: 0% IL, B: 19% IL (article I and article II).

The utilization of the IL in electrospinning also affected the process itself. For example, during the electrospinning experiments it was found that the longest fiber-forming distance at voltages up to 20 kV for a pure 13% SAN solution in 1,2-DCE was 15 cm. With an addition of at least 0.5% of IL the distance increased up to 20 cm. At longer distances, the electrospinning jet has more time to dry into a fiber. The drier the fiber is when it reaches the collector, the less post-processing the membrane needs. The process stability was also improved for solutions in 1,2-DCE. With an addition of 0.5% IL, no needle clogging was observed during electrospinning due to the stronger stretching of the solution in the electrical field because of higher solution electrical conductivity.

3.1.3 Effect of IL and CNTs on properties of electrospinning solutions and fiber morphology

In this subsection, the application of unmodified CNTs in the electrospinning of solutions with and without IL will be discussed. Solutions for the next experiments with the addition of the CNTs were prepared with the application of the ultrasound in an ice bath. At ultrasonic treatment imparts a large amount of energy to the solution and dramatically increases its temperature. Due to that, 1,2-DCE evaporated quickly and the polymer concentration rapidly increased. For this reason, it was decided to continue further experiments only with SAN in DMSO system.

Fig. 3.7 represents the impact of IL and CNTs on the SAN polymer solution viscosity. It can be seen that increasing the content of CNTs increases viscosity in both solution types, with and without IL. This is caused by the dispersion of CNTs into the polymer solution. CNTs are entangled with polymer chains and this increases the solution viscosity. The higher the content of CNTs is, the higher the solution viscosity is. The same phenomenon is described in [90], where the viscosity of PVDF/DMF solutions with various CNTs concentrations was studied.

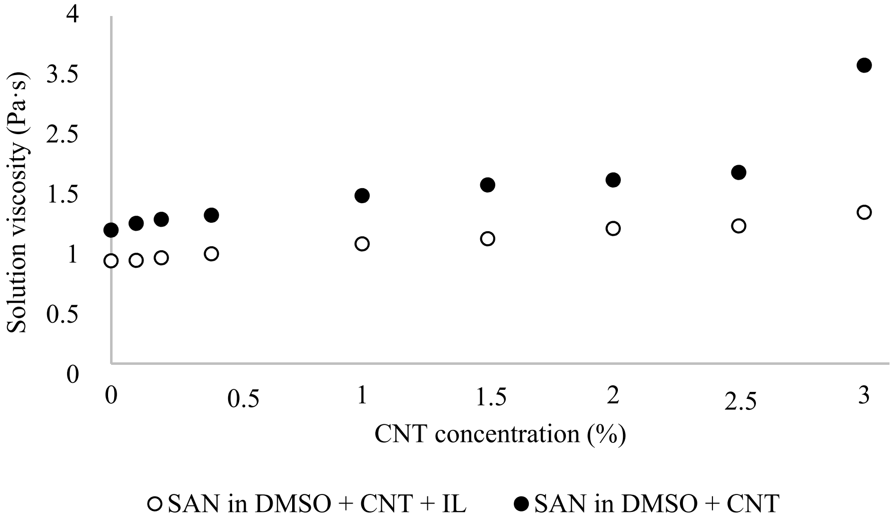

Figure 3.7. Solution viscosity dependence on addition of CNTs (article II).

By comparing the solutions with and without IL it can be seen that solutions with IL have lower viscosity values than the solutions without IL at the same CNT concentrations. IL-free solution viscosity increased from 1.537 Pa·s at 0% CNT up to 3.436 Pa·s at 3% concentration of CNT. At the same time, the viscosity of IL containing solutions increased from 1.184 up to 1.742 Pa·s at the same concentrations of CNT. This is caused by the improved dispersion of CNTs into the polymer solution. This phenomenon is wider discussed in the section 3.2.2. In addition, the decrease of the viscosity of the solutions is related to a decrease of intermolecular interactions resulting from IL dilution in DMSO. The same phenomenon is described by G. Yanfang *et al.* in [89].

While studying the effect of CNT concentration on the electrical conductivity of the solutions, it was found that with increasing of the content of CNTs, the solution electrical conductivity also increases. This is true for both solutions, with and without the IL. This can be explained by the conductive nature of CNTs, thus the higher the CNTs content in the solution is, the higher the solution's electrical conductivity is. However, there is also a difference in three orders of magnitude between electrical conductivity values of the solutions with and without IL, which is explained by ionic nature of IL. There is also a difference in the effect of the addition of CNTs in IL-free and IL containing solutions. The effect of IL and CNTs on solution properties considering preparation technique is discussed in depth below in the section 3.2.2.

3.1.4 Effect of IL and CNTs on properties of electrospun membrane

First, the effect of IL and CNTs on the electrical conductivity of electrospun membrane will be discussed. It was found that the addition of 20% of IL alone increases the electrical conductivity of the membrane from 0 up to 0.244 μS/cm (see Fig. 3.8). This is caused by the conductive nature of IL.

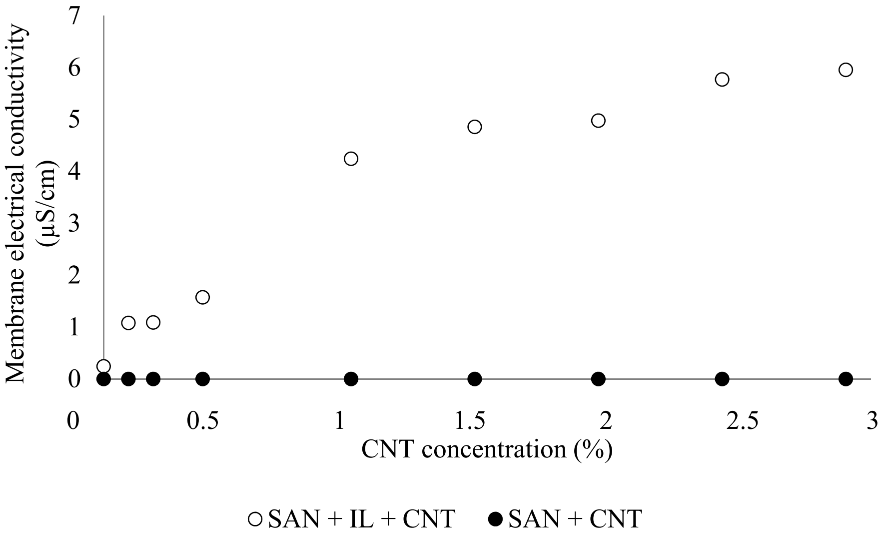

Figure 3.8. Membrane electrical conductivity dependence on addition of CNTs (article II).

The addition of CNTs into pure SAN in DMSO solution does not affect the electrical conductivity of electrospun membranes. The electrical conductivity of all SAN + CNT membranes is below nS/cm range. This phenomenon can be explained by the poor dispersion of CNTs in SAN polymer solution. With the increase of the concentration of the CNTs in SAN + IL membrane, the electrical conductivity of the membrane is also increased. This phenomenon is caused by the role of IL as a dispersant and its conductive nature. The IL creates conductive linkages between separate CNTs and its agglomerates thus making a conductive network inside the SAN polymer fibers.

The effect of CNTs and IL on membranes tensile stress at maximum load was evaluated. The addition of IL increases the tensile stress at maximum load of a SAN membrane from 2 up to 4.8 MPa (see Fig. 3.9). This can be explained by the increase of the electrical conductivity of the solution with the addition of IL. As a result, the stretching force of the solution due to the electrical field increases. This, in turn, promotes the formation of the fibers of smaller average diameter (see Fig. 3.10). The stronger stretching during electrospinning increases the molecular orientation in the obtained fibers results in the higher tensile stress of the electrospun membrane [91].

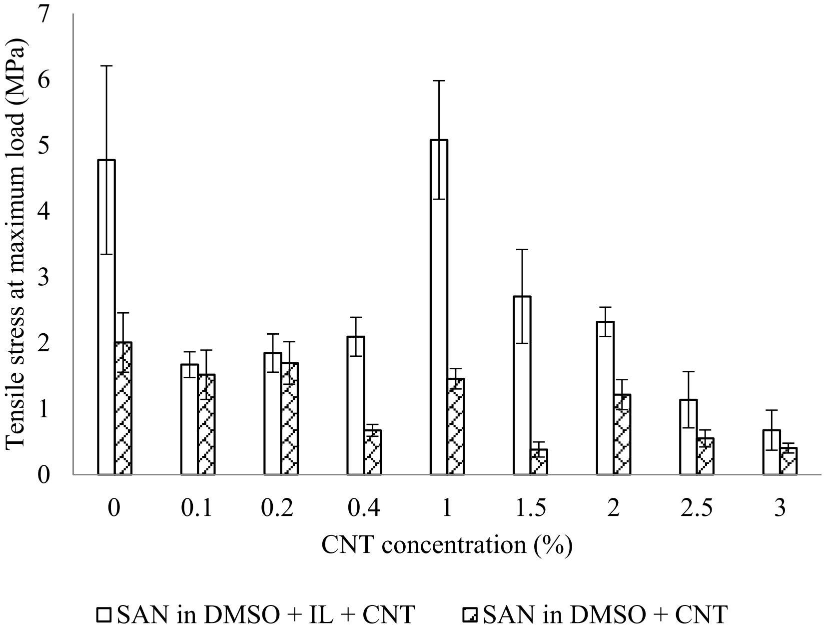

Figure 3.9. Membrane tensile stress at maximum load dependence with the addition of CNTs (article II).

It should be marked that no dependence of membranes tensile stress on the addition of CNTs was found in SAN + CNT membranes. The tensile stress at the maximum load of SAN membranes decreases at all CNT concentrations. This phenomenon is explained by the poor dispersion of CNTs into polymer solutions. The agglomerates of CNTs inside SAN fibers create stress location areas. It results in micro-crack diffusion in the membrane and deterioration of the membrane's mechanical properties [92]. The same is true for all SAN + IL + CNT membranes at CNT concentrations above 1%. The decrease of the membrane's tensile stress at CNTs concentrations above 1% is caused by the repletion of CNTs in the solution. Another reason for the decrease of the tensile stress at the maximum load of SAN + IL + CNT membranes is the increase of solution viscosity with an increase if CNTs concentration is above 1%. At higher viscosity values, electrospinning solutions resist more the stretching by the charges on the jet. As a result, fibers of greater diameter (see Fig. 3.10) are produced, which are weaker [91]. This, in turn, promotes the production of membranes with lower tensile stress at maximum load.

For SAN + IL + CNT membranes it was found, that the tensile stress at maximum load is higher at all CNTs concentrations compared to SAN + CNT membranes. This can be explained by the effect of the IL as a dispersant, which helps to create more uniform dispersion of single CNTs, which reduces the amount and size of agglomerates and therefore improves the strength of the membrane. More detailed discussion about the IL assisted mechanism of the dispersion of the CNTs is presented in the sections 3.2.2 and 3.2.3. Another reason of the increasing of the tensile stress is an increase of polymer solution electrical conductivity with the addition of IL and CNTs, which allows the production of fibers of smaller average diameter. The best result of the tensile stress was achieved for SAN + IL + 1% CNTs membrane, which is 5.1 MPa.

Finally, in this subsection, the effect of IL and CNTs on the obtained fiber morphology will be discussed. It should be noted that no clear dependence between CNTs concentration and fiber average diameter for SAN + CNT membranes was found in this study. However, it was found, that the addition of IL + CNT into polymer solution reduces the average diameter of the obtained fibers until the certain concentration of the CNTs (see Fig. 3.10).

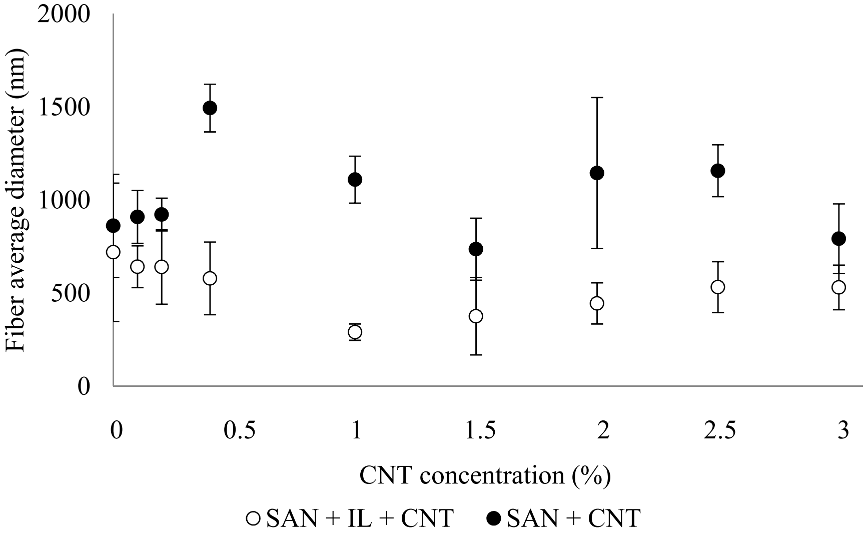

Figure 3.10. Average fiber dimeter dependence on the addition of CNTs (article II).

From the Fig. 3.10 it can be seen that with the addition of CNT, the average fiber diameter decreases to 290 nm at 1% CNTs but increases continuously above this concentration. It was also noted that the deviation of fiber diameter gets smaller until 1% CNTs and again starts growing above this concentration. For these two phenomena, there is one explanation – the counteraction of the solution electrical conductivity and viscosity during the electrospinning process. With the addition of CNTs into SAN in DMSO + IL solution, its electrical conductivity and viscosity increase continuously (see the section 3.1.3). Until 1% of CNTs, the electrical conductivity during electrospinning plays a major role. With the increase of electrical conductivity not only is the stretching of solution increasing, but also the bending instability of the electrospinning jet. Lastly, this means that the deposition area is also increased, which, in turn, promotes higher elongation and favors the formation of finer fibers of lower average diameter [93]. Either way, at concentrations above 1% of CNTs the average fiber diameter and its stability increases. This is caused by the increase of the solution viscosity that starts playing a major role in electrospinning process at these concentrations.

SEM investigations (see Fig. 3.11) showed bead formation in both SAN + CNT and SAN + IL + CNT fibers starting from 1.5% of CNTs. This is possibly due to the unstable process, which was caused by inefficient CNT dispersion. The same phenomenon was observed by J. Xu *et al.* [94]. At higher CNTs concentrations, the amount and size of the agglomerates also increase and thus promoting solution flow instability. Beaded fiber structure can also be reasons for the decreasing tensile stress of the obtained membranes because the shape of single fibers is not uniform.

To summarize, the optimization of the major parameters was performed and the following values were chosen as optimum: voltage 20 kV, distance 20 cm, SAN in DMSO solution concentration 20%, IL concentration 20% by weight of SAN, CNTs concentration 1% by weight of SAN. The main outcome of this section is a decision to move from non-covalent bonding between CNTs and polymer to creation of the covalent bond between them. During the optimization of electrospinning parameters, it was found that the dispersion of CNTs into polymer solutions has a key role in reinforcement of the electrospun membrane. Utilization of the IL as a functional additive for CNTs gave certain results. Membrane electrical conductivity reached μS/cm range. Unfortunately, the tensile stress at maximum load of SAN + IL + CNT membranes is only two times higher, on average, compared to the SAN + CNT values. At the same time, the addition of only CNTs into electrospinning solutions reduces the tensile stress at maximum load of membranes compared to SAN membrane due to CNTs tendency to agglomerate. To overcome this problem, it was decided to create a covalent bond between SAN and CNTs while enhancing the dispersion through that, which will be discussed in the section 3.2.

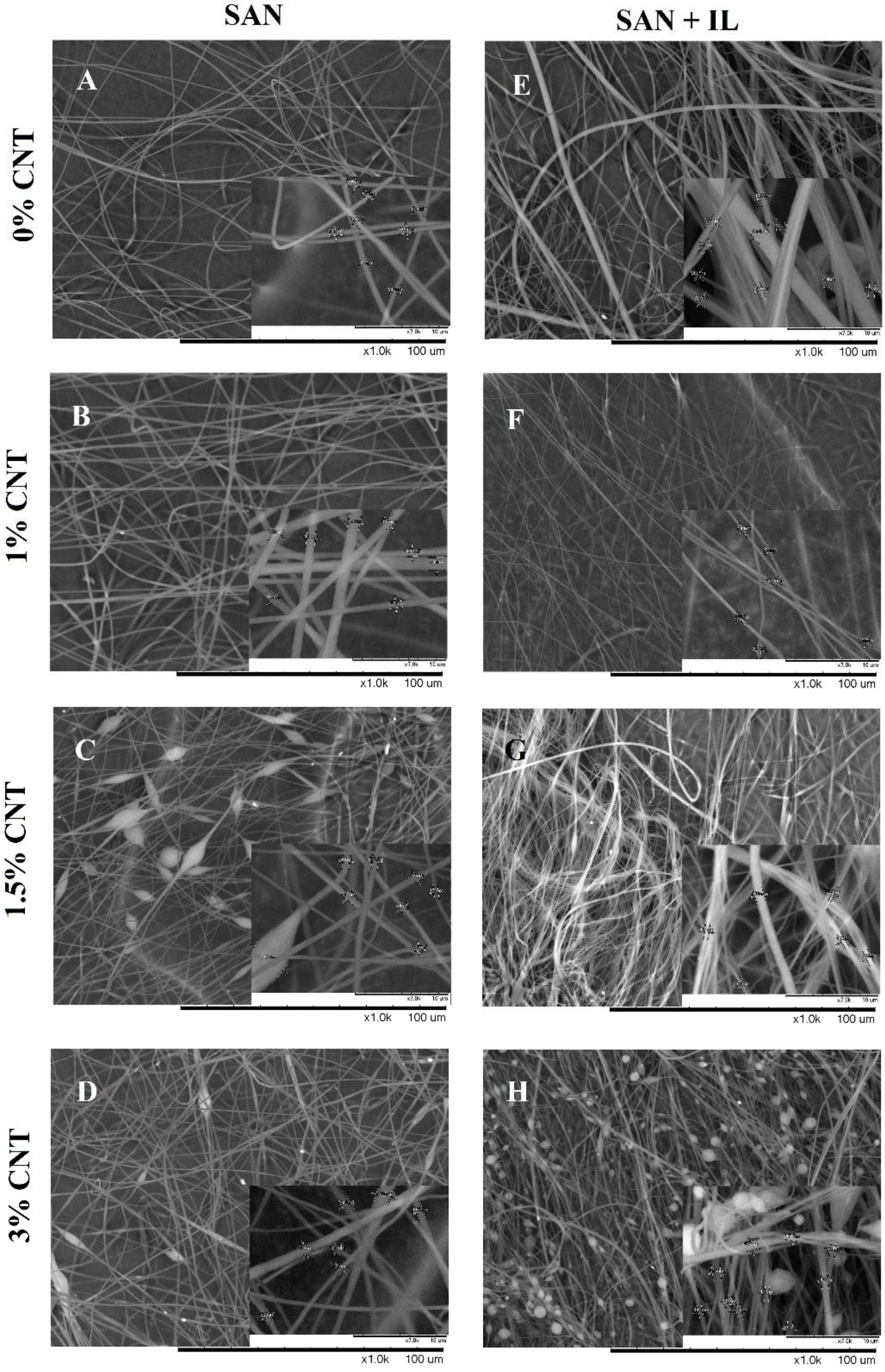

Figure 3.11. SEM micrographs of SAN + CNT (A-D) and SAN + IL + CNT (E-H) fibers.

3.2 CNT grafting with SAN for electrospinning

Reactive melt blending was chosen as an appropriate grafting technology for the creation of SANm-g-CNTs. This research method, which was proposed by J.-H. Shi, *et al.* was modified: unnecessary steps were removed, solvents changed to more efficient, time-consuming filtering was replaced with quick and effective centrifugation. Finally, this new procedure (see section 2.2) was developed for the production of SANm-g-CNTs, which has even more chances to be adopted by the industrial field.

In this section, the creation of covalent bond between CNTs and SAN is discussed. FT-IR, ^{1}H NMR, TGA and TEM were used to confirm the covalent bonds between SANm and CNTs. After the CNT surface modification, the obtained nanotubes were effectively dispersed into SAN in DMSO solution and electrospun. Solutions, prepared with different methods and obtained membranes were carefully studied for electrical, rheological and mechanical properties. All results are presented and compared to unmodified CNTs. The section 3.2 is based on article III.

3.2.1 Characterization of SANm and SANm-g-CNTs

There are a few methods for the preparation of oxazolines by the utilization of amino alcohols. The simplest and cost-efficient method usually involves the reaction of amino alcohol and carboxylic acid [95]. A literature survey showed that at temperatures below 200°C, the rate of a linking reaction is insufficient [96]. At higher temperatures, it was reasonable to make a reaction of SAN attachment to CNTs surface in a melt. The decomposition temperature of SAN is 375°C. SAN is also a thermoplastic polymer. These two properties, in addition to amino functional group, make it a perfect polymer for grafting reaction on CNT-COOHs in a compounder at high temperature.

At first, cyano groups of SAN polymer molecules were reacted with AE in presence of $Zn(Ac)_2$ catalyst. The SANm or oxazoline-modified polymer was formed through this reaction. In order to confirm the formation of oxazoline group, FT-IR spectra of SAN and SANm were recorded and compared (see the Fig. 3.12). The peaks of the mono-substituted C=C bond of the aromatic ring of styrene at 1601 cm^{-1} and C≡N bond of acrylonitrile functional group at 2237 cm^{-1} are present in both spectra of SAN and SANm [84]. But, SANm spectra have an additional strong peak at 1664 cm^{-1}, corresponding to expected oxazoline functional group (vibration of N=C bond). This confirms the formation of new bonds in the SAN molecule [82].

After the oxazoline group forms, the CNT-COOHs were immediately added to SANm in compounder. Grafting reactions between oxazoline groups of SANm and carboxylic groups of nanotubes took place to form covalent bonding and cover CNTs with polymer molecules (see Fig. 3.15). ^{1}H NMR was performed for SANm-g-MWCNTs to confirm the reaction between SANm oxazoline group and carboxylic group on the surface of carbon nanotubes (see Fig. 3.13). The styrene aromatic protons between 6.84 and 7.17 ppm are clearly identifiable. Unfortunately, the solvent peaks are overlapping the acrylonitrile peaks around 2.0-3.5 ppm. Regardless, the signal from styrene units shows, after extensive purification steps, that a grafting reaction took place and the CNTs' surface is covalently coated with SANm.

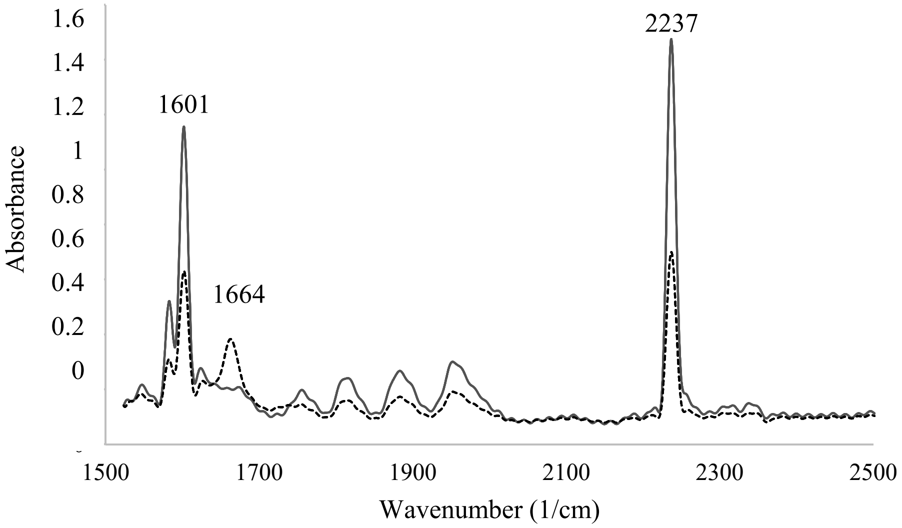

Figure 3.12. FT-IR spectra of SAN (solid line) and SANm (dotted line) (article III).

To characterize the thermal behavior of SAN, SANm, CNT-COOHs, and SANm-g-CNTs to determine the amount of SANm grafted onto CNT-COOHs, TGA was performed (see Fig. 3.14). The TG curve of CNT-COOHs shows a continuous decomposition with the increase of temperature. The same is true for the SANm-g-CNTs at the temperature above 445°C. The continuous decomposition of the SANm-g-CNTs at the temperatures above 445°C can be explained by the decomposition of unreacted –COOH groups on the CNTs and impurities that the CNT-COOHs sample contained. SAN starts to decompose at 375°C and loses its weight completely at 445°C [97]. SANm TG curve is very similar to SAN curve, despite this, SANm starts to decompose at 360°C. The modification reaction of SAN into SANm changed the degradation pathway of polymer molecules and induced decomposition at a lower temperature. In case of SANm-g-CNTs, weight loss starts at the same temperature as SANm, 360°C. This is attributed to the grafted SANm onto the CNTs. The SAN polymer content on the CNTs is about 35 wt%, as estimated by TGA.

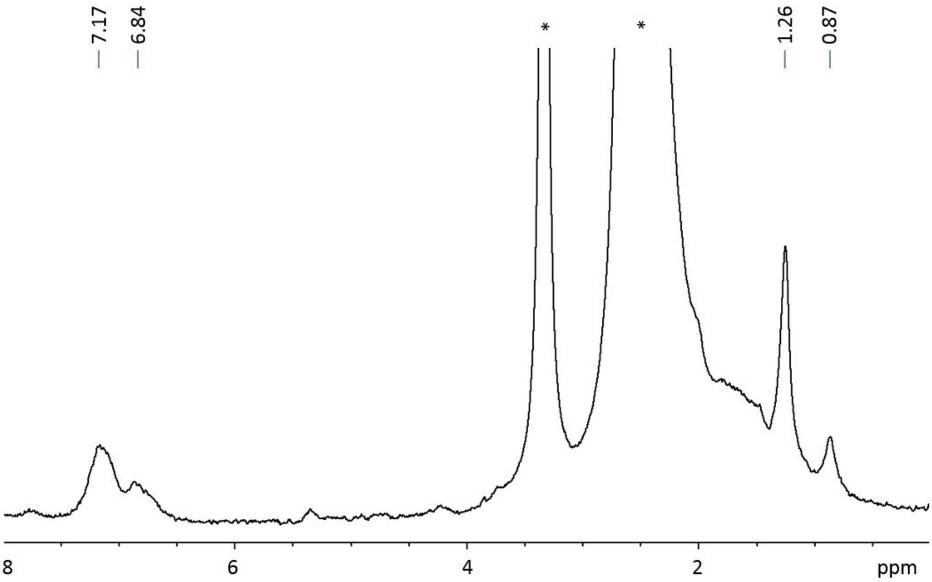

Figure 3.13. ^{1}H NMR spectrum of SANm-g-CNTs in d6-DMSO (article III).

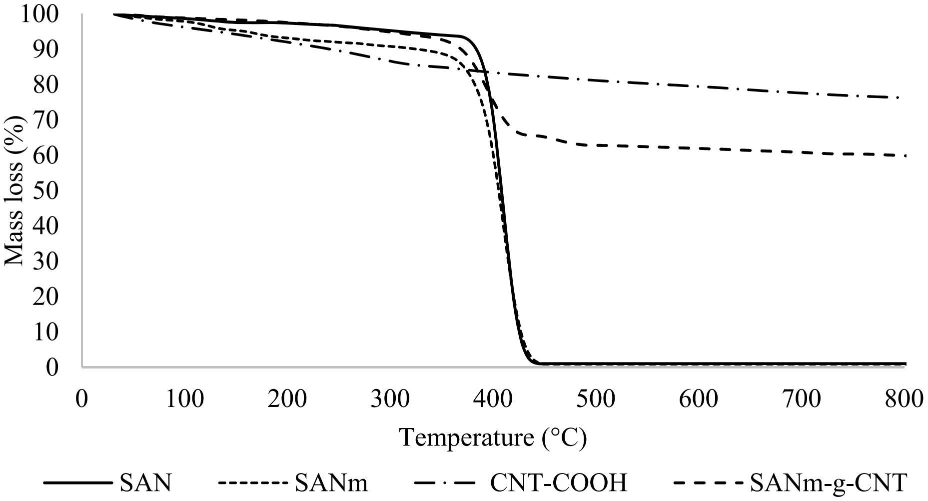

Figure 3.14. TG curves for SAN, SANm, CNT-COOHs and SANm-g-CNTs (article III).

TEM microscopy analysis was performed to confirm the existence of a SANm layer on the CNT surface (see the Fig. 3.15). After CNT grafting with SANm the structure of nanotubes takes a core and shell structure where inside layer is nanotube and outside layer is modified polymer. From the Fig. 3.15, the graphite sheet structure of the inner layer of SAN-g-CNT can be clearly observed. The polymer layer thickness on CNT is near 8 nm.

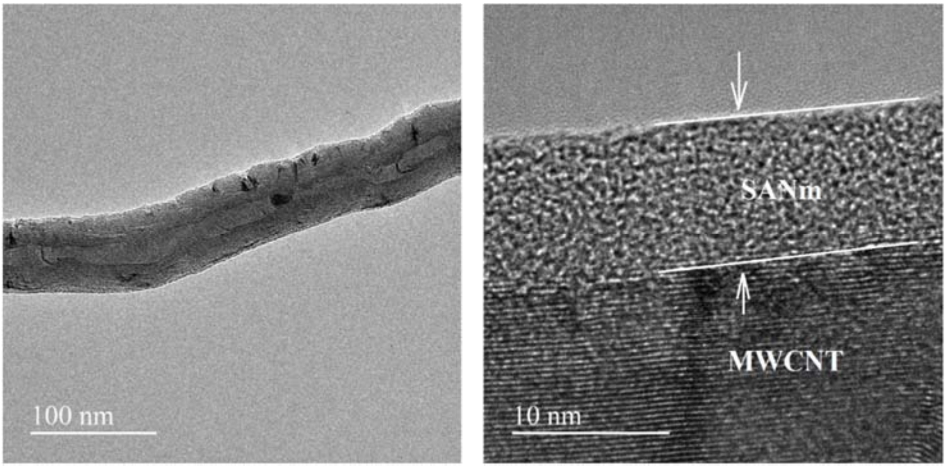

Figure 3.15. TEM micrographs of SANm-g-CNTs (article III).

3.2.2 Effect of CNT grafting with SANm on properties of electrospinning solutions

First, the solution electrical conductivity dependence on the addition of different CNTs and solution preparation method will be discussed. In mechanically mixed solutions, an increase of the electrical conductivity was observed with the addition of CNTs for almost twice compared to pure polymer solutions (see the Fig. 3.16). This is due to the excellent electrical properties of CNTs, which improve the electrical conductivity of polymer solutions.

A difference between mechanically and ultrasonically mixed solutions was discovered. The ultrasonic treatment was used for improving the dispersion of CNTs into polymer solutions. The Fig. 3.16 shows, that the application of ultrasonic treatment increases the electrical conductivity of the solutions compared to mechanically mixed in IL-free systems. The ultrasonication reduces the size and amount of nanotube agglomerates thus helping to enhance the electrical conductivity of the polymer solution [98].

In the article II [99], the positive impact of IL addition on the dispersion of CNTs into electrospinning solutions is discussed. The IL acts as a dispersive agent for CNTs. The size and amount of the agglomerates of the CNTs were reduced with the addition of IL into electrospinning solutions. For this reason, the IL was added, and the same series of the solutions prepared. It was found that addition of IL increases the electrical conductivity of all solutions by three orders of magnitude (see Fig. 3.16) compared to IL-free solutions. This phenomenon is caused by the ionic nature of IL molecules, which was previously discussed in the section 3.1.2.

It was also found that ultrasonic treatment reduces electrical conductivity of SAN in DMSO + IL electrospinning solutions compared to IL-free series. The decrease in electrical conductivity after ultrasonication can be explained by the decrease of electrical conductivity of IL during ultrasonication. The initial electrical conductivity of the IL was 78.3 µS/cm and after 3h of ultrasonication, it reduced to 71.1 µS/cm. The decrease of the electrical conductivity of the IL is caused by oxidative degradation of IL under ultrasonication, which is discussed below [100].

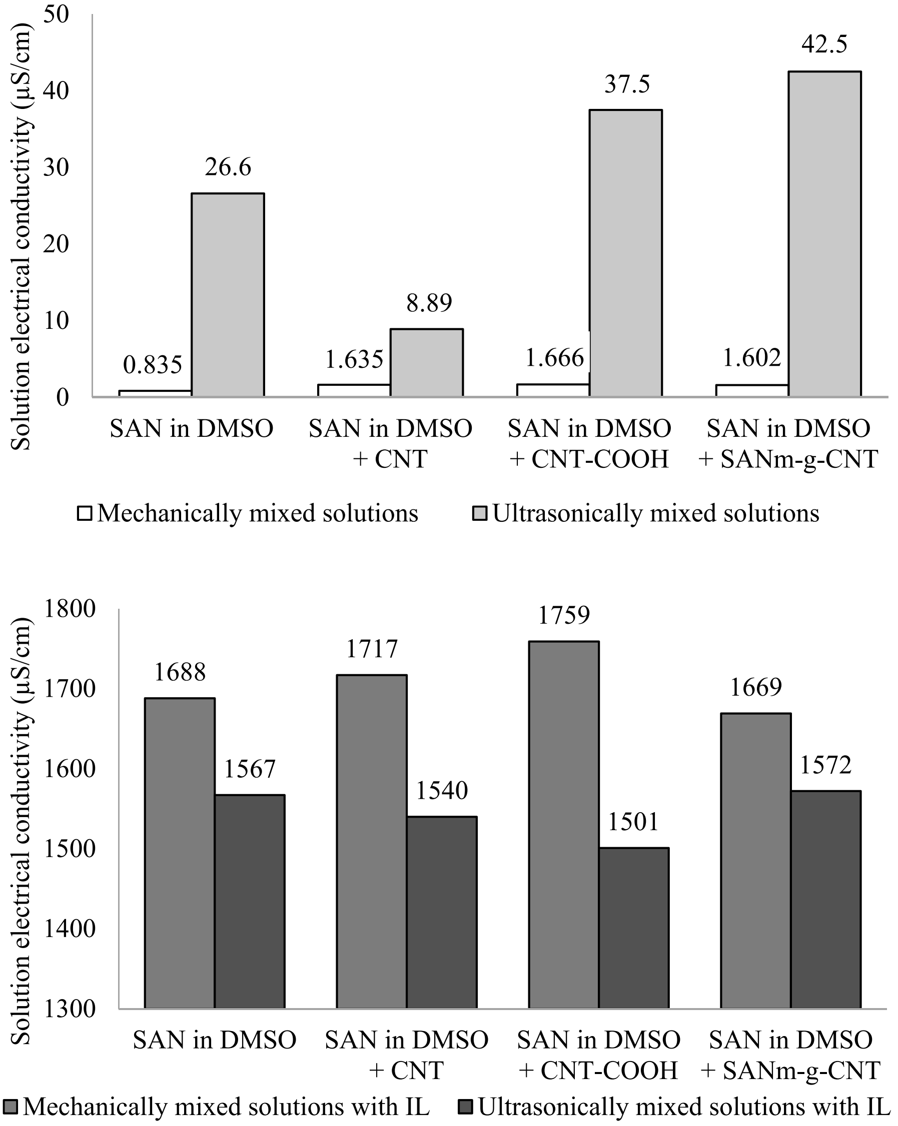

Figure 3.16. Solution electrical conductivity dependence on the addition of different CNTs, IL and solution preparation method (article III).

The literature review and personal experience showed that morphology and consequently mechanical properties of electrospun membrane strongly depend on rheological properties of the electrospinning solutions, especially on viscosity. To evaluate the influence of CNT grafting with the polymer on the solutions, the viscosity was measured at the 100/s shear rate. Results are presented in the Table 3.1.

Table. 3.1. Viscosity of solutions (Pa·s, article III).

	Mechanically mixed	Ultrasonically mixed
SAN in DMSO	2.26	2.12
SAN in DMSO + CNT	2.91	2.90
SAN in DMSO + CNT-COOH	2.31	1.90
SAN in DMSO + SANm-g-CNT	2.50	1.91
SAN in DMSO + IL	0.79	3.58
SAN in DMSO + CNT + IL	2.81	4.93
SAN in DMSO + CNT-COOH + IL	0.87	3.86
SAN in DMSO + SANm-g-CNT + IL	5.80	3.23

A decrease of the solution viscosity was observed in SAN in DMSO, SAN in DMSO + CNT and SAN in DMSO + CNT-COOH solutions with the addition of IL into mechanically mixed solutions. It was previously discussed in the section 1.2.2, that imidazolium ILs can be used to re-bundle the agglomerated CNTs. “Cation-π” interactions between imidazolium ions and a large π-electronic surface of CNTs causes the CNTs to re-bundle [58]. With the addition of the IL into solution, the strong π-π interactions of CNTs are shielded due to the large dielectric constant of ILs that prevent exfoliated CNTs and smaller agglomerates from aggregation [58]. As the dispersion of CNTs into polymer solution was improved by adding the IL the viscosity of mechanically mixed solutions also decreased. Z.Fan and S.G.Advani found the same phenomenon while the study of the rheology of MWCNTs suspensions [101]. The viscosity is known as a fluid's resistance to flow. The viscosity of pure IL is lower compared to the viscosity of SAN in a DMSO solution. For this reason, it acts as a lubricant in solutions. The decrease of the viscosity of the solutions with the addition of IL can be also explained by the decrease of intermolecular interactions resulting from IL dilution in DMSO [89].

Alternatively, the viscosity of the mechanically mixed solution with SANm-g-CNTs increases with the addition of IL. This effect can be explained by covalent grafting of CNTs by the polymer. During current research, it was found that [Bmim]Cl has poor compatibility with SAN and SANm: pure SAN and SANm do not dissolve in pure IL. Due to this fact, IL ions can reach only the ungrafted surface of SANm-g-CNTs. Therefore, IL cannot play the role of dispersant for solutions with SANm-g-CNTs. For the current moment, no explanation was found for this phenomenon. No relevant literature was found for a better explanation of interactions between SAN and SANm, SAN and IL, or SANm and IL. More precise rheological research is needed to explain this effect.

The effect of ultrasonic treatment on electrospinning solutions viscosity will be now discussed. In IL-free solutions, viscosity decreases after ultrasonication. During the ultrasonic treatment, more energy is applied to solutions thus increasing the dispersion of CNTs and consequently, a decrease of the viscosity value is observed. The similar results were observed in the study of Y. Y. Huang *et al.* in [50]. Authors found that high-energy ultrasonication during mixing dispersed CNTs into a polymer matrix is better and consequently, the viscosity reduces.

However, the opposite effect of ultrasonication was observed in all IL containing solutions: the viscosity increases after ultrasonication. The reason may be in the increase of viscosity of IL itself during ultrasonication. The viscosity of pure IL before and after ultrasonication was measured. Obtained values are 0.97 and 1.38 Pa·s respectively. During the oxidative degradation under ultrasonication, some ions are degraded. Consequently, not all degraded ions have lower mobility in solution [100]. Due to this reason, the decrease of the electrical conductivity and increase of the viscosity of IL containing solutions under ultrasonic treatment are observed.

3.2.3 Effect of CNT grafting with SANm on properties of electrospun membrane

First, it should be marked that electrospinning of mechanically mixed SAN in DMSO + IL + CNT solution was not stable. No continuous fibers were produced for the evaluation of membrane mechanical and electrical properties. Due to this reason, this membrane is excluded from the further discussion.

The results of electrical conductivity measurements described in 3.1.4 were confirmed: the electrical conductivity of all membranes without IL is below nS/cm. Grafting of CNTs with SANm also did not affect the electrical conductivity of SAN + SANm-g-CNTs membrane. Once again, the utilization of IL increases the electrical conductivity of the membranes up to the µS/cm range. It was noted that the electrical conductivity of mechanically mixed SAN + IL and SAN + IL + SANm-g-CNT is almost the same.

The results that are more interesting were achieved by ultrasonic treatment: an electrical conductivity decrease was observed in pure SAN + IL and SAN + IL + CNT-COOH membranes (see Fig. 3.17). This can be caused by a decrease in electrical conductivity of IL itself during ultrasonication. Alternatively, the electrical conductivity of SAN + SANm-g-CNT membrane increased with the application of ultrasound as a mixing technique to the electrospinning solutions. This phenomenon can be caused by the grafting of SANm on CNTs. SANm-g-CNTs disperse easily compared to ungrafted ones due to the polymer which is covalently bonded to CNTs surface. Better dispersion of CNTs ensures the enhancement of the electrical conductivity of the electrospun membrane overcoming the observed decrease in conductivity of IL itself.

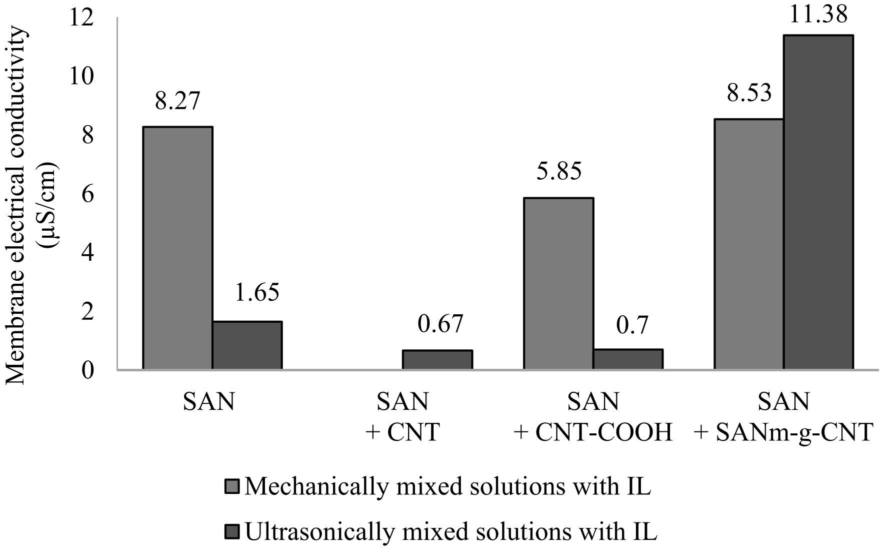

Figure 3.17. Membrane electrical conductivity dependence on addition of different CNTs, IL and solution preparation method (article III).

The effect of CNTs grafting, IL and ultrasonic treatment on membrane mechanical properties will be discussed. First, the effect of CNTs grafting by SANm on membrane mechanical properties should be evaluated. The SAN membrane has the lowest tensile stress at maximum load and modulus. With the addition of different CNTs, the tensile stress and modulus of SAN membranes increase from 0.18 and 5.2 MPa up to 0.43 and 9.7 MPa for SAN + CNT, up to 1.31 and 41 MPa for SAN + CNT-COOH, and up to 2.91 and 72 MPa for SAN + SANm-g-CNT, respectively (see Fig. 3.18 and Fig. 3.19 mechanically mixed IL-free systems). The addition of CNTs increases mechanical properties of electrospun membranes due to the outstanding mechanical properties of CNTs [102]. Membranes with CNT-COOHs and SANm-g-CNTs have higher tensile stress at maximum load and modulus compared to the unmodified CNTs. According to the literature, all functionalized CNTs provide higher strength than unmodified CNT due to the better dispersion [103] in a certain matrix.

The effect of added IL on mechanical properties of membranes that was described in 3.1.4. was confirmed. The tensile stress at the maximum load and modulus diagrams on the Fig. 3.18 and the Fig. 3.19 show that in both preparation methods, mechanical and ultrasonic mixing, the improvement of mechanical properties was achieved with the addition of IL. As an example, the membrane modulus of mechanically mixed SAN + SANm-g-CNT system increased from 72 up to 420 MPa. The same behavior is true for ultrasonically mixed systems; the increase of membrane modulus was from 110 up to 139 MPa. This is indirectly related to the increase of electrical conductivity of electrospinning solutions, which was described above in 3.1.4 and deeply evaluated by X.-L. Xie *et al.* in [99].

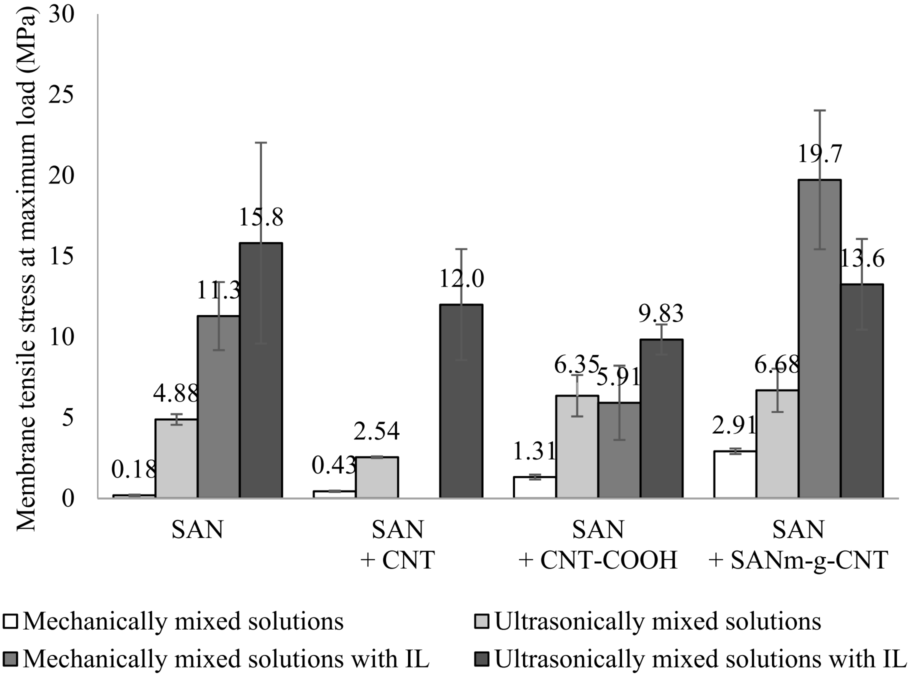

Figure 3.18. Membrane tensile stress dependence on the addition of different CNTs, IL and solution preparation method (article III).

The impact of ultrasonication on mechanical properties of obtained membranes is also shown in the Fig. 3.18 and Fig. 3.19. The tensile stress at maximum load and modulus of the membrane increases drastically with the utilization of ultrasound in IL-free solutions preparation. A higher amount of energy is applied to polymer solution during ultrasonication, which provides better dispersion of CNTs into the polymer matrix. Finally, a better load transfer to the filled network is achieved, resulting in more uniform stress distribution, which in turn enhance the mechanical properties of the composite polymer membrane [82, 4].

During the current study, the opposite effect of ultrasonication was found for polymer-grafted CNTs in presence of IL. It was found that the behavior of SAN + IL + SANm-g-CNT system is opposite to other ones: ultrasonication caused a decrease of the tensile stress and modulus of the membrane. This can be explained by CNTs grafting with SANm. In case of ungrafted nanotubes, IL can easily cover the CNTs. The application of the ultrasound enhances the dispersion of unmodified CNTs and CNT-COOHs. IL is connected to CNTs surface in those systems. For example, during fiber formation when the solvent is evaporated, in dry SAN + IL + CNT and SAN + IL + CNT-COOH membranes IL is distributed on the surface of CNTs and connected by discussed above "cation-π" interactions. Nevertheless, in SAN + IL + SANm-g-CNTs membranes separate nanotubes are covalently bonded to the polymer. This means that the surface of the separate CNTs is fully or partially covered with the modified SAN. Due to this reason, the IL cannot reach the CNT surface fully and play a role of dispersant and the opposite effect appears during ultrasonic mixing in SAN + IL + SANm-g-CNT system.

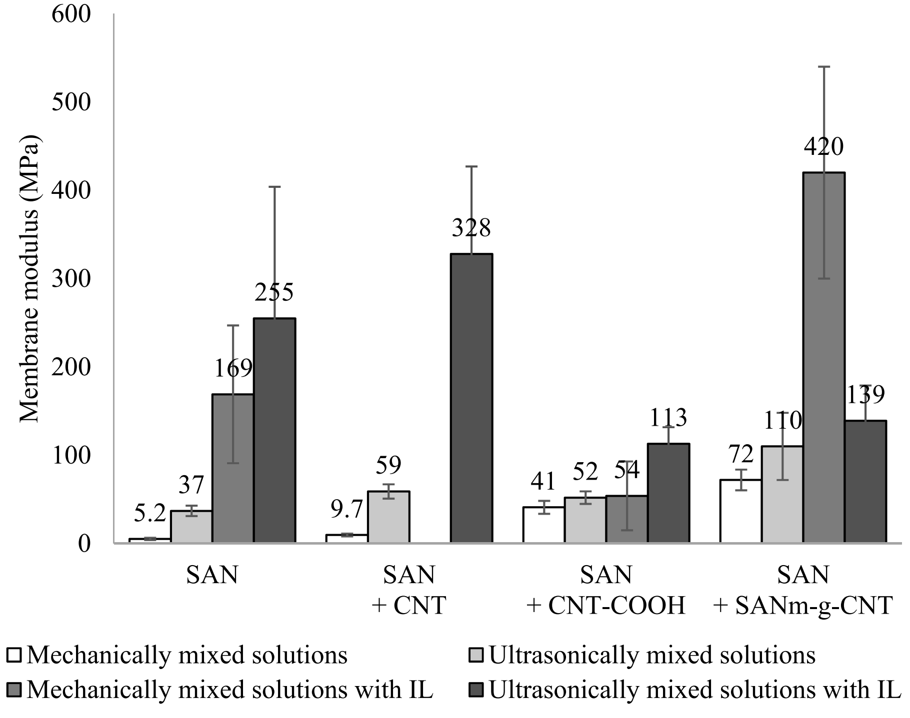

Figure 3.19. Membrane modulus dependence on addition of different CNTs, IL and solution preparation method (article III).

In case of SAN + IL + SANm-g-CNT, the system with two polymers, which are very close but not identical, is formed. Both SAN and SANm do not dissolve in IL. During ultrasonication, a more homogeneous distribution of SAN, IL, and SANm-g- CNTs is achieved in the solution. This means that in the dry SAN + IL + SANm-g-CNT membrane IL is distributed more homogeneously, compared to the membrane electrospun from the mechanically mixed solution. As IL cannot stay on the surface of SANm-g-CNTs, more stress location sites appear in the fiber after ultrasonication of the electrospinning solution. This can cause the decrease of SAN + IL + SANm-g CNTs membrane mechanical properties after ultrasonication of electrospinning solution. Unfortunately, no relevant literature about SAN(SANm)/IL fiber structure after mechanical stress was found to prove this theory. A deeper study of SAN(SANm)/IL membranes behavior and structure under mechanical stress is needed to experimentally confirm this theory.

Finally, it can be concluded, that the best mechanical and electrical properties were achieved by utilization of SANm-g-CNTs and IL. Membrane mechanical properties increased by two orders of magnitude compared to SAN membranes.

In comparison to membranes with unmodified CNTs and CNT-COOHs, the increase was two times in average. From one point of view the IL and SANm-g-CNTs together enhance the electrical conductivity of the electrospinning solution and affect membrane morphology and mechanical properties of the membrane. From another point of view, the covalent bonding of SANm to CNT-COOHs provides better dispersion of CNTs into the polymer matrix. A uniform load transfer in the final product is reached through this and the material strength properties are enhanced.

The morphology of the obtained fibers was carefully studied by SEM. Illustrative pictures are presented in the Fig. 3.20 and in the Fig. 3.21. The average fiber diameter was calculated (see the Fig. 3.22) and the dependence of the average fiber diameter in the addition of different CNTs, IL and the application of different mixing techniques was analyzed. Ultrasonication was found to have certain effects on fiber morphology. In IL-free membranes, smoother fibers of lower average diameter can be produced with the ultrasonic mixing of electrospinning solutions. This is explained by an increase of the the solution’s electrical conductivity. However, as evident from Fig. 3.22, in case of IL containing solutions, the effect of ultrasound on fiber average diameter is weaker compared to IL-free systems. Comparing membranes with and without IL shows that the addition of IL decreases fiber average diameter. It should be also marked that SAN and SAN + SANm-g-CNT membranes average diameter dependence on the addition of IL and ultrasonic treatment is the same: a systematic decrease. This can be explained by the formation of a covalent bond in SANm-g-CNTs between CNTs and SANm, which helps the CNTs act as integrated part of polymer solution during electrospinning.

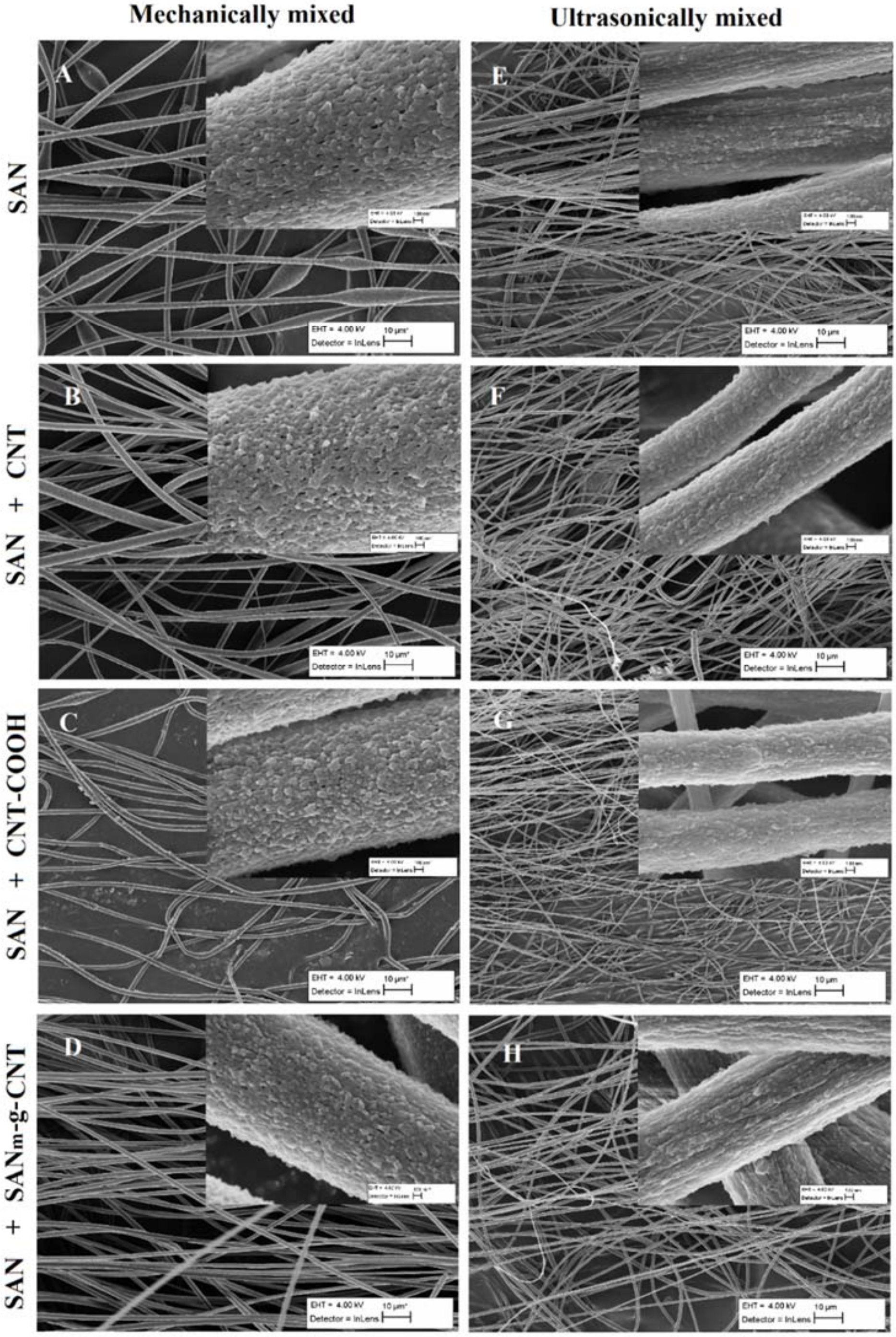

Figure 3.20. SEM micrographs of SAN fibers with different CNTs electrospun from mechanically (A-D) and ultrasonically (E-H) mixed solutions (article III).

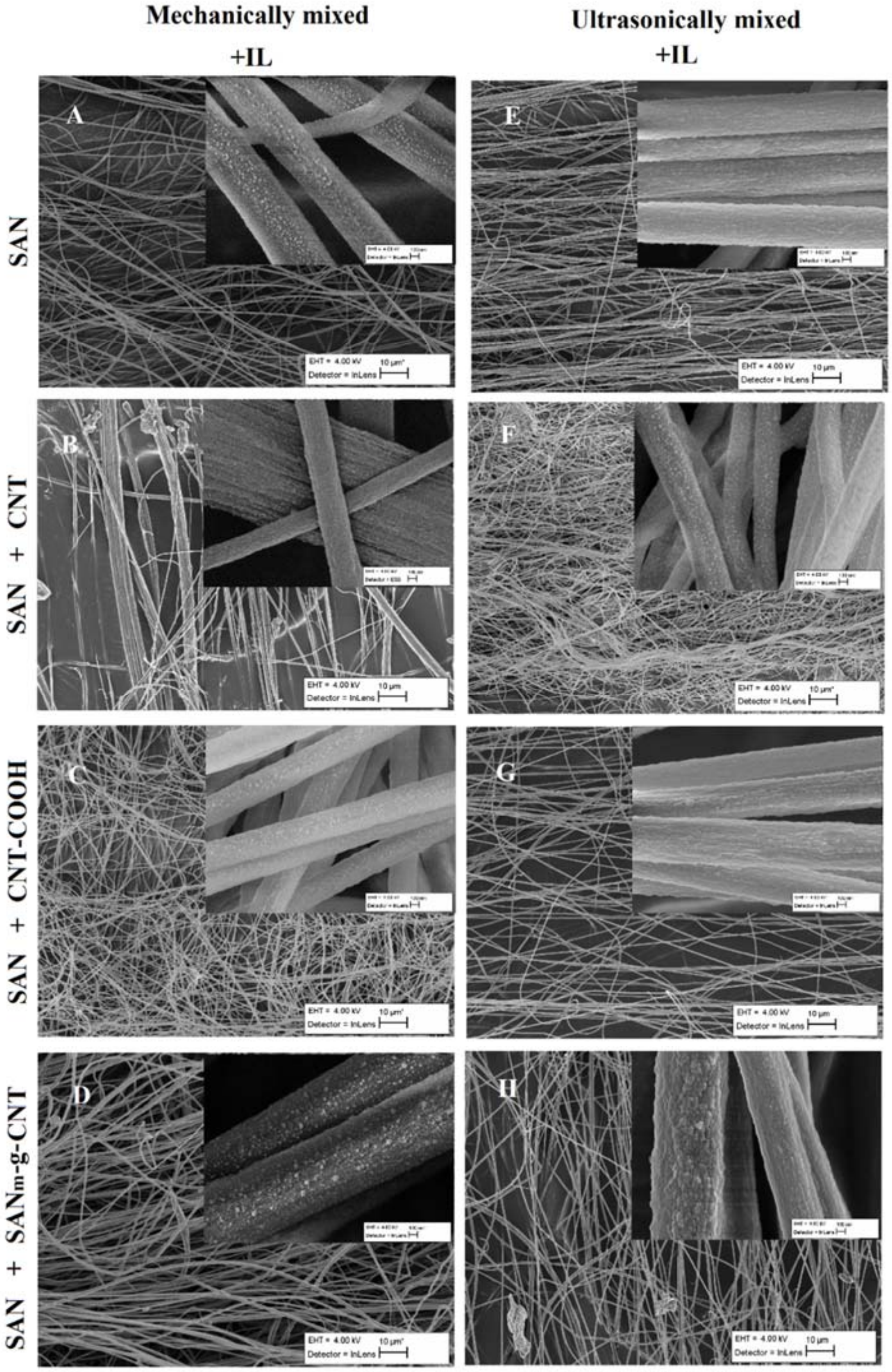

Figure 3.21. SEM micrographs of SAN fibers with IL and different CNTs electrospun from mechanically (A-D) and ultrasonically (E-H) mixed solutions (article III).

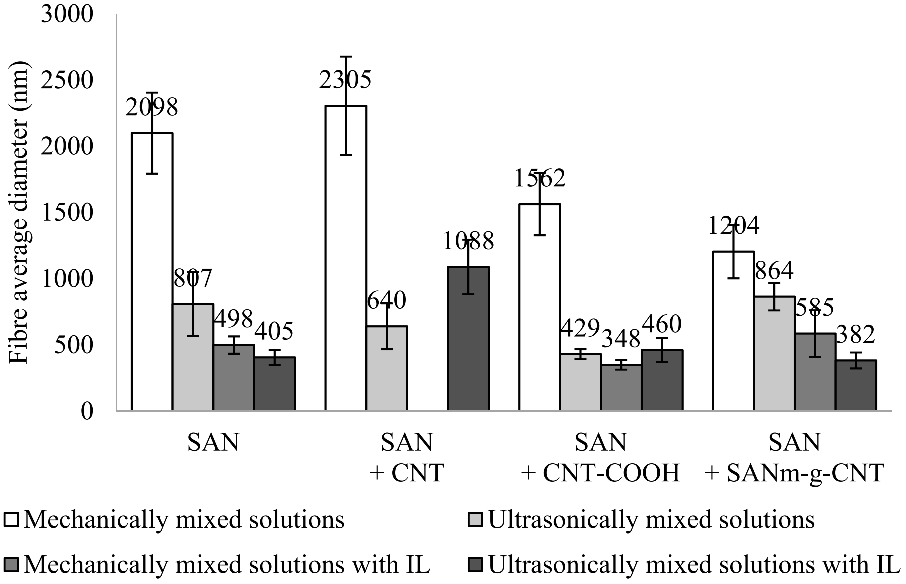

Figure 3.22. Fiber average diameter dependence on the addition of different CNTs, IL and solution preparation method (article III).

During the current research, it was also found that obtained fibers have a porous structure (see Fig. 3.20 and Fig 3.21) which means that volume to weight ratio increases as well. According to the literature review, porous fibers can be formed using phase separation [104]. If the electrospinning solution contains a volatile solvent, rapid solvent evaporation occurs and pores appear in the fiber structure as the solvent-rich phase is dried out [105, 106]. In this research, the DMSO was used as a solvent for SAN in electrospinning experiments to prevent this. It has opposing properties, high boiling point and low evaporation speed [107], which make electrospinning of SAN continuous. However, as it is a poor solvent for SAN, a porous structure was obtained. It was not the main aim of this research, but as high porosity is desirable in several applications such as healthcare, energy, environmental engineering and biotechnology, defense and security, the potential application field list for the obtained mats is wider now due to the porous structure of the fiber surface [106].

CONCLUSIONS

Concluding from the research carried out in this thesis, the main outcomes are presented in next paragraphs.

For the electrospinning process, DMSO was chosen as an appropriate solvent for SAN spinning. Because of its low evaporation rate and high boiling temperature the electrospinning process was continuous unlike with 1,2-DCE. Also, solutions with DMSO can be electrospun at higher polymer concentrations compared to 1,2-DCE, which is always preferable from an environmental point of view. At higher polymer concentrations, the fibers have more uniform less-beaded cylindrical shape.

The influence of IL on the SAN solution properties as electrical conductivity and viscosity of the SAN + (0-20%)IL solutions was investigated. The electrical conductivity increases linearly because of the conductive nature of IL. The results of electrical conductivity measurements showed that IL effects stronger electrical conductivity of solutions with DMSO. Despite low electrical conductivity of IL itself, which is 78.3 µS/cm, the electrical conductivity of SAN in 1,2-DCE solutions increases up to 272 µS/cm at 19% of IL. With the addition of 20% of the IL into SAN in DMSO solution, the electrical conductivity increased up to 1698 µS/cm. The addition of IL into SAN solutions caused a decrease of the viscosity of solutions. However, at all IL concentrations, the viscosity of solutions with DMSO is almost 10 times higher compared to solutions with 1,2-DCE. The described differences of solution electrical conductivity and viscosity are caused by different chemical and physical properties of solvents and, as a consequence, their intermolecular interactions with SAN and IL.

The IL and its concentration have a notable effect on the morphology of electrospun fibers. No solvent beads were observed with concentrations ≥1.5% of IL. The biggest effect of [Bmim]Cl was observed on fiber morphology. With the addition of 0.5% of IL fiber diameter decreases by almost half and at 20% of IL, it reduces seven times compared to pure SAN fibers.

The impact of CNTs on the properties of SAN polymer solutions and membranes with and without IL was studied. CNTs increase viscosity in both solution types, with and without IL. Nevertheless, the viscosity of SAN in DMSO + IL + CNT is lower at the same CNTs concentrations compared to SAN in DMSO + CNT solutions.

As for membranes, it was found that CNTs have different impacts on the electrical conductivity, the tensile stress and fiber morphology of SAN + CNT and SAN + IL + CNT membrane. The electrical conductivity of all SAN + CNT membranes is below nS/cm in the studied range. CNTs do not form any conductive network in pure SAN fibers. The addition of IL creates a conductive network inside the SAN fibers between separate CNTs and their agglomerates and assists the production of membranes with conductivity in μS/cm range. It was also found that CNTs increase the tensile stress of the membrane only in presence of IL. The highest tensile stress of 5.2 MPa was achieved at the CNTs concentration of 1% in presence of IL. It was three times higher than the tensile stress of SAN membrane, but only 0.3 MPa higher comparing to SAN + IL membrane. However, SEM investigation showed that both types of membranes, with and without IL, contain beads at CNTs concentrations over 1.5%. Membranes of SAN + CNT showed no dependence of fiber diameter on the concentration of CNTs. Alternatively, there was a marked clear relation between CNT concentration and fiber average diameter in SAN + IL + CNT membranes. The fiber diameter decreases up to 290 nm at 1% CNTs and increases above this concentration. This is caused by the relation of solutions viscosity, electrical conductivity and applied force during electrospinning.

For increasing the efficiency of CNTs as a reinforcing filler, it was decided to graft their surface with SAN polymer. For this purpose, SAN was modified by reactive melt blending with an oxazoline group to SANm and attached covalently to CNTs surface in a one-step blending procedure. FT-IR confirmed the presence of the oxazoline group. A strong peak at 1664 cm-1 in SANm corresponding to the expected oxazoline functional group (vibration of N=C bond). ^{1}H NMR and TEM confirmed the presence of SANm on the surface of CNTs. According to TGA results, it was estimated that polymer content on the CNTs is about 35wt%. In addition, a modification reaction of SAN into SANm changed the degradation pathway of polymer molecules and induced decomposition at a lower temperature. The process yield was 55%. It should be also marked that proposed method for grafting of CNTs by SANm has many advantages compared to previously reported in literature procedures. It is simple, time efficient and can be easily adopted by industry.

SANm-g-CNTs were effectively dispersed into SAN in DMSO as well as SAN in DMSO + IL solutions and electrospun. Two different methods for solution preparation, mechanical and ultrasonic, were used and compared. Electrospun membranes were studied for electrical and mechanical properties. IL increased solution electrical conductivity by three orders of magnitude on average. Ultrasonic treatment increases solutions electrical conductivity in all IL-free systems because of enhanced dispersion. However, with the application of the ultrasonic treatment to IL containing solutions, the electrical conductivity of all solutions decreased, which can be caused by a decrease in the conductivity of IL. Viscosity measurement showed that SANm-g-CNTs do not cause the significant change in polymer solution viscosity. This is very important for electrospinning process, as solution processing strongly depends on viscosity values.

The highest mechanical strength was achieved in membranes with SANm-g-CNTs. The membrane tensile stress at maximum load and modulus were 16 and 14 times higher compared with pure SAN membrane and 7 times higher compared to ungrafted CNTs and CNT-COOHs. Even more, during the current research, an increase of mechanical strength of two orders of magnitude was achieved by the combination of a grafting method and ultrasonic treatment, which is a very promising result. It was also discovered that the electrical conductivity of SAN membranes could not be increased by only the addition of CNTs. The IL is needed to produce membranes with the electrical conductivity of at least µS/cm range. The last one was achieved by the addition of IL and SANm-g-CNTs with the application of an ultrasonic treatment.

In general, it can be concluded that a combined approach is needed to create SAN/CNTs conductive reinforced membranes. CNTs should be covalently grafted with relevant polymers for effective load transfer between CNT and polymer matrix in final membrane. Conductive additive is needed to create linkages between separate CNTs or their agglomerates inside the electrospun fiber. Finally, ultrasonic treatment is needed to enhance the dispersion of CNTs, IL and as a consequence mechanical and electrical properties of the composite membrane.

ACKNOWLEDGEMENTS

First, I would like to express my deepest thanks to my supervisor professor Andres Krumme for his valuable advice, continuous support and encouragement during this work.

I would like to express my gratitude to my opponents Prof. Heikki Tenhu from the University of Helsinki, Finland and Dr. Jaan Leis from the University of Tartu, Estonia.

The present research was carried out at the Department of Materials and Environmental Technology, Tallinn University of Technology, from 2012-2017. I would like to thank all my colleagues for friendly atmosphere and cosy work conditions. Special thanks to Dr. Elvira Tarasova for fruitful discussions we had. I would also like to thank my students Merit Rikko and Kaia-Kristina Kirikal for assistance with the experiments.

I am grateful to Dr. Tiit Kaljuvee for performing and explanation of TGA results, to Dr. Sami Hietala (University of Helsinki, Finland) for carrying out and interpretation of ^{1}H NMR measurements, to Dr. Valdek Mikli for SEM and to Ph.D. Mihkel Rähn (University of Tartu, Estonia) for TEM analysis. I also would like to thank Dr. James Mendez (Indiana University, U.S.) for revising the language of the manuscript.

I acknowledged the Archimedes Foundation Implementing Agency of Structural Support for its support under grant “CNT Reinforced Electrospun Nano-fibers and Yarns”, no. 3.2.1101.12-0018. In addition, I would like to thank ASTRA “TUT Institutional Development Program for 2016-2022” Graduate School of Functional Materials and Technologies (2014-2020.4.01.16-0032) for giving me the opportunity to attend conferences and meet so many interesting people.

Finally, my warmest thanks are to my family, my daughter Ulyana, my son Timofei and friends for the patient and kind support. My special gratitude belongs to my husband Nikolai for his advice, his patience, and his faith.

ABSTRACT

Electrospinning of a polymer membrane reinforced with carbon nanotubes.

The aim of the current research was to electrospin a reinforced composite polymer membrane. SAN polymer was chosen from the variety of different polymers as a matrix polymer and CNTs were used as the functional additive. CNTs are often utilized for improvement of material properties such as strength, electrical and thermal conductivity for special applications. However, literature survey and personal experience showed there are several problems with CNTs used as filler. For example, poor dispersion of CNTs into the polymer solution and weak interfacial adhesion between CNTs and polymer matrix. The first is limited by agglomeration of CNTs and the second causes inefficient load transfer between the matrix polymer and the CNTs inside the fiber.

In the current dissertation, different approaches were applied to overcome the named problems to achieve the aim. Ultrasonication was applied as a powerful mixing technique to achieve a better distribution of CNTs in electrospun fibers. The IL was used as a functional additive, which improved dispersion of CNTs and created conductive linkages between CNTs. Finally, a new covalent grafting method of CNTs with modified SAN polymer was developed to enhance CNT dispersion and improve interfacial adhesion between CNTs and polymer matrix.

The dissertation is based on three publications. The thesis composes a literature overview, experimental, results, and discussion sections.

In the literature overview, the audience can read about electrospinning and utilization of CNTs. In the subsection dedicated to principles of electrospinning with the scheme of typical setup, variables and their influence on fiber morphology as well as properties and application of electrospun fibers are presented. In the subsection related to CNTs structure, properties and application are briefly described. More attention is given to dispersion methods, especially to the utilization of dispersive agents and the modification of CNTs by the polymer. In the experimental part, all used materials, electrospinning variables, solution preparation conditions, and samples characterization methods are fully described. In addition, a full scheme and a description of new modified SAN grafting to CNTs method are presented.

The section with results and discussion is divided into two subsections. First, a solution optimization procedure is discussed. Based on the solution and membrane properties such as viscosity, electrical conductivity, and the tensile stress, 20% SAN in DMSO with the addition of 1% of the CNTs and 20% of IL were chosen as optimal concentrations. Secondly, an evidence of formation of covalent bonds between modified SAN and CNTs by reactive melt blending are presented. TGA, ^{1}H NMR, FT-IR and TEM results are discussed. Finally, the

effect of IL, CNTs grafting by polymer and utilization of ultrasonication for better CNTs dispersion is deeply discussed.

An outcome of the thesis is an electrospun reinforced SAN/SANm-g-CNTs composite membrane, produced by a combined method. Ultrasonication was used for better dispersion of CNTs, IL – for enhancement of membrane electrical conductivity and CNTs grafting by polymer – for better load transfer between the polymer matrix and CNTs under load. In addition, a new method for the preparation of polymer grafted CNTs was developed. Novel “grafting to” process is simpler, less time consuming and can be easily adopted by industry compared to the previously proposed methods.

KOKKUVÕTE

Süsinik nanotorudega tugevdatud polümeerse membraani elektroketrus

Antud uurimistöö põhieesmärk oli elektrokedrata tugevdatud polümeerne komposiitmembraan. SAN (stüreen-akrüülnitriilkopolümeer) oli valitud maatriksiks ja CNT-sid (süsiniknanotorusid) kasutati funktsionaalse lisandina. CNT-sid kasutatakse tihti selliste materjalide omaduste parendamiseks nagu tugevus, elektri- ja soojusjuhtivus. Seevastu kirjanduse ülevaade ja isiklik kogemus näitasid, et CNT-de kasutamisel lisandina on mõned raskused, näiteks CNT-de kehv dispersioon polümeeri lahuses ja nõrk faasidevaheline adhesioon CNT-de ja polümeerse maatriksi vahel. Esimene probleem on selgitatav CNT-de aglomeratsiooniga, aga teine põhjustab kiu sees ebaefektiivset koormuse ülekandmist polümeerse maatriksi ja CNT-de vahel.

Käesolevas doktoritöös on nimetatud raskuste ületamiseks ja eesmärgi saavutamiseks kasutatud erinevad lähenemisviise. Ultraheli oli rakendatud kui võimsat segamismeetodit, et saavutada CNT-de paremat jaotumist elektrokedratud kius. IL-i (ioonvedelikku) kasutati funktsionaalse lisandina, mille ülesandeks oli parandada CNT-de dispergeerimist ja luua CNT-de vahel juhtiv võrgustik. Lõpuks töötati välja uus meetod kovalentse sideme loomiseks CNT-de ja modifitseeritud SAN polümeeri vahel selleks, et suurendada faasidevahelist adhesiooni.

Antud doktoritöö põhineb kolmel publikatsioonil. Väitekiri koosneb kirjanduse ülevaatest, eksperimentaalsest ja tulemusi kokkuvõtvast osast.

Kirjanduse ülevaates on kirjeldatud elektroketruse meetodit ja CNT-de kasutamise võimalusi. Elektroketruse põhimõttele pühendatud alajaotises on esitatud tüüpilise elektroketrusseadme skeem, elektroketrust mõjutavad faktorid ja nende mõju kiu morfoloogiale. Samas alajaotises on kirjeldatud elektrokedratud membraanide kasutamisalasid. CNT-dega seotud alajaotises on esitatud CNT-de struktuur, nende kasutamisalad ja omadused. Suurem tähelepanu on pööratud CNT-de dispergeerimise meetoditele, dispergeerumist parandavate lisandite kasutamisele ja CNT-de modifitseerimisele polümeeriga. Eksperimentaalses osas on täielikult kirjeldatud kõik kasutatud kemikaalid, elektroketruse tingimused, lahuste valmistamise meetodid, lahuste ja membraanide uurimismeetodid. Samas jaotises on esitatud uus meetod kovalentse sideme loomiseks CNT-de ja modifitseeritud SAN polümeeri vahel ning selle meetodi detailne skeem ja kirjeldus.

Tulemusi kokkuvõttev osa on jagatud kolmeks alajaotiseks. Esmalt on käsitletud lahuste parameetrite optimiseerimist. Lahuste ja membraanide omadusi on selgitatud lähtuvalt viskoossusest, elektrijuhtivusest ja tõmbetugevusest. Leiti, et parim lahuse koostis on 20% SAN polümeeri lahustatuna dimetüülsulfoksiidis koos 1% CNT-de ja 20% IL lisandiga. Teises alajaotises on esitatud tõestus modifitseeritud SAN-i ja CNT-de vahel kovalentse sideme moodustumise kohta. TGA (termogravimeetriline analüüs), ^{1}H NMR (tuuma magnetresonants), FT-IR (Fourier' infrapunaspektroskoopia) ja TEM (läbilaske-elektronmikroskoopia) analüüsi tulemusi on selgitatud. Viimases alajaotises on laialdaselt käsitletud IL-i lisamise, CNT-de polümeeriga katmise ja ultraheliga segamise mõju.

Antud uurimistöö tulemuseks on elektrokedratud SAN/CNT komposiitne membraan, mis oli valmistatud kombineeritud meetodi alusel. Ultraheliga segamist kasutati ja IL lisati paremaks CNT-de dispergeerimiseks polümeerses maatriksis. CNT-d kaeti modifitseeritud polümeeriga, et saavutada parem CNT-de ja polümeerse maatriksi vaheine adhesioon. Elektrokedratud membraanide elektrijuhtivus saavutas tänu IL ja CNT-de lisamisele µS/cm taseme. Väljatöötatud CNT-de SAN-ga katmise meetod on lihtsam, kiirem ning tööstuses kergesti rakendatav.

REFERENCES

[1] Rutledge, G.C., Fridrikh, S.V. 2007. "Formation of fibers by electrospinning." *Advanced Drug Delivery Reviews,* 59: 1384–1391.

[2] Ramakrishna, S. 2005. *An introduction to electrospinning and nanofibers.* Singapore: World Scientific Publishing Co. Pte. Ltd.

[3] Huang, Z.-M., Zhang, Y.-Z., Kotaki, M., Ramakrishna, S. 2003. "A review on polymer nanofibers by electrospinning and their applications in nanocomposites." *Composites Science and Technology*, 8: 2223-2253.

[4] Bhattacharya, M. 2016. "Polymer Nanocomposites—A Comparison between Carbon Nanotubes, Graphene, and Clay as Nanofillers." *MDPI,* 9: 1-10.

[5] Huang, C., Chen, S., Lai, C., Reneker, D.H., Qiu, H., Ye, Y., Hou, H. 2006. "Electrospun polymer nanofibres with small diameters." *Nanotechnology,* 17: 1558–1563.

[6] Bhardwaj, N., Kundu, S.C. 2010. "Electrospinning: A fascinating fiber fabrication technique." *Biotechnology Advances*, 325-347. doi:10.1016/j.biotechadv.2010.01.004.

[7] Boys, C.V. 1887. "On the Production, Properties, and some suggested Uses of the Finest Threads." *Proceedings of the Physical Society,* 9: 8-19. doi:10.1088/1478-7814/9/1/303.

[8] Cooley, J.F. 1902. US Patent US692631 A.

[9] Morton, W.J. 1902. US Patent US705691 A.

[10] Electrospinning – *Elsevier*. "www.scopus.com" (Online: 08.12.2016)

[11] Mitchell, G.R. 2015. *Electrospinning. Principles, practice and possibilities.* The royal Society of Chemistry.

[12] Taylor, G. 1969. "Electrically driven jets." *Proceedings of the Royal Society Series A,* 313: 453-475.

[13] Theron, A., Zussman, E., Yarin, A.L. 2001. "Electrostatic field-assisted alignment of electrospun nanofibres." *Nanotechnology,* 12: 384–390.

[14] Shenoy, S.L., Bates, W.D., Frischb, H.L., Wnek, G.E. 2005. "Role of chain entanglements on fiber formation during electrospinning of polymer solutions: good solvent, non-specific polymer–polymer interaction limit." *Polymer*, 25: 3372–3384. (doi:http://dx.doi.org/10.1016/j.polymer.2005.03.011.)

[15] Manas, C., Salil, K. R. 2007. *Plastics Technology Handbook, fourth edition.* New York: Taylor & Francis Group, LLC.

[16] Li, Z., Wang, C. 2013. *One-dimensional nanostructures. Electrospinning technique and unique nanofibers.* Springer.

[17] Andrady, A.L. 2008. *Science and technology of polymer nanofibers.* New Jersey: John Wiley & Sons, Inc.

[18] Qin, Y. 2010. *Micro-Manufacturing Engineering and Technology.* Oxford: William Andrew.

[19] Tripatanasuwan, S., Zhong, Z., Reneker, D.H. 2007. "Effect of evaporation and solidification of the charged jet in electrospinning of poly(ethylene oxide) aqueous solution." *Polymer*, 26: 5742-5746. doi:http://dx.doi.org/10.1016/j.polymer.2007.07.045.

[20] Subbiah, T., Bhat, G. S, Tock, R. W., Parameswaran, S., Ramkumar, S. S. n.d. "Electrospinning of Nanofibers." *Journal of Applied Polymer Science,* 96: 557–569.

[21] Huang, Z.-M., Zhang, Y.-Z., Kotaki, M., Ramakrishna, S. 2003. "A review on polymer nanofibers by electrospinning and their applications in nanocomposites." *Composites Science and Technology,* 63: 2223-2253.

[22] Reneker, D.H., Yarin, A.L., Zussman, E., XU, H. 2007. "Electrospinning of Nanofibers from Polymer Solutions and Melts." *Advances in Applied Mechanics,* (41): 43-195, 345-346.

[23] Cramariuc, B., Cramariuc, R., Scarlet, R., Manea, L. R., Lupu, G. I, Cramariuc, O. 2013. "Fiber diameter in electrospinning process." *Journal of Electrostatics,* 71 (3): 189-198.

[24] Huang, L., Bui, N.-N., Manickam, S.S., McCutcheon, J.R. 2011. "Controlling electrospun nanofiber morphology and mechanical properties using humidity." *Journal of Polymer Science Part B-Polymer Physics,* 49 (24): 1734–1744.

[25] Chronakis, I.S. 2005. "Novel nanocomposites and nanoceramics based on polymer nanofibers using electrospinning process—A review." *Journal of Materials Processing Technology,* 167 (2-3): 283-293.

[26] Raghavana, P., Zhaoa, X., Kima, J.-K., Manuel, J., Chauhana, G.S., Ahna, J.-H., Nah, C. 2008. "Ionic conductivity and electrochemical properties of nanocomposite polymer electrolytes based on electrospun poly(vinylidene fluoride-co-hexafluoropropylene) with nano-sized ceramic fillers." *Electrochimica Acta,* 54 (2): 228-234.

[27] Wutticharoenmongkol, P., Sanchavanakit, N., Pavasant, P., Supaphol, P. 2005. "Preparation and Characterization of Novel Bone Scaffolds Based on Electrospun Polycaprolactone Fibers Filled with Nanoparticles." *Macromolecular Bioscience,* 6 (1): 70-77.

[28] Shi, Q., Zhou, C., Yue, Y., Guo, W., Wu, Y., Wu, Q. 2012 "Mechanical properties and in vitro degradation of electrospun bio-nanocomposite mats from PLA and cellulose nanocrystals." *Carbohydrate Polymers,* 90: 301-308.

[29] Iijima, S. 1991. "Helical Microtubules of Graphitic Carbon," *Nature,* 354: 56-58.

[30] Saito, R., Dresselhaus, G., Dresselhaus, M.S. 1998. *Physical properties of carbon nanotubes.* London: Imperial College Press.

[31] Properties and Applications of Carbon Nanotubes – *Nanoscience*. “www.nanoscience.com” (Online: 29.08.2017)

[32] Eatemadi, A., Daraee, H., Karimkhanloo, H., Kouhi, M., Zarghami, N., Akbarzadeh, A., Abasi, M., Hanifehpour, Y., Joo, S.W. 2014. "Carbon nanotubes: properties, synthesis, purification, and medical applications." *Nanoscale Research Letters,* 9 (393): 1-13.

[33] Donaldson, K., Poland, C.A., Duffin, R., Bonner, J. 2012. *The Toxicology of Carbon Nanotubes.* Campridge: Cambridge University Press.

[34] Low, I.M. 2006. *Ceramic-Matrix Composites: Microstructure, Properties and Applications.* . Cambridge: Woodhead Publishing.

[35] Zhang, R., Zhang, Y., Zhang, Q., Xie, H., Qian, W., Wei, F. 2013. "Growth of Half-Meter Long Carbon Nanotubes Based on Schulz–Flory Distribution." *ACS Nano,* 7: 6156–6161.

[36] Iijima, S., Ichihashi, T. 1993. "Single-shell carbon nanotubes of 1-nm diameter" *Nature*, 363: 603-605.

[37] Ando, Y., Iijima, S. 1993. "Preparation of Carbon Nanotubes by Arc-Discharge Evaporation." *Journal of Applied Physics,* 32: 107-109.

[38] Che, G., Lakshmi, B.B., Martin, C.R., Fisher, R., Ruoff, R.S. 1998. "Chemical Vapor Deposition Based Synthesis of Carbon Nanotubes and Nanofibers Using a Template Method." *Chemistry of Materials,* 10 (1): 260-267.

[39] Hsu, W.K., Terrones, M., Hare, J.P., Terrones, H., Kroto, H.W., Walton, D.R.M. 1996. "Electrolytic formation of carbon nanostructures." *Chemical Physics Letters,* 262 (1-2): 161-166.

[40] Lebedkin, S., Schweiss, P., Renker, B., Malik, S., Hennrich, F., Neumaier, M., Stoermer, C., Kappes, M.M. 2002. "Single-wall carbon nanotubes with diameters approaching 6 nm obtained by laser vaporization." *Carbon,* 40 (3): 417-423.

[41] Morales, A.M., Lieber, C.M. 1998. "A Laser Ablation Method for the Synthesis of Crystalline Semiconductor Nanowires." *Science,* 279 (5348): 208-211.

[42] Journet, C., Bernier, P. 1998. "Production of carbon nanotubes." *Journal of Applied Physics,* 67: 1-9.

[43] CNT Technology Overview – *Nanoscience*. “www.nanoscience.com” (Online: 29.08.2017)

[44] De Volder, M.F.L., Tawfick, S.H., Baughman, R.H., Hart, A.J. 2013. "Carbon Nanotubes: Present and Future Commercial Applications." *Science,* 339 (6119): 535-539.

[45] Chou, T.-W., Gao, L., Thostenson, E.T., Zhang, Z., Byun, J.-H. 2010. "An assessment of the science and technology of carbon nanotube-based fibers and composites." *Composites Science and Technology,* 70 (1): 1-19.

[46] Wu, Z. et al. 2004. "Transparent, conductive carbon nanotube films." *Science,* 305 (5688): 1273 -1276.

[47] Tans, S.J., Verschueren, A.R.M., Dekker, C. 1998. "Room-temperature transistor based on a single carbon nanotube." *Nature,* 393 (6680): 49 -52.

[48] Huang, Y.Y., Terentjev, E.M. 2012. "Dispersion of Carbon Nanotubes: Mixing, Sonication, Stabilization, and Composite Properties." *Polymers,* 4: 275-295.

[49] Villmow, T., Pötschke, P., Pegel, S., Häussler, L., Kretzschmar, B. 2008. "Influence of twin-screw extrusion conditions on the dispersion of multi-walled carbon nanotubes in a poly(lactic acid) matrix." *Polymer,* 49 (16): 3500-3509.

[50] Huang, Y., Y., Ahir, S., V., Terentjev, E., M. 2006. "Dispersion rheology of carbon nanotubes in a polymer matrix." *Physical Review B,* 73: 125422.

[51] Osorio, A.G., Silveira, I.C.L., Bueno, V.L., Bergmann, C.P. 2008. "$H_2SO_4/HNO_3/HCl$—Functionalization and its effect on dispersion of carbon nanotubes in aqueous media." *Applied Surface Science,* 255: 2485–2489.

[52] Saito, T., Matsushige, K., K.Tanaka, K. 2002. "Chemical treatment and modification of multi-walled carbon nanotubes." *Physica B,* 323: 280–283.

[53] Hirsch, A., Vostrowsky, O. 2005. "Functionalization of Carbon Nanotubes." *Top Curr Chem,* 245: 193– 237.

[54] Datsyuk, V., Kalyva, M., Papagelis, K., Parthenios, J., Tasis, D., Siokou, A., Kallitsis, I., Galiotisa, G. 2008. "Chemical oxidation of multiwalled carbon nanotubes." *Carbon,* 46: 833 – 840.

[55] Vaisman, L., Wagner, H.D., Marom, G. 2006. "The role of surfactants in dispersion of carbon nanotubes." *Advances in Colloid and Interface Science,* 128–130: 37–46.

[56] Weingärtner, H. 2008. "Understanding ionic liquids at the molecular level: Facts, problems, and controversies." *Angewandte Chemie International Edition,* 247: 654-670.

[57] Greaves, T.L., Drummond, C.J. 2007. "Protic ionic liquids: Properties and applications." *Chemical Reviews,* 108: 206-237.

[58] Wang, J.Y., Chu, H.B., Li, Y. 2008. "Why single-walled carbon nanotubes can be dispersed in imidazolium-based ionic liquids." *ACS Nano,* 2: 2540–2546.

[59] Bellayer, S., Gilman, J.W., Eidelman, N., Bourbigot, S., Flambard, X., Fox, D.M., and H.C., Trulove, P.C. de Long. 2005. "Preparation of

homogeneously dispersed multiwalled carbon nanotube/polystyrene nanocomposites via melt extrusion using trialkyl imidazolium compatibilizer." *Advanced Functional Materials,* 15: 910-916.

[60] Shim, Y., Kim, H.J. 2009. "Solvation of carbon nanotubes in a room-temperature ionic liquid." *ACS Nano,* 3: 1693–1702.

[61] Liu, P. 2005. "Modifications of carbon nanotubes with polymers." *European Polymer Journal,* 41 (11): 2693-2703.

[62] Wypych, G. 2012. *Handbook of polymers.* Toronto: GhemTec Publishing.

[63] Chrisochoou, A., Dufour, D. 2003. *Styrenic copolymers.* Shrewsbury: Smithers Rapra.

[64] Hill, D.E., Lin, Y., Rao, A.M., Allard, L.F., Sun, Y.P. 2002. "Functionalization of carbon nanotubes with polystyrene." *Macromolecules,* 35: 9466-9471.

[65] Huang, W., Lin Y., Taylor, S., Gaillard, J., Rao, A.M., Sun, Y.P. 2002. "Sonication-assisted functionalization and solubilization of carbon nanotubes." *Nano Letters,* 2: 231-234.

[66] Lou, X., Detrembleur, C., Sciannamea, V., Pagnoulle, C., Jerome, R. 2004. "Grafting of alkoxyamine end-capped (co)polymers onto multi-walled carbon nanotubes." *Polymer,* 45: 6097-6102.

[67] Xie, L., Xu, F., Qiu, F., Lu, H., Yang, Y. 2007. "Single-walled carbon nanotubes functionalized with high bonding density of polymer layers and enhanced mechanical properties of composites." *Macromolecules,* 40: 3296-3305.

[68] Li, H., Cheng, F., Duft, A.M., Adronov, A. 2005. "Functionalization of single-walled carbon nanotubes with well-defined polystyrene by “click” coupling." *Journal of the American Chemical Society,* 127: 14518-14524.

[69] Jung, Y.C., Sahoo, N.G., Cho, J.W. 2006. "Polymeric nanocomposites of polyurethane block copolymers and functionalized multi-walled carbon nanotubes as crosslinkers." *Macromol Rapid Commun,* 27: 126-131.

[70] Koshio, A., Yudasaka, A.M., Zhang, M., Iijima, S. 2001. "A simple way to chemically react single-wall carbon nanotubes with organic materials using ultrasonication." *Nano Letters,* 1: 361-363.

[71] Yao, Z., Braidy, N., Botton, G.A., Adronov, A. 2003. "Polymerization from the surface of single-walled carbon nanotubes—preparation and characterization of nanocomposites." *Journal of the American Chemical Society,* 125: 16015-16024.

[72] Cui, J., Wang, W.P., You, Y.Z., Liu, C., Wang, P. 2004. "Functionalization of multiwalled carbon nanotubes by reversible addition fragmentation chain-transfer polymerization." *Polymer,* 45: 8717-8721.

[73] Yoon, K.R., Kim, W.J., Choi, I.S. 2004. "Functionalization of shortened single-walled carbon nanotubes with poly(p-dioxanone) by “grafting-from” approach." *Macromolecular Chemistry and Physics,* 205: 1218-1221.

[74] Blond, D., et al. 2016. "Enhancement of modulus, strength, and toughness in poly(methyl methacrylate)-based composites by the incorporation of poly(methyl methacrylate)-functionalised nanotubes." *Advanced Functional Materials,* 16: 1608-1614.

[75] Wang, X., Liu, H., Qiu, L. 2007. "Cationic polymerization of tetrahydrofuran from multiple-walled carbon nanotubes: Preparation and glass transition kinetics." *Materials Letters,* 61: 2350-2353.

[76] Meng, Q.J., Zhang, X.X., Wang, X.C. 2006. "Preparation and characterization of poly-(1, 3-propylene glycol-hexanedioic acid)-functionalized carbon nanotubes." *High Performance Materials,* 19: 451-461.

[77] Philip, B., Xie, J., Abraham, J.K., Varadan, V.K. 2004. "A new synthetic route to enhance polyaniline assembly on carbon nanotubes in tubular composites." *Smart Materials and Structures,* 13: N105-N108.

[78] Funck, A., Kaminsky, W. 2007. "Polypropylene carbon nanotube composites by in situ polymerization." *Composites Science and Technology,* 67: 906-915.

[79] Santhosh, P., Gopalan, A., Lee, K.P. 2006. "Gold nanoparticles dispersed polyaniline grafted multiwall carbon nanotubes as newer electrocatalysts: preparation and performances for methanol oxidation." *Journal of Catalysis,* 238: 177-185.

[80] Datsyuk, V., et al. 2007. "In situ nitroxide-mediated polymerized poly(acrylic acid) as a stabilizer/compatibilizer carbon nanotube/polymer composites," *Journal of Nanomaterials,* 2007: 74769.

[81] Shanmugharaj, A.M., Bae, J.H., Nayak, R.R., Ryu, S.H. 2007. "Preparation of poly(styrene-co-acrylonitrile)-grafted multiwalled carbon nanotubes via surface-initiated atom transfer radical polymerization." *J Journal of Polymer Science Part A: Polymer Chemistry,* 45: 460-470.

[82] Shi, J.-H., Yang, B.-X., Goh, S.H. 2009. "Covalent functionalization of multiwalled carbon nanotubes with poly(styrene-co-acrylonitrile) by reactive melt blending." *European Polymer Journal,* 45: 1002-1008.

[83] Huddleston, J.G., Visser, A.E., Reichert, W.M., Willauer, H.D., Broker, G.A., Rogers, R.D. 2001. "Characterization and comparison of hydrophilic and hydrophobic room temperature ionic liquids incorporating the imidazolium cation." *Green Chemistry,* 3 (4): 156-164.

[84] Hu, G.-H., Scaffaro, R., La Mantia, F. 1998. "Chemical Modification of Nitrile to Oxazoline Functionality on a StyreneAcrylonitrile Copolymer in the Melt." *Journal of Macromolecular Science, Part A: Pure and Applied Chemistry,* 35: 457-474.

[85] Ki, C.S., Baek, D.H., Gang, K.D., Lee, K.H., Um, I.C., Park, Y.H. 2005. "Characterization of gelatin nanofiber prepared from gelatin–formic acid solution." *Polymer,* 46: 5094-5102.

[86] Lin, T., Wang, H., Wang, H., Wang, X. 2004. "The charge effect of cationic surfactants on the elimination of fibre beads in the electrospinning of polystyrene." *Nanotechnology,* 15: 1375–1381.

[87] Pimenta, A.F.R. et al. 2012. "Electrospinning of Ion Jelly fibers." *Materials Letters,* 83: 161–164.

[88] Walker, M. 1992. *DMSO: Nature's Healer.* New York: Avery Publishing Group Inc

[89] Yanfang, G., Tengfang, W., Dahong, Y., Changjun, P., Honglai, L., Ying, H. 2011. "Densities and viscosities of the ionic liquid [C4mim][PF6]+ N,N-dimethylformamide binary mixtures at 293.15 K to 318.15 K." *Chinese Journal of Chemical Engineering,* 16 (2): 256-262.

[90] Seoul, C., Kim, Y.-T., Baek, C.-K. 2003. "Electrospinning of poly(vinylidene fluoride)/dimethylformamide solutions with carbon

nanotubes." *Journal of Polymer Science Part B Polymer Physics* 41: 1572-1577.

[91] Papkov, D., Zou, Y., Andalib, M.N., Goponenko, A., Cheng, S.Z.D., Dzenis, Y. A. 2013. "Simultaneously strong and tough ultrafine continuous nanofibers." *ACSNano,* 7: 3324-3331.

[92] Zha, J-W., Sun, F., Wang, S-J., Wang, D., Lin, X., Chen, G., Dang, Z-M. 2014. "Improved mechanical and electrical properties in electrospun polyimide/multiwalled carbon nanotubes nanofibrous composites." *Journal of Applied Physics,* 116: 134104 (1-5).

[93] Macossay, J., et al. 2014. "Imaging, spectroscopic, mechanical and biocompatibility studies of electrospun Tecoflex®EG 80A nanofibres and composites thereof containing multiwalled carbon nanotubes." *Applied Surface Science,* 321: 205–213.

[94] Xu, J., Xie, Y., Zhang, H., Ye, Z., Zhang, W. 2014. "Fabrication of PLGA/MWNTs composite electrospun fibrous scaffoldsfor improved myogenic differentiation of C2C12 cells." *Colloids and Surfaces B: Biointerfaces,* 123: 907–915.

[95] Frump, J., A. 1971. "Oxazolines. Their preparation, reactions, and applications." *Chemical Reviews,* 71: 483–505.

[96] Plackett, D. 2011. *Biopolymers – New materials for sustainable films and coatings.* United Kingdom: Wiley.

[97] Ma, Y., Pang, Y. 2015. "Mechanism Study on Char Formation of Zinc Acetylacetonate on ABS Resin." *Chinese Journal of Polymer Science,* 33 (5): 772-782.

[98] Lee, J., Kim, M., Hong, C., K., Shim, S., E. 2007. "Measurement of the dispersion stability of pristine and surface-modified multiwalled carbon nanotubes in various nonpolar and polar solvents." *Measurement Science and Technology,* 18: 3707-3712.

[99] Xie, X.-L., Mai, Y.-W., Zhou, X.-P. 2005. "Dispersion and alignment of carbon nanotubes in polymer matrix: A review." *Materials Science and Engineering R,* 49: 89-112.

[100] Gudkova, V., Märtson, T., Rikko, M., Tarasova, E., Savest, N., Viirsalu, M., Krumme, A. 2015. "1-butyl-3-methylimidazolium chloride assisted

electrospinning of SAN/MWCNTs conductive reinforced composite membranes." *Journal of Electrostatics* 78: 11-16.

[101] Ewa, M.S., Malgorzata, C., Stolte, S., Stepnowski, P. 2011. "Stability of Ionic Liquids." *Current Organic Chemistry,* 15: 1974-1991.

[102] Fan, Z., Advani, S.G. 2007. "Rheology of multiwall carbon nanotube suspensions." *Journal of Rheology,* 51: 585-604.

[103] Spitalsky, Z., Tasis, D., Papagelis, K., Galliotis, C. 2009. "Carbon nanotube–polymer composites: Chemistry, processing, mechanical and electrical properties." *Progress in Polymer Science,* 5: 357-401.

[104] Eren, O., Ucar, N., Onen, A., Karacan, I., Kizildag, N., Demirsoy, N., Vurur, O., Borazan, I. 2016. "Effect of differently functionalized carbon nanotubes on the properties of composite nanofibers." *Indian Jorunal of Fibre & Textile Research,* 41: 138-144.

[105] Ramakrishna, S., Fujihara, K, Teo, W., E., Yong, T., Ma, Z., Ramaseshan, R. 2006. "Electrospun nanofibers: solving global issues.," *Materials Today,* 9: 40-50.

[106] Fiber physical structure – ElectrospinTech. "www.electrospintech.com/porousfiber.html" (Online: 11.03.2017)

[107] Dayal, P., Kyu, T. 2006. "Porous fiber formation in polymer-solvent system undergoing solvent evaporation." *Journal of Applied Physics,* 100: 043512-1.

[108] Katsogiannis, K., A., G., Vladisavljevic´, G., T., Georgiadou, S. 2015. "Porous electrospun polycaprolactone (PCL) fibres by phase separation." *European Polymer Journal,* 69: 284-295.

[109] Smallwood, I., M. 1996. Handbook of organic solvent properties. London: Gray Publishing.

APPENDIX A

Article I

Gudkova, V., Krumme, A., Märtson, T., Rikko, M., Tarasova, E., Viirsalu, M. (2014). The impact of 1-butyl-3-methylimidazolium chloride on electrospinning process of SAN polymer solutions and electrospun fiber morphology. *Journal of Electrostatics*, 72, 433−436. (https://doi.org/10.1016/j.elstat.2014.08.003)

Journal of Electrostatics 72 (2014) 433–436

Contents lists available at ScienceDirect

Journal of Electrostatics

journal homepage: www.elsevier.com/locate/elstat

The impact of 1-butyl-3-methylimidazolium chloride on electrospinning process of SAN polymer solutions and electrospun fiber morphology

V. Gudkova*, A. Krumme, T. Märtson, M. Rikko, E. Tarassova, M. Viirsalu

Department of Polymer Materials, Tallinn University of Technology, Tallinn, Estonia

ARTICLE INFO

Article history:
Received 28 July 2014
Accepted 14 August 2014
Available online 2 September 2014

Keywords:
Electrospinning
Ionic liquid
SAN
Fiber
Morphology

ABSTRACT

The aim of this research was to investigate how addition of IL [Bmim]Cl[1] into SAN[2] solution in 1,2-DCE[3] will influence electrospinning variables, stability of process and morphology of obtained nanofibers and find out the appropriate way of utilizing [Bmim]Cl in the electrospinning process. The solutions of pure SAN in 1,2-DCE of different concentrations (10–20%) and solutions with different concentrations (0.5–20%) of IL were spun at different variables (10–20 cm and 10–20 kV). All results were investigated by optical and SEM microscopy. Also solution parameters like electrical conductivity, surface tension and viscosity were measured and their effect on the obtained fibers morphology estimated.

1. Introduction

Electrospinning is a fascinating fiber formation method that creates nanofibers through an electrically charged jet of polymer solution or polymer melt [4]. The advantages of this fiber formation method are high speed of process, low cost, easy application in production, continuous fiber, easy to achieve nanoscale diameter, flexibility in process parameters [3]. The electrospinning process is governed by many parameters, classified broadly into solution parameters, process parameters, and ambient parameters. Solution parameters include viscosity, conductivity, molecular weight, and surface tension [2]. It was found from the literature that each of these parameters significantly affect the fiber morphology obtained as a result of electrospinning, and by proper manipulation of these parameters we can get nanofibers of desired morphology and diameters [2].

Nanofibrous materials produced by electrospinning have many extraordinary properties, such as very large surface area to volume ratio, flexibility in surface functionalities, and superior mechanical performance (e.g. stiffness and tensile strength) compared with any other known form of the materials [1]. These outstanding characteristics make the polymer nanofibers optimal candidates for many important applications like filter media, nano-sensors, military protective clothing, cosmetic skin mask, tissue engineering scaffolding and industrial application etc. [1,3].

The list of solvent/polymer systems that can be electrospun is endless. As a basic solution component SAN copolymer was used. SAN copolymer has excellent transparency, high tensile modulus, good rigidity and hardness, high dimensional stability and accuracy, good heat and excellent chemical resistance [6]. The last one is very important in filtering materials that can be produced by electrospinning. Chemical resistant ultrafine SAN fibers can be produced by electrospinning according to the literature [8]. T. Senthil, G. Gibin, S. Anandhan studied electrospinning of SAN in DMSO at different variables and optimized the process. It is known that properties of final products made of SAN strongly depend on styrene (S) and acrylonitrile (AN) ratio in the polymer chain. Strength, stiffness, impact resistance, heat resistance and resistance to stress cracking increase with increasing of the molecular weight or AN content of the copolymer [5]. That is why using SAN copolymer is of interest for future studies. Literature review showed that SAN can be modified by reactive melt blending [10], atom transfer radical polymerization [11] or chemical modification [12]. Modified SAN can react with functionalized carbon nanotubes, modify their surface and help to disperse CNTs in SAN or PAN electrospinning solutions, thus improving mechanical properties of the final product.

Unlike simple inorganic salts (such as NaCl) which often melt at very high temperature, ionic liquids (ILs) are a kind of organic salts

---

* Corresponding author. Ehitajate tee 5, 19086 Tallinn, Estonia. Tel.: +372 56260175.

E-mail address: viktoria.gudkova@ttu.ee (V. Gudkova).

[1] [Bmim]Cl - 1-butyl-3-methylinmidazolium chloride.

[2] SAN - styrene-acrylonitrile copolymer.

[3] 1,2-DCE - 1,2-dichloethane.

http://dx.doi.org/10.1016/j.elstat.2014.08.003
0304-3886/© 2014 Elsevier B.V. All rights reserved.

that are liquid at or near room temperature, always taking 100 °C as an upper limit. So far, ILs have attracted much attention and been widely used as a promising class of green solvents in the field of chemical reactions, organic and material synthesis, solvent extraction and electrochemistry because of their negligible vapor pressure, nonflammability, high thermal and chemical stability, high polarity, wide electrochemical window and tuneable physicochemical properties. The imidazolium cation, especially 1-alkyl-3-methylimidazolium ($C_n mim^+$), is one of the most popular cations [7]. The literature review showed, that ionic liquid 1-butyl-3-methylimidazolium hexafuluorophosphate ($BMIPF_6$) can be used to produce SAN nanofibers as chemiresistors for alcohol vapors [9]. The authors found that addition of $BMIPF_6$ into SAN solution increases electrical conductivity and viscosity of the solution and reduces surface tension which strongly affects fiber morphology.

Motivated by the search of new solvent systems for electrospinning that could reduce the obtained fiber diameter, in this research we studied the impact of 1-butyl-3-methylimidazolium chloride [Bmim]Cl IL on the electrospinning process of SAN polymer solutions, electrospun fiber morphology and solution parameters, such as electrical conductivity, viscosity and surface tension.

To the best of our knowledge, this is the first report on [Bmim]Cl assisted SAN copolymer electrospinning. This opens up new opportunities for the application of [Bmim]Cl as an important additive in electrospinning solutions.

2. Experimental

2.1. Materials

The solutions used in the electrospinning experiments were prepared using SAN, purchased from Polimeri Europa SRL (Italy). All solutions were mixed mechanically at 50 °C using reflux to prevent solvent evaporation. 1,2-DCE was purchased from Merck KGaA (Germany), purity 99.5. [Bmim]Cl was synthesized in the laboratory of the Department of Polymeric Materials, TUT, Tallinn, using the procedure reported in Ref. [13]. In a typical preparation, 1.5 mol of chlorobutan and 1 mol of 1-methylimidazole were mixed in a round-bottomed flask fitted with a reflux condenser and stirred for 3 days at 80 °C. Of the two phases formed, the top phase containing the reagents, was removed by washing several times with ethyl acetate. The yellowish IL product of [Bmim]Cl was further heated to 50 °C under vacuum to eliminate traces of ethyl acetate solvent.

2.2. Electrospinning experiments

All electrospinning solutions were spun from a 1 ml syringe with a medical needle of 0.6 mm diameter. A MK Series power supply (GLASSMAN EUROPE Limited, UK) was used to generate voltages ranging from 0 to 20 kV. Fibers were collected to an aluminum foil flat collector 4 × 4 cm. The distance between the top of the needle and the collector was 10–20 cm in all experiments. To pump the electrospinning solutions, NE-1000 Single Syringe Pump (New Era Pump Systems, Inc.) was used.

2.3. Characterization

Optical micrographs were taken with Axiskop 2 optical microscope (Carl Zeiss Microscopy, LLC). Morphology of the electrospun fibers was analyzed by SEM (TM1000, Hitachi). For each electrospinning solution, surface tension was determined with Dataphysics Contact Angle System OCA 20, electrical conductivity was measured with SevenCompact Conductivity S230 (Mettler Toledo). Solution viscosities were measured with Brookfield Rheometer RVDV II+ (Brookfield eng labs Inc.). Each experiment was performed at standard temperature (23 °C).

3. Results and discussion

3.1. Impact of solution concentration on fiber morphology

To investigate the impact of SAN concentration on fiber morphology, SAN solutions in 1,2-DCE of concentrations from 10 to 20% were prepared and electrospun at different variables: distance 10–20 cm and voltage 10–20 kV. The obtained fibers were studied with optical microscopy (see Fig. 1).

An increase in concentration results in more extensive polymer chain entanglements within the solution which is necessary for maintaining the continuity of the jet during electrospinning [3]. The lowest concentration of SAN in 1,2-DCE for the continuous electrospinning jet to be able to form (see Fig. 1A) is 10%. The evaporation speed of 1,2-DCE was too high and needle was clogged for a few times even at the lowest solution concentration that would be otherwise appropriate for the continuous electrospinning process. With the increasing concentration the diameter of the fiber also increases (see Fig. 1B, C) because of the greater resistance of the solution to the stretching forces caused by the charges on the jet. At a lower concentration, the higher amount of 1,2-DCE molecules and fewer chain entanglements of SAN means that the surface tension of 1,2-DCE is higher than the interaction of solvent molecules with polymer chains and is dominant during the electrospinning process. This promotes beads formation at lower solution concentrations (see Fig. 1A). When the SAN concentration is increased the entanglement of SAN molecules during electrospinning also increased resulting in higher diameter, decreased beads number and change of their shape from spherical to spindle-like. Anyway the concentration cannot be increased infinitely. At 20% concentration the SAN solution dries at the tip of the needle before electrospinning can be initiated because of the high evaporation speed

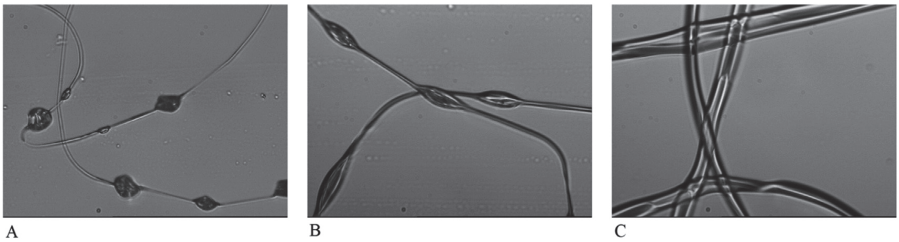

Fig. 1. [A] 10% SAN in 1,2-DCE; [B] 13% SAN in 1,2-DCE; [C] 17% SAN in 1,2-DCE. All fibers are obtained at the same variables: 10 kV and 10 cm (optical microscope, amplification 50×).

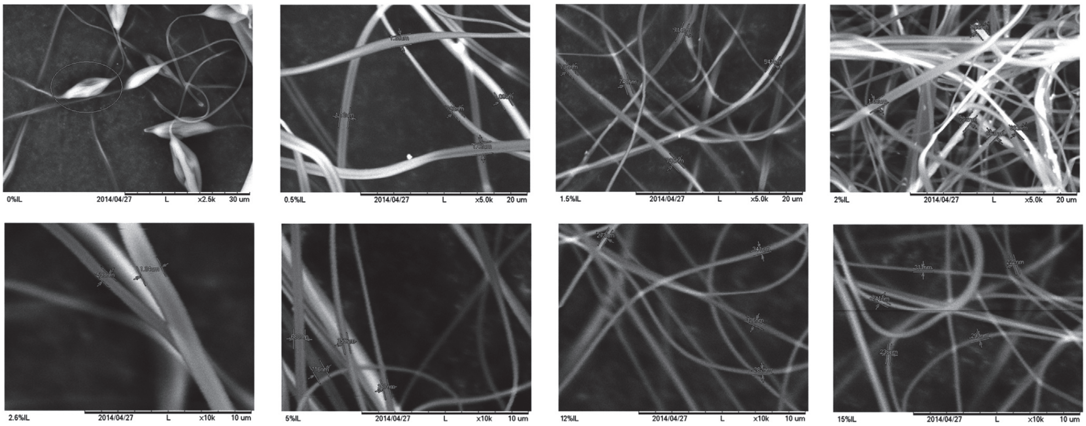

Fig. 2. SEM micrograph of 13% SAN in +1,2-DCE + different concentration of [Bmim]Cl. All pictures are made by SEM. All fibers on pictures are obtained at the same variables: 20 kV and 20 cm.

of 1,2-DCE. Solution concentration 13% was chosen for further research as an optimum.

One of the possibilities to eliminate beads formation in fibers is increasing the stretching force. Addition of charged particles into the electrospinning solution can increase the stretching force of the electrospinning jet. ILs consist of ions and [Bmim]Cl was chosen for further experiments.

3.2. [Bmim]Cl impact on electrospinning conditions of SAN solutions

To investigate the impact of [Bmim]Cl on the stability of the electrospinning process of SAN solution in 1,2-DCE different amounts of [Bmim]Cl (0–20% from SAN content w/w) was added into 13% SAN solution and the obtained solutions were electrospun at the same variables: distance 10–20 cm and voltage 10–20 kV.

During the electrospinning experiments it was found that for pure 13% SAN solution in 1,2-DCE the longest fiber-forming distance at voltages up to 20 kV was 15 cm. With an addition of at least 0.5% of [Bmim]Cl into the solution the distance increased up to 20 cm. With the increasing distance, the electrospinning jet has more time to dry into a fiber. The drier the fiber reaches the collector the less postprocessing the material needs, the less stuck-together are the fibers obtained, the less beads and smaller beads they contain. Process stability was also improved. With an addition of 0.5% [Bmim]Cl no needle clogging was observed during electrospinning.

Both phenomena are related to the increased content of charged particles and, as a consequence, to the electrical conductivity of the solution and the nature of the ionic liquid (see Fig. 3). [Bmim]Cl dissolves easily in 1,2-DCE into two ions $[\text{Bmim}]^+$ and Cl^-. $[\text{Bmim}]^+$ and Cl^- increases the electrical conductivity of the electrospinning solution and at the same time the stretching force to the collector. With an addition of ions the stretching force becomes high enough to overcome the surface tension and to initiate electrospinning. Higher stretching forces prevent the needle from clogging at higher distances. [Bmim]Cl is a nonvolatile liquid and stays in the electrospinning jet during the whole fiber formation process.

3.3. [Bmim]Cl impact on fiber morphology

To investigate the impact of [Bmim]Cl and it's concentration on fiber morphology, 13% SAN solution in 1,2-DCE with an addition of 0–20% of [Bmim]Cl was electrospun at the same variables: distance 10–20 cm and voltage 10–20 kV. The obtained fibers were investigated by optical and SEM microscopy (see Fig. 2.).

3.3.1. Impact of [Bmim]Cl addition on beads formation in SAN fibers and their shape

First positive impact of the addition of [Bmim]Cl on the electrospun fiber morphology was detected during SEM analysis – no solvent beads were observed even with an addition of 1.5% into the solution of SAN (see Fig. 2. 0% and 1.5%). This phenomenon is caused by dissolution of [Bmim]Cl in 1,2-DCE. As [Bmim]Cl is dissolved in 1,2-DCE the electrical conductivity of the solution increases (see Fig. 3). Electrical conductivity of pure SAN solution in 1,2-DCE is 0.35 μS/cm. Addition of 1.5% of IL increases the electrical conductivity of the solution up to 2630 μS/cm. As a consequence the stretching force of electrospinning jet to the collector increases and this in turn prevents beads formation during electrospinning.

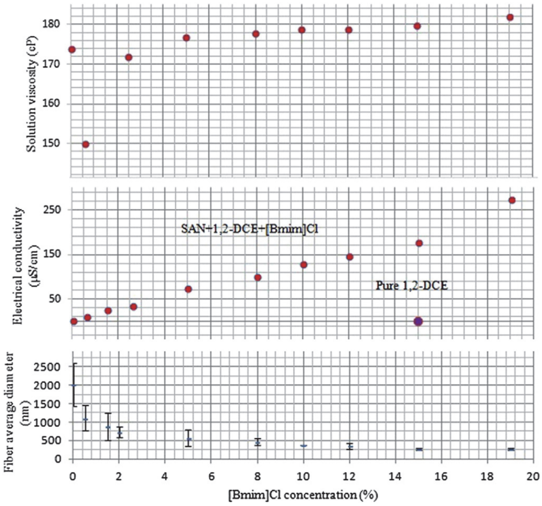

Fig. 3. Dependence of SAN in 1,2-DCE solutions electrical conductivity, viscosity and electrospun fiber diameter on [Bmim]Cl concentration.

The addition of 0.5% [Bmim]Cl changes the shape of the obtained fibers from trode-like to ribbon-like (see Fig. 2. 0% and 0.5%). Ribbon-like shape formation is determined by the presence of liquid components inside the fibers that makes the walls of the fibers stick together from inside.

3.3.2. *Impact of [Bmim]Cl addition on obtained fiber diameter*

Next positive impact of [Bmim]Cl addition into the electrospinning solution is a decrease of the obtained fibers diameter down to nanoscale. From Fig. 3 it can be seen that an addition of at least 0.5% of [Bmim]Cl reduces the obtained fiber diameter almost twice from 2015 nm down to 1110 nm. Addition of 20% of [Bmim]Cl reduces the fiber diameter more than seven times, from 2015 nm down to 275 nm. Sharp reduction in fiber diameter at lower [Bmim]Cl concentrations is caused by the increased electrical conductivity and decreased solution viscosity. From Fig. 3 it can also be seen that with the increasing [Bmim]Cl concentration the diameter fluctuates less.

3.4. *The impact of [Bmim]Cl on surface tension and viscosity of electrospinning solutions*

Surface tension and viscosity of the electrospinning solutions were measured to investigate the impact of [Bmim]Cl on appropriate solution parameters and as consequence on fiber morphology and diameters. Surface tension of pure 13% SAN solution in 1,2-DCE is 21.78 mN/m. Surface tension of 13% SAN+1,2-DCE+20%[Bmim]Cl is 21.36 mN/m. It can be concluded that [Bmim]Cl does not influence the surface tension of SAN solutions in 1,2-DCE at concentrations up to 20%. Fig. 3 represents the impact of [Bmim]Cl on the solution viscosity. From the diagram it can be seen, that an addition of 0.6% of IL reduces the viscosity of the SAN solution abruptly. Viscosity of pure 13% SAN solution in 1,2-DCE is 174 cP and an addition of 0.6% [Bmim]Cl into the solution brings the viscosity down to 150 cP value. With further addition of [Bmim]Cl the viscosity values grow. The growth is fast up to [Bmim]Cl concentration of 2.5% and turns slower and linear from that value on. A.F.R. Pimenta, A.C. Baptista et al. have reported the same results for gelatin/[C2OMIM]BF_4 fibers [14].

4. Conclusions

In this work the impact of [Bmim]Cl on the electrospinning process of SAN polymer solutions and electrospun fiber morphology was studied. We have found that solution concentration, addition of [Bmim]Cl and its concentration in the electrospinning solution have a certain effect on the electrospinning process and fiber morphology. We have found that fiber diameter increases with higher polymer concentration in the solution. Also the number of beads decreases and their form changes from spherical to spindle-like. During the experiments we have found, that the distance between the top of the needle and the collector can be increased with an addition of at least 0.5% of [Bmim]Cl into the electrospinning solution. The process stability is also improved. With the addition of [Bmim]Cl no needle sticking, clogging was observed during electrospinning. [Bmim]Cl and its concentration have a notable effect on the obtained fiber morphology. No solvent beads were observed even with addition of as little as 1.5% into solution. Another effect is the change in fiber shape from trode-like to ribbon-like. And the last and biggest effect is reduction in fiber diameter with very small quantity of [Bmim]Cl. With the addition of 0.5% of [Bmim]Cl fiber diameter decreases almost twice. With the addition of 1.5% of [Bmim]Cl fiber diameter reaches nanoscale. Fibers of the diameter of 275 nm can be produced with the addition of 20% of [Bmim]Cl.

As the solution parameters have a certain impact on the electrospinning process and the obtained fiber morphology, the electrical conductivity, viscosity and surface tension of the SAN + [Bmim]Cl solutions were studied. With an addition of [Bmim]Cl into the solution, the electrical conductivity increases linearly and surface tension almost does not change. The highest impact has been detected on the solution viscosity. At lower IL concentrations in the solution (up to 2.5%) there is a significant drop and race in solution viscosity. With higher [Bmim]Cl concentrations the viscosity grows slowly and linearly.

Acknowledgments

The Archimedes Foundation Implementing Agency of Structural Support is acknowledged for support under grant no. AR12135.

References

[1] Z.-M. Huang, Y.-Z. Zhang, M. Kotaki, S. Ramakrishna, A review on polymer nanofibers by electrospinning and their applications in nanocomposites, Compos. Sci. Technol. 63 (2003) 2223–2253.

[2] N. Bhardwaj, S.C. Kundu, Electrospinning: a fascinating fiber fabrication technique, Biotechnol. Adv. 28 (2010) 325–347.

[3] Ramakrishna, Introduction to Electrospining and Nanofibers, World Scientific Publishing Co, USA, 2005.

[4] G.C. Rutledge, S.V. Fridrikh, Formation of fibers by electrospinning, Adv. Drug Deliv. Rev. 59 (2007) 1384–1391.

[5] A. Chrisochoou, D. Dufour, Styrenic Copolymers, Smithers Rapra, GBR, Shrewsbury, 2003.

[6] G. Wypych, Handbook of Polymers, GhemTec Publishing, Canada, Toronto, 2012.

[7] A. Kokorin, Ionic Liquids: Theory, Properties, New Approaches, InTech, Croatia, 2011.

[8] T. Senthil, G. Gibin, S. Anandhan, Chemical-resistant ultrafine poly(styrene-coacrylonitrile) fibers by electrospinning: process optimization by design of experiment, Polym. Plast. Technol. Eng. 52 (4) (2013) 407–421.

[9] K. Minjae, K. Eunsoo, W.P. Dong, S.S. Bong, E.S. Sang, Ionic liquid/styrene–acrylonitrile copolymer nanofibers as chemiresistor for alcohol vapours, Bull. Korean Chem. Soc. 33 (9) (2012) 2867–2872.

[10] J.-H. Shi, B.-X. Yang, S.H. Goh, Covalent functionalization of multiwalled carbon nanotubes with poly(styrene-co-acrylonitrile) by reactive melt blending, Eur. Polym. J. 45 (2009) 1002–1008.

[11] A.M. Shanmugharaj, J.H. Bae, R.R. Nayak, S.H. Ryu, Preparation of poly(styrene-co-acrylonitrile)-grafted multiwalled carbon nanotubes via surface-initiated atom transfer radical polymerization, J. Polym. Sci. Part A Polym. Chem. 45 (2007) 460–470.

[12] G. Schmidt-Naake, H. Becker, W. Becker, Chemical modification of poly(styrene-co-acrylonitrile) with 2-aminoalcohols and 3-aminoalcohols, Die Angew. Makromol. Chem. 267 (1999) 63–66.

[13] R. Rogers, D. Heather, J. Huddleston, W. Reichert, A. Visser, G. Broker, Green Chem. 3 (2001) 156–164.

[14] A.F.R. Pimenta, A.C. Baptista, T. Carvalho, P. Brogueira, N.M.T. Lourenço, C.A.M. Afonso, S. Barreiros, P. Vidinha, J.P. Borges, Electrospinning of ion jelly fibers, Mater. Lett. 83 (2012) 161–164.

Article II

Gudkova, V., Krumme, A., Märtson, T., Rikko, M., Tarasova, E., Savest, N., Viirsalu, M. (2015). 1-butyl-3-methylimidazolium chloride assisted electrospinning of SAN/MWCNT conductive reinforced composite membranes. Journal of Electrostatics, 78, 11−16. (https://doi.org/10.1016/j.elstat.2015.09.002)

Journal of Electrostatics 78 (2015) 11–16

Contents lists available at ScienceDirect

Journal of Electrostatics

journal homepage: www.elsevier.com/locate/elstat

1-butyl-3-methylimidazolium chloride assisted electrospinning of SAN/MWCNTs conductive reinforced composite membranes

V. Gudkova*, A. Krumme, T. Märtson, M. Rikko, E. Tarasova, N. Savest, M. Viirsalu

Department of Polymer Materials, Tallinn University of Technology, Tallinn, Estonia

ARTICLE INFO

Article history:
Received 7 July 2015
Received in revised form
5 September 2015
Accepted 6 September 2015
Available online 25 September 2015

Keywords:
Composite materials
Electrospinning
Polymers
SEM
Electrical conductivity
Mechanical testing

ABSTRACT

The aim of this research was to investigate how the addition of IL [Bmim]Cl* and MWCNTs** into SAN*** solution will influence the viscosity and the electrical conductivity of the electrospinning solution and to find out the impact of IL and CNTs on the electrical and mechanical properties of the obtained membranes and on the morphology of the produced nanofibres. MWCNTs were added into two types of SAN solutions, with and without [Bmim]Cl, and then electrospinning was performed. All membranes were investigated by SEM analysis. The electrical conductivity and viscosity of the solutions were measured and their effect on the morphology of the fibres, as well as electrical and mechanical properties was estimated.

1. Introduction

Electrospinning is a fascinating fibre formation method that creates nanofibres through an electrically charged jet of polymer solution or polymer melt [1]. The advantages of this fibre formation method are high speed of process, low cost, easy application in production, continuous fibre, easy to achieve nanoscale diameter, flexibility in process parameters [2]. The electrospinning process is governed by many solution, process and ambient parameters. It was found from the literature that each of the solution parameters, which include viscosity, conductivity, molecular weight and surface tension, has a significant impact on the morphology of the fibres and on the properties of the material obtained. By proper manipulation of these parameters membranes of desired structure and properties can be electrospun [2].

Nanofibrous materials produced by electrospinning have many extraordinary properties, such as very large surface area to volume ratio, flexibility in surface functionalities, and superior mechanical performance (e.g. stiffness and tensile strength) compared with any other known form of materials [3]. These outstanding characteristics make the polymer nanofibres optimal candidates for many important applications like filter media, nano-sensors, military protective clothing, cosmetic skin mask, tissue engineering scaffolding etc. [2,3].

Basic components of the solutions used were SAN and [Bmim]Cl. SAN copolymer has many advantages in comparison with others polymers like excellent transparency, high tensile modulus, good rigidity and hardness, high dimensional stability and accuracy, good heat and excellent chemical resistance [27]. It is known that styrene (S) and acrylonitrile (AN) ratio in the polymer chain have significant effect on properties of final products made of SAN [28]. Last is the reason why SAN copolymer is of interest for future research. Literature review showed that SAN can be modified by chemical modification [29] and react after the process with functionalized carbon nanotubes. This can help to disperse CNTs in SAN electrospinning solutions and improve mechanical properties of the final product.

Our previous research showed a positive impact of [Bmim]Cl addition to the polymer solution on the electrospinning process and on the morphology of the fibres obtained [4]. During the experiments it was found that the distance between the top of the needle and the collector could be increased if at least 0.5% of [Bmim]Cl by weight of SAN was added into the electrospinning solution. With increased distance the electrospinning jet has longer flying time and larger deposition area which in case leads to

---

Abbreviations: [Bmim]Cl*- 1-butyl-3-methylimidazolium chloride; MWCNTs**- multiwalled carbon nanotubes; SAN***- styrene-acrylonitrile copolymer.

* Corresponding author. Ehitajate tee 5, 19086 Tallinn, Estonia.
E-mail address: viktoria.gudkova@ttu.ee (V. Gudkova).

http://dx.doi.org/10.1016/j.elstat.2015.09.002
0304-3886/© 2015 Elsevier B.V. All rights reserved.

production of drier and thinner fibres with smaller diameter fluctuation. The process stability was also improved. [Bmim]Cl concentration has a notable effect on the obtained fibre morphology. No solvent beads were observed even when only 1.5% of MWCNTs by weight of SAN was added into the solution. Another effect is the change in fibre shape from cylindrical to ribbon-like. And the (last and) biggest effect is reduction in fibre diameter with very small additions of [Bmim]Cl. E.g. 0.5% of [Bmim]Cl by weight of SAN reduced the fibre diameter almost twice, with an addition of 1.5% of [Bmim]Cl the fibre diameter reached nanoscale, 20% of [Bmim]Cl yielded fibres with a diameter of 275 nm, i.e. more than seven times smaller compared to pure SAN fibres.

Carbon nanotubes (CNTs) have been known for longer than a hundred years [5] but got intensive attention only in 1991 after Iijima research publication [6]. CNTs are ideal reinforcing agents for high performance polymer composites. The properties of polymer composites that can be improved due to the presence of CNTs include tensile strength [7,8], tensile modulus [9,10], toughness [11], glass transition temperature [12,13], thermal conductivity [14,15], electrical conductivity [16,17], solvent resistance [18], optical properties [19,20], etc.

A literature review showed efficient utilization of carbon nanotubes with the help of ionic liquids. E.g. Yonghui Liu, Li Yu et al. report good and stable dispersion of MWCNTs by an ionic liquid of the type gemini imidazolium surfactants in aqueous solution [24].

Motivated by the aim of creating reinforced conductive membranes, in this research we studied the impact of [Bmim]Cl and MWCNTs on the properties of SAN polymer solution, on the morphology of electrospun fibres and electrical and mechanical properties of the membranes.

2. Experimental

2.1. Materials

The solutions for the electrospinning experiments were prepared using SAN purchased from Polimeri Europa SRL (Italy) and DMSO purchased from Merck KGaA (Germany). First a 1:4 solution of SAN in DMSO was made by mechanical stirring at 50 °C for 8 h. After that, [Bmim]Cl ionic liquid (20% by weight of SAN) and various amounts of MWCNTs (0.1 up to 3.0% by weight of SAN) solutions were added to the 1:4 SAN in DMSO solutions. Before electrospinning and measuring of the viscosity and electrical conductivity the solutions were ultrasonicated for 3 h using Sonoplus HD 2070 (BANDELIN electronic GmbH & Co. KG). MWCNTs with an average diameter of 9.5 nm, average length 1.5 μm and 95% purity were purchased from Nanocyl S.A. (Belgium). [Bmim]Cl was synthesised at the laboratory of the Department of Polymeric Materials, TUT, Tallinn, using the procedure reported in Ref. [21]. In standard preparation, 1.5 mol of chlorobutan and 1.0 mol of 1-methylimidazole were mixed in a round-bottomed flask fitted with a reflux condenser and stirred for 3 days at 80 °C. Of the two phases formed, the top phase containing the reagents, was removed by washing several times with ethyl acetate. The yellowish IL product of [Bmim]Cl was further heated up to 50 °C under vacuum to eliminate traces of ethyl acetate solvent.

2.2. Electrospinning experiments

All electrospinning solutions were electrospun from a 2.5 ml syringe with a medical needle of a diameter 0.6 mm. A MK Series power supply (GLASSMAN EUROPE Limited, UK) was used to generate a voltage of 20 kV. Fibres were collected to the drum, which had been covered with an aluminium foil beforehand. The distance between the tip of the needle and the collector was 20 cm. To pump the electrospinning solutions, NE-1000 Single Syringe Pump (New Era Pump Systems, Inc.) was used. Pumping rates were between 0.5 and 0.9 ml/h.

2.3. Characterization

For each solution the viscosity was measured with concentric cylinder viscometer Brookfield RVDVII+ (Brookfield ENG LABS Inc., USA), using spindle No 21 at 23.3 °C. The temperature was held constant with a MGW Lauda C6 thermostat (Berner Osakyhtio, Finland). The electrical conductivities of the solutions were measured with SevenCompact Conductivity S230 (Mettler Toledo, Switzerland) at room temperature.

Mechanical properties of the membranes were measured at room temperature with Instron 5866 (Instron Corporation, USA) using Bluehill™ 2 Version 2.17 software with a cross-head speed of 20 mm/min and a clamps distance of 15 mm. The electrical conductivity of the membranes were measured with High Resistance Meter Model HR2 (AlphaLab, Inc., USA) at room temperature. Distance between electrodes was 10 mm. For both conductivity and mechanical measurements six samples of each membrane were prepared with dimensions of 5 × 25 mm. The thickness of each sample was measured from three different places with a Sony U30-F Digital Indicator (Sony Magnescale Inc., Japan) and the average was calculated.

The morphology of the electrospun fibres was analysed using SEM microscope TM1000 (Hitachi High-Technologies Europe GmbH, Germany).

3. Results and discussion

3.1. Impact of MWCNTs and [Bmim]Cl on SAN solution viscosity and electrical conductivity

3.1.1. Solution viscosity

Fig. 1 represents the impact of [Bmim]Cl and MWCNTs on the solution viscosity. From the viscosity diagram it can be seen that with increasing content of MWCNTs in both solution types, with

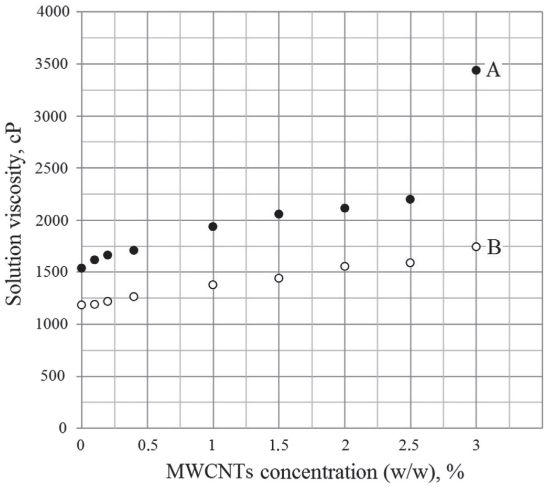

Fig. 1. Dependence of SAN in DMSO solutions viscosity on [Bmim]Cl addition and MWCNTs concentration. A: 1:4 SAN in DMSO + (0–3)% MWCNTs by weight of SAN. B: 1:4 SAN in DMSO + 20% [Bmim]Cl + (0–3)% MWCNTs by weight of SAN.

and without [Bmim]Cl, the viscosity also increases. This is caused by the dispersion of CNTs in the polymer solution. MWCNTs are entangled with polymer chains and this increases the solution viscosity. The higher the content of MWCNTs, the higher the solution viscosity. The same phenomenon is described in Ref. [25], where the viscosity of PVDF/DMF solutions with various CNTs concentrations is studied.

By comparing the solutions with and without [Bmim]Cl it can be seen, that the solutions with [Bmim]Cl have lower viscosities than the solutions without [Bmim]Cl. Solution viscosity without [Bmim]Cl increased from 1537cP at 0% concentration up to 3436cP at 20% concentration by weight of SAN, while the viscosity of solutions containing [Bmim]Cl increased from 1184cP up to 1742cP at the same concentrations. This is related to the decrease of intermolecular interactions resulting from [Bmim]Cl dilution in DMSO. The same phenomenon is described by Yanfang G. et al. in "Densities and Viscosities of the Ionic Liquid [C4mim][PF6] + N,N-dimethylformamide Binary Mixtures at 293.15 K–318.15 K" [26].

3.1.2. *Electrical conductivity of solutions*

The electrical conductivity of SAN in DMSO solution increases with the addition of MWCNTs from 0.919 μS/cm at 0.1% up to 5.09uS/cm at 3.0% of MWCNTs by weight of SAN. This is caused by the highly conductive nature of MWCNTs. From Fig. 2 it can be seen that there is a rapid rise between 0.1 and 1.0% MWCNTs by weight of SAN. From 1.0 up to 3.0% of MWCNTs by weight of SAN the electrical conductivity of the solution increases only for 0.78 μS/cm. It can be concluded that SAN in DMSO solution without [Bmim]Cl gets saturated at 1.0% of MWCNTs by weight of SAN and further dispersion of carbon nanotubes is not efficient.

With an addition of 20% [Bmim]Cl by weight of SAN the electrical conductivity of SAN polymer solution increases up to 178 μS/cm. This phenomenon is caused by the nature of [Bmim]Cl molecules. [Bmim]Cl is a liquid salt at room temperature, that consists of large $[Bmim]^+$ cations and small Cl^- anions, the electrical conductivity of which is 3.41 μS/cm. With an addition of [Bmim]Cl into the SAN polymer solution the ionic pairs dissociate in DMSO and increase the amount of charge carriers. With an addition of MWCNTs into the [Bmim]Cl containing SAN polymer solution the electrical conductivity increases rapidly from 178 μS/cm at 0.1 up to 209 μS/cm at 3.0% of MWCNTs by weight of SAN. The dependence has a linear character from 1.0 up to 3.0% of MWCNTs by weight of SAN. These can be explained by the effect of [Bmim]Cl as a dispersant. [Bmim]Cl helps to reduce the amount and size of agglomerates of MWCNTs in SAN polymer solution. It also creates conductive linkages between separate MWCNTs and agglomerates thus creating a conductive network in SAN polymer solution.

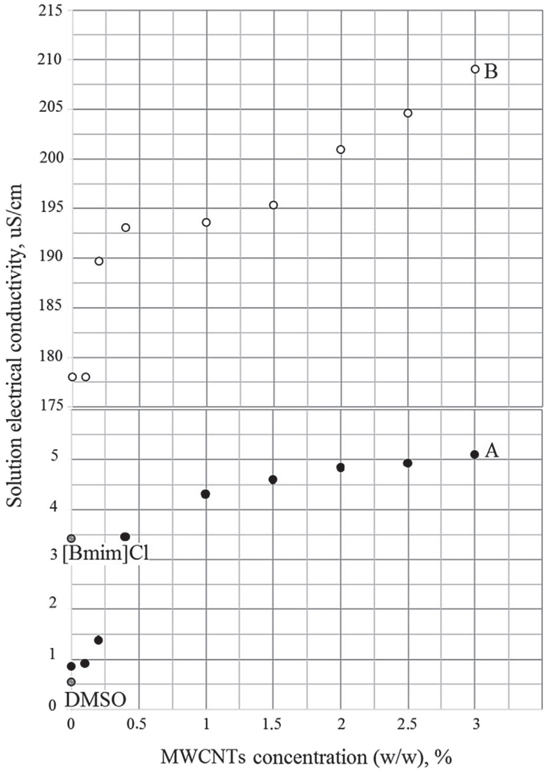

Fig. 2. Dependence of SAN in DMSO solutions electrical conductivity and viscosity on [Bmim]Cl addition and MWCNTs concentration. A: 1:4 SAN in DMSO + (0–3)% MWCNTs by weight of SAN, B: 1:4 SAN in DMSO + 20% [Bmim]Cl + (0–3)% MWCNTs by weight of SAN.

3.2. *Impact of MWCNTs and [Bmim]Cl on SAN membrane mechanical properties, electrical conductivity and fibres morphology*

3.2.1. *Membrane electrical conductivity*

Fig. 3 represents the impact of [Bmim]Cl and MWCNTs on the electrical conductivity of the membrane. From the diagram it can be seen that an addition of 20% of [Bmim]Cl by weight of SAN increases the electrical conductivity of the membrane from 0 up to 0.244 μS/cm. This is caused by the conductive nature of ionic liquid.

The addition of MWCNTs into pure 1:4 SAN in DMSO solution does not affect the electrical conductivity of membranes obtained. The electrical conductivity of SAN + (0–3)% MWCNTs by weight of SAN membraines is 0 μS/cm. This phenomenon is caused by poor dispersion of MWCNTs in SAN polymer solution.

The addition of MWCNTs into 1:4 SAN in DMSO solution containing [Bmim]Cl increases the electrical conductivity of the membranes from 1.08 μS/cm at 0.1% up to 5.9 μS/cm at 3.0% MWCNTs by weight of SAN. This phenomenon is caused by the role

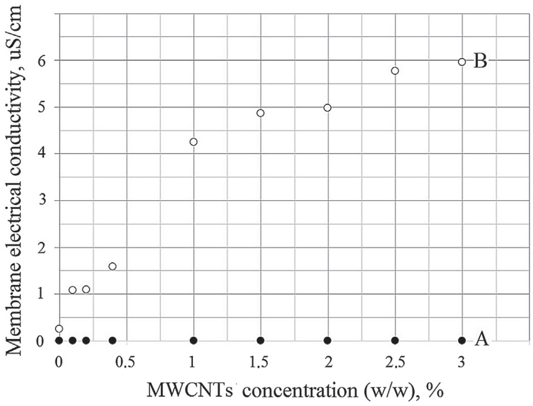

Fig. 3. Dependence of SAN membrane electrical conductivity on [Bmim]Cl and MWCNTs concentration. A: SAN + (0–3)% MWCNTs by weight of SAN, B: SAN + 20% [Bmim]Cl + (0–3)% MWCNTs by weight of SAN.

of [Bmim]Cl as a dispersant and it's conductive nature. [Bmim]Cl creates conductive linkages between separate MWCNTs and MWCNTs agglomerates thus making a conductive network inside SAN polymer fibres.

3.2.2. Mechanical properties of the membranes

From Fig. 4 it can be seen that an addition of 20% of [Bmim]Cl by weight of SAN increases the tensile stress of a SAN membrane from 2.0 up to 4.8 MPa. This phenomenon can be explained by the increase of the electrical conductivity of the solution when [Bmim]Cl is added. As a consequence the stretching force of the electrospinning jet to the collector increases and this in turn makes SAN polymer molecules more aligned inside the obtained fibre, increasing polymer crystallinity inside the electrospun fibres resulting in the higher tensile stress of the SAN membrane.

Fig. 4 represents the impact of MWCNTs on the mechanical properties of electrospun SAN membranes. With an addition of 0.1 up to 3.0% of MWCNTs by weight of SAN the tensile stress of the SAN membrane reduces at all concentrations. No dependence of the tensile tension of the membrane on MWCNTs concentration was found in [Bmim]Cl free membranes. These results can be explained by the poor dispersity of MWCNTs in pure SAN polymer electrospinning solution. The agglomerates of MWCNTs inside SAN fibres create stress location areas. At these points crackes appear when force is applied to fibres thus reducing the tensile stress of the obtained membranes.

It was found that the addition of [Bmim]Cl increases the tensile stress of MWCNTs containing SAN polymer membranes at all MWCNTs concentrations compared to membranes without the ionic liquid. This can be explained by the role of [Bmim]Cl as a dispersant. With improved dispersity of MWCNTs less stress location sites are generated and more separate carbon nanotubes can be aligned during electrospinning inside the SAN fibres. Another reason of this phenomenon is the improved electrical conductivity of the electrospinning solution due to the addition of ionic liquid and carbon nanotubes. It was also found that with an addition of MWCNTs into the ionic liquid containing polymer solution the tensile stress of the membrane increases three times from 1.7 MPa at 0.1% up to 5.1 MPa at 1.0% of MWCNTs by SAN weight where it reaches its maximum. Further addition of MWCNTs reduces the tensile stress which can be explained by saturation of the polymer solution with MWCNTs. The dispersion of MWCNTs is efficient up to 1.0% by weight of SAN. Beyond this concentration neither the ionic liquid nor ultrasonication can help to disperse MWCNTs in the SAN solution. Another reason for this phenomenon is the increase of viscosity of the polymer solution. The viscosity of the solution has a significant effect on the morphology and mechanical properties of the obtained fibres. Due to the increased viscosity the electrospinning solution resists more to being stretched by the charges on the jet. As a result, at weaker stretching the alignment of polymer molecules and MWCNTs is lower. This in turn leads to production of membranes with lower tensile stress.

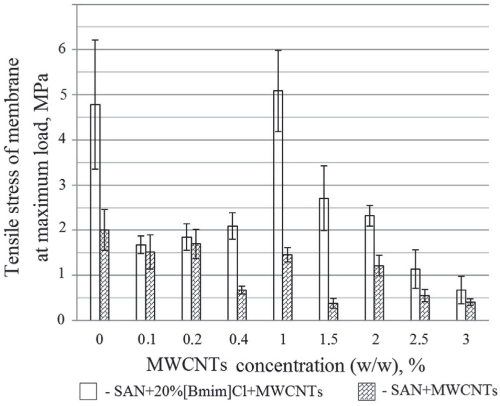

Fig. 4. Dependence of SAN membrane tensile stress at maximum load on [Bmim]Cl and MWCNTs concentration.

3.2.3. Membrane morphology

From Fig. 5 it can be seen that with the addition of 20% [Bmim]Cl by weight of SAN into the electrospinning polymer solution the average diameter of the obtained fibres decreases from 862 nm at 0% down to 720 nm at 20% of [Bmim]Cl by weight of SAN. This phenomenon can be explained by the increased electrical conductivity of the electrospinning solution due to the addition of an ionic liquid. The greater the electrical conductivity of the solution, the more charges it carries and the stronger is the stretching force to the collector. The shape of the fibres is also more uniform at higher electrical conductivities of the solution. Moreover, the increased electrical conductivity of the solution influences also the jet bending instability, which means that the depositing area is increased and this in turn will also favour the formation of finer fibres since the jet path is now increased.

It was found that with addition of MWCNTs from 0.1 up to 1.0% by weight of SAN into the [Bmim]Cl containing electrospinning solution the diameter of the obtained fibres decreases from 642 down to 291 nm. It is known that the addition of MWCNTs reduces the resistivity of polymeric systems. This increases the conductivity and charge density of the jet during electrospinning. These effects in turn promote higher elongation of the fibre during the jet pass to the collector, resulting in the decrease of the fibre diameter. The same effect was observed by J. Macossay et al. who studied the incorporation of MWCNTs into electrospun Tecoflex®EG80A class of polyurethane nanofibers [22]. It was also found that with a further addition of MWCNTs into the solution the average fibre diameter stably increases. This can be explained by an increase in the solution viscosity that hinders the rise of the electrical conductivity of

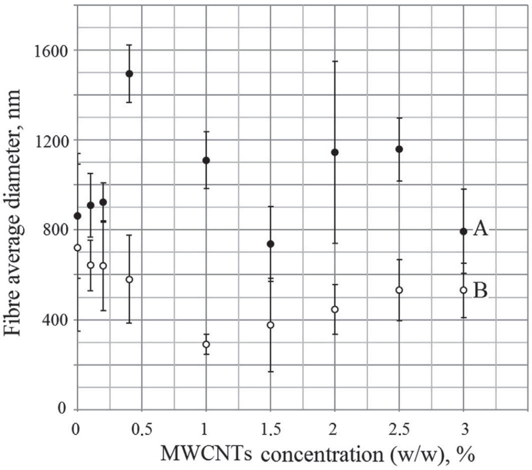

Fig. 5. Dependence of SAN fibre average diameter on [Bmim]Cl and MWCNTs concentration. A: SAN + (0–3)% MWCNTs by weight of SAN, B: SAN + 20%[Bmim]Cl + (0–3)% MWCNTs by weight of SAN.

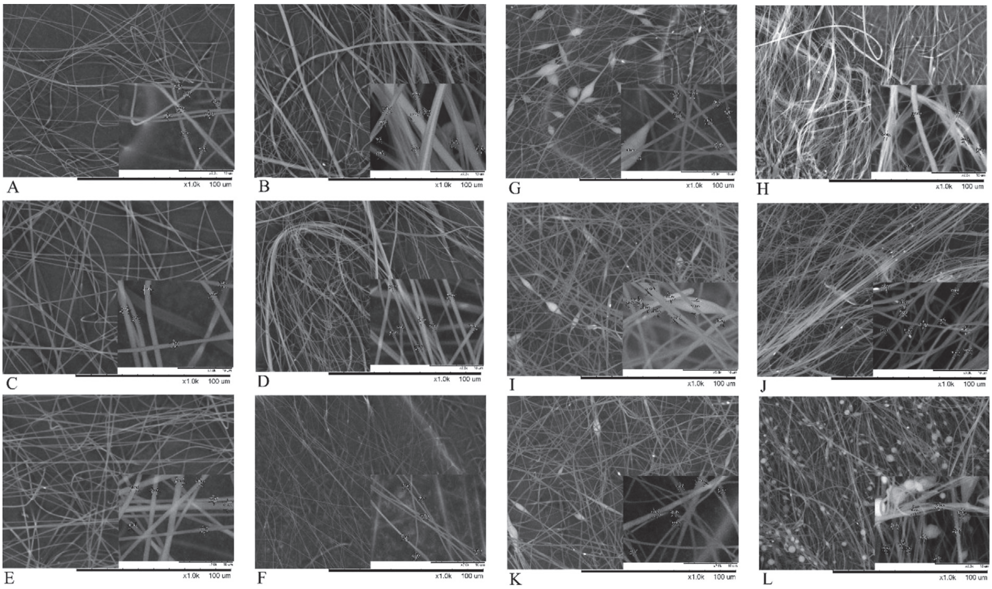

Fig. 6. SEM micrograph of SAN two types fibres, with and without [Bmim]Cl, with different concentration of MWCNTs (0 up to 3.0% by weight of SAN). A: SAN, B: SAN + 20%[Bmim]Cl, C: SAN + 0.1%MWCNTs, D: SAN + 20%[Bmim]Cl + 0.1%MWCNTs, E: SAN + 1.0%MWCNTs, F: SAN + 20%[Bmim]Cl + 1.0%MWCNTs, G: SAN + 1.5%MWCNTs, H: SAN + 20%[Bmim]Cl + 1.5%MWCNTs, I: SAN + 2.5%MWCNTs, J: SAN + 20%[Bmim]Cl + 2.5%MWCNTs, K: SAN + 3.0%MWCNTs, L: SAN + 20%[Bmim]Cl + 3.0%MWCNTs. [Bmim]Cl concentration is calculated by weight of SAN.

the solution (see Figs. 1 and 2). The growth of the viscoelastic force of the electrospinning solution acts against the stretching force thus promoting greater diameter of the fibres.

SEM investigation (see Fig. 6) showed beads formation in both types of fibres, with and without [Bmim]Cl, starting from 1.5% of MWCNTs by weight of SAN. This is possibly due to the unstable solution jet during electrospinning which was caused by inefficient carbon nanotubes dispersion. The same phenomenon was observed by X. Jiazhu et al. in their study "Fabrication of PLGA/MWNTs composite electrospun fibrous scaffolds for improved myogenic differentiation of C2C12 cells" [23]. With increasing concentration the amount and size of the agglomerates also increase thus promoting jet instability. Beads formation and jet instability can also be reasons of the decreasing tensile stress of the obtained membranes.

4. Conclusions

In this work the impact of [Bmim]Cl and MWCNTs on the parameters of SAN polymer solution and electrical and mechanical properties of the electrospun membranes was studied. We have found that the concentrations of [Bmim]Cl and MWCNTs have a certain effect on the viscosity and electrical conductivity of SAN polymer solution. The addition of MWCNTs into the polymer solution increases viscosity in both solution types, with and without [Bmim]Cl. But the viscosity of [Bmim]Cl containing solutions is lower at the same MWCNTs concentrations compared to ionic liquid containing solutions. The electrical conductivity of SAN in DMSO solution increases with the addition of MWCNTs in both types of solutions, with and without [Bmim]Cl. But the solutions with [Bmim]Cl have at least 20 times higher electrical conductivity and the dependence is more pronounced. It means that the same quantity of MWCNTs has a greater effect in ionic liquid containing solutions.

Presence of [Bmim]Cl and MWCNTs and their concentration have a notable effect on the electrical conductivity, tensile stress and fibre morphology of the obtained membrane. The electrical conductivity of all membranes without the ionic liquid is zero. MWCNTs do not form any conductive network in pure SAN fibres. The addition of [Bmim]Cl increases the electrical conductivity only up to 0.244 μS/cm. But the addition of MWCNTs into the ionic liquid containing solution increases the electrical conductivity of the membrane up to 5.95 μS/cm. Thus, [Bmim]Cl and MWCNTs create a conductive network inside the SAN fibres and yield conductive membranes. It was found that MWCNTs have a certain effect on the tensile stress of the membrane only in [Bmim]Cl containing membranes. The highest tensile stress was achieved at the MWCNTs concentration 1.0% by weight of SAN. SEM investigation showed that both types of membranes, with and without [Bmim]Cl, contain beads at MWCNTs concentrations higher than 1.5% by weight of SAN. But ionic liquid content has a certain effect on the average diameter of the fibres – below 1.0% of MWCNTs by weight of SAN it reduces it and above 1.0% it increases again (till 3.0%). The solutions without ionic liquid showed no dependence of fibre diameter on the concentration of MWCNTs.

Acknowledgements

The Archimedes Foundation Implementing Agency of Structural Support is acknowledged for its support under grant "Carbon Nanotube Reinforced Electrospun Nano-fibres and Yarns", no. 3.2.1101.12-0018.

References

[1] G.C. Rutledge, S.V. Fridrikh, Formation of fibres by electrospinning, Adv. Drug Deliv. Rev. 59 (2007) 1384–1391.
[2] Ramakrishna, Introduction to Electrospining and Nanofibres, World Scientific Publishing Co, USA, 2005.
[3] Z.-M. Huang, Y.-Z. Zhang, M. Kotaki, S. Ramakrishna, A review on polymer

nanofibres by electrospinning and their applications in nanocomposites, Compos. Sci. Technol. 63 (2003) 2223–2253.

[4] V. Gudkova, A. Krumme, T. Märtson, M. Rikko, E. Tarassova, M. Viirsalu, The impact of 1-butyl-3-methylimidazolium chloride on electrospinning process of SAN polymer solutions and electrospun fibre morphology, J. Electrost. 72 (2014) 433–436.

[5] M. Monthioux, V.L. Kuznetsov, Who should be given the credit for the discovery of carbon nanotubes? Carbon 44 (2006) 1621–1623.

[6] S. Iijima, Helical microtubules of graphitic carbon, Nature 354 (1991) 56–58.

[7] S. Kanagaraj, F.R. Varanda, T.V. Zhiltsova, M.S.A. Oliveira, J.A.O. Simoes, Mechanical properties of high density polyethylene/carbon nanotube composites, Compos. Sci. Technol. 67 (2007) 3071–3077.

[8] J.Y. Kim, S.I. Han, S.H. Kim, Crystallization behaviors and mechanical properties of poly(ethylene 2,6-naphthalate)/multiwall carbon nanotube nanocomposites, Polym. Eng. Sci. 47 (2007) 1715–1723.

[9] S.H. Jin, Y.B. Park, K.H. Yoon, Rheological and mechanical properties of surface modified multi-walled carbon nanotube-filled PET composite, Compos. Sci. Technol. 67 (2007) 3434–3441.

[10] Z. Wang, P. Ciselli, T. Peijs, The extraordinary reinforcing efficiency of singlewalled carbon nanotubes in oriented poly(vinyl alcohol) tapes, Nanotechnology 18 (2007) 455709/1–455709/9.

[11] B.X. Yang, J.H. Shi, K.P. Pramoda, S.H. Goh, Enhancement of stiffness, strength, ductility and toughness of poly(ethylene oxide) using phenoxy-grafted multiwalled carbon nanotubes, Nanotechnology 18 (2007) 125606/1–125606/7.

[12] J.Q. Pham, C.A. Mitchell, J.L. Bahr, J.M. Tour, R. Krishanamoorti, P.F. Green, Glass transition of polymer/single-walled carbon nanotube composite films, J. Polym. Sci. Part B Polym. Phys. 41 (2003) 3339–3345.

[13] X.Y. Gong, J. Liu, S. Baskaran, R.D. Voise, J.S. Young, Surfactant-assisted processing of carbon nanotube/polymer composites, Chem. Mater. 12 (2000) 1049–1052.

[14] I.V. Singh, M. Tanaka, J. Zhang, M. Endo, Evaluation of effective thermal conductivity of CNT-based nano-composites by element free Galerkin method, Int. J. Numer. Methods Heat Fluid Flow 17 (2007) 757–769.

[15] S. Sergei, L. Xue, O. Rahmi, K. Pawel, G.C. David, Role of thermal boundary resistance on the heat flow in carbon-nanotube composites, J. Appl. Phys. 95 (2004) 8136–8144.

[16] B.R. Sankapal, K. Setyowati, J. Chen, H. Liu, Electrical properties of airstable, iodine-doped carbon-nanotube-polymer composites, Appl. Phys. Lett. 91 (2007) 173103/1–173103/3.

[17] N. Grossiord, H.E. Miltner, J. Loos, J. Meuldijk, B. Van Mele, C.E. Koning, On the crucial role of wetting in the preparation of conductive polystyrene-carbon nanotube composites, Chem. Mater. 19 (2007) 3787–3792.

[18] H. Guo, T.V. Sreekumar, T. Liu, M. Minus, S. Kumar, Structure and properties of polyacrylonitrile/single wall carbon nanotube composite films, Polymer 46 (2005) 3001–3005.

[19] M. Ichida, S. Mizuno, H. Kataura, Y. Achiba, A. Nakamura, Anisotropic optical properties of mechanically aligned single-walled carbon nanotubes in polymer, Appl. Phys. A 78 (2004) 1117–1120.

[20] U.D. Weglikowska, M. Kaempgen, B. Hornbostel, V. Skakalova, J. Wang, J. Liang, et al., Conducting and transparent SWNT/polymer composites, Phys. Status Solidi (b) 243 (2006) 3440–3444.

[21] R. Rogers, D. Heather, J. Huddleston, W. Reichert, A. Visser, G. Broker, Green Chem. 3 (2001) 156–164.

[22] J. Macossay, F.A. Sheikh, T. Cantu, T.M. Eubanks, M.E. Salinas, C.S. Farhangi, H. Ahmad, et al., Imaging, spectroscopic, mechanical and biocompatibility studies of electrospun Tecoflex®EG 80A nanofibres and composites thereof containing multiwalled carbon nanotubes, Appl. Surf. Sci. 321 (2014) 205–213.

[23] J. Xu, Y. Xie, H. Zhang, Z. Ye, W. Zhang, Fabrication of PLGA/MWNTs composite electrospun fibrous scaffoldsfor improved myogenic differentiation of C2C12 cells, Colloids Surf. B Biointerfaces 123 (2014) 907–915.

[24] L. Yonghui, Y. Li, Z. Shaohua, Y. Jie, S. Lijuan, Z. Liqiang, *Dispers*ion of multiwalled carbon nanotubes by ionic liquid-type Gemini imidazolium surfactants in aqueous solution, Colloids Surf. A Physicochem. Eng. Asp. 359 (2010) 66–70C.

[25] C. Seoul, Y.-T. Kim and C.-K. Baek, Article, Electrospinning of Poly(-vinylidenefluoride)/Dimethylformamide solutions with carbon nanotubes, where authors studied viscosity of PVDF/DMF solutions with various CNT concentrations.

[26] G. Yanfang, W. Tengfang, Y. Dahong, P. Changjun, L. Honglai, H. Ying densities and viscosities of the ionic liquid [C4mim][PF6]+ N,N-dimethylformamide binary mixtures at 293.15 K to 318.15 K, Chin. J. Chem. Eng. 16(2) 256–262.

[27] G. Wypych, Handbook of Polymers, GhemTec Publishing, Canada, Toronto, 2012.

[28] A. Chrisochoou, D. Dufour, Styrenic Copolymers, GBR, Shrewsbury: Smithers Rapra, 2003.

[29] G. Schmidt-Naake, H. Becker, W. Becker, Chemical modification of poly(styrene-co-acrylonitrile) with 2-aminoalcohols and 3-aminoalcohols, Die Angew. Makromol. Chem. 267 (1999) 63–66.

Article III

Vassiljeva, V., Kirikal, K.-K., Hietala, S., Kaljuvee, T., Mikli, V., Rähn, M., Tarasova, E., Krasnou, I., Viirsalu, M., Savest, N., Plamus, T., Javed, K., Krumme, A. (2017). One-step carbon nanotubes grafting with styrene-co-acrylonitrile by reactive melt blending for electrospinning of conductive reinforced composite membranes. *Fullerenes, Nanotubes and Carbon Nanostructures* - Manuscript ID FNCN17204.R2 (accepted)

Fullerenes, Nanotubes and Carbon Nanostructures

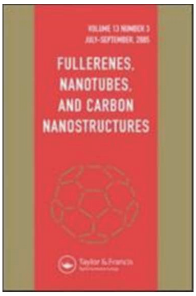

One-step carbon nanotubes grafting with styrene-co-acrylonitrile by reactive melt blending for electrospinning of conductive reinforced composite membranes

Journal:	*Fullerenes, Nanotubes and Carbon Nanostructures*
Manuscript ID	FNCN17204.R2
Manuscript Type:	Original Article
Date Submitted by the Author:	09-Oct-2017
Complete List of Authors:	Vassiljeva, Viktoria; Tallinna Tehnikaulikool, Kirikal, Kaia-Kristina; Tallinna Tehnikaulikool Hietala, Sami; University of Helsinki Kaljuvee, Tiit; Tallinna Tehnikaulikool Mikli, Valdek; Tallinna Tehnikaulikool Rähn, Mihkel; Tartu Ulikool Tarasova, Elvira; Tallinn University of Technology, Department of Polymer Materials Krasnou, Illia; Tallinn University of Technology, Department of Polymer Materials Viirsalu, Mihkel; Tallinna Tehnikaulikool Savest, Natalja; Tallinn University of Technology, Plamus, Tiia; Tallinna Tehnikaulikool Javed, Kashif; Tallinna Tehnikaulikool Krumme, Andres; Tallinna Tehnikaulikool
Keywords:	electrospinning, CNT grafting, reactive melt blending, membrane, fiber

Hello,

First of all, we would like to thank you for so reasonable comments and suggestions, especially in part of IL and it's impact on the viscosity of different solutions and membrane mechanical properties. You will find the response for all of them in the list below:

1. Reviewer(s):

The data should be explained clearly. For example, on page 12, the authors present that "The decrease in electrical conductivity of IL containing solutions after ultrasonic irradiation can be explained by the decrease of electrical conductivity of IL itself during ultrasonication. Initial electrical conductivity of IL was 78.3 and after 3h of ultrasonication it reduced to 71.1μS/cm.". Please give the experimental details or the references which can explain "decrease of electrical conductivity of IL itself during ultrasonication".

Author:

The decrease of electrical conductivity of IL is caused by oxidative degradation of IL under ultrasonication. Related discussion and reference are presented now on page 11 and page 13 in a revised version of the manuscript.

2. Reviewer(s):

On page 13, the authors present that "Addition of SANm-g-CNTs into SAN polymer solution does not affect much viscosity values in comparison to SAN solution. This can be explained by the covalent attaching of SANm molecules to CNT, which improves dispersion level of CNTs into the polymer matrix." Please interpret how dispersion affects viscosity.

Authors:

In general, during the mechanical dispersion of ungrafted CNTs, they have a tendency to stay in agglomerated form. Agglomerates are larger and harder compared to entangled polymer molecules in a concentrated polymer solution and for this reason, the viscosity values increase. Literature review (and our experience) show, that modified CNTs can be dispersed more homogeneously. This means that more separate CNTs and smaller agglomerates present in solution. For this reason, the viscosity of the solutions with modified CNTs is lower compared to solutions with unmodified CNTs, but still higher compared to the pure polymer solution. Also, the solution with CNT-COOH has lower viscosity value compared to SANm-g-CNTs for the same reason. CNT-COOH are smaller compared to SANm-g-CNTs because –COOH is smaller compared to SANm.

It was decided to remove named statement ("Addition of SANm-g-CNTs into SAN polymer solution does not affect much viscosity values in comparison to SAN solution. This can be explained by the covalent attaching of SANm molecules to CNT, which improves dispersion level of CNTs into the polymer matrix.") from the article, as compatibility of SAN and SANm is still unclear and should be studied more precisely. This should be studied more precisely, but this is out of the range of current research. We hope you will agree with this decision. In case if you agree with the explanation above and consider it is appropriate to current manuscript we will be happy to add it into the manuscript.

3. Reviewer(s):

On page 14, the authors present that "In case of ungrafted nanotubes, IL can easily cover the CNTs. Nevertheless, in case of polymer- grafted CNTs separate nanotubes are coated with the polymer, IL cannot reach the CNTs surface and play a role of dispersant." The reviewer suggests the authors to clearly commentate the mechanism of their opinion.

Authors:

More detailed explanation of the interaction between the surface of CNT and the IL on page 12 with relevant references is added. Also, the scheme is presented in figure 7 for better understanding.

4. Reviewer(s):

The changing viscosity of solution after adding the IL maybe be given a better explanation if the authors want to display this data on page 12.

Authors:

The viscosity of pure IL before and after ultrasonication was measured and values are 0.97 and 1.38 Pa·s respectively. During the oxidative degradation under ultrasonication, some ions are degraded and as a consequence not degraded ions have lower mobility in solution. This causes the decrease of the electrical conductivity and increase of the viscosity of IL-containing solutions under ultrasonic treatment.

The effect of IL on solution viscosity under ultrasonication is different compared to mechanically mixed systems. Please see the extended discussion about the effect of IL and ultrasonication on pages 11-13 with the relevant references.

5. Reviewer(s):

Figure 2 can be seen the difference between the two lines (solid line or dotted line).

Authors:

The figure was modified. Now two lines are placed separately.

6. Reviewer(s):

On page 5, the authors do not give the ultrasonic power.

Authors:

We are not sure about this comment if we understood it correctly. We used ultrasonication to dissolve and achieve better homogenization of $Zn(Ac)2·2H2O$ in AE. The mixture in ratio 1:83 was ultrasonically mixed for 10 minutes.

7. Reviewer(s):

Figures that express the same meaning can be put together. For example, fig. 6 and 7 can be combined together.

Authors:

The figures 6 and 7 are combined under name „Solutions electrical conductivity dependence on addition of different CNTs, IL, and solution preparation method". See new figure 6.

Thank you very much again for indication of weak points in our manuscript. It was useful and helpful for current research. We hope that corrected version of manuscript will find positive feedback from you.

Best regards,

Authors

One-step carbon nanotubes grafting with styrene-co-acrylonitrile by reactive melt blending for electrospinning of conductive reinforced composite membranes

V. Vassiljeva[1*], **K.-K.Kirikal**[1], **S.Hietala**[2], **T.Kaljuvee**[1], **V.Mikli**[1], **M.Rähn**[3], **E.Tarasova**[1], **I.Krasnou**[1],

M.Viirsalu[1], **N.Savest**[1], **T.Plamus**[1], **K.Javed**[1], **A.Krumme**[1]

[1,3,4]*Department of Materials and Environmental technology, Tallinn University of Technology, Tallinn, Estonia*

viktoria.vassiljeva@ttu.ee, Ehitajate tee 5, 19086 Tallinn, Estonia

[2]*Department of Chemistry, University of Helsinki, Helsinki, Finland*

[3]*Institute of Physics, University of Tartu, Tartu, Estonia*

Abstract

Aim of this research was to electrospin conductive composite membrane of styrene-co-acrylonitrile (SAN) reinforced with carbon nanotubes (CNTs). To improve electrical conductivity of final membrane ionic liquid (IL) was used. For better dispersion of CNTs in SAN matrix one-step reactive melt blending method for grafting of SAN onto CNTs was developed. Influence of SANm-g-CNTs on solutions properties was studied and compared to solutions with ungrafted CNTs and carboxyl group functionazed CNTs (CNT-COOHs). Combination of IL and SANm-g-CNTs increase in to orders of magnitude SAN membrane tensile stress and modulus. Electrical conductivity of obtained membranes achieved the level of semi-conductor materials.

1. Introduction

Nanotechnology has attracted more and more interest during last few decades. In addition, carbon nanotube-polymer composites have gained attention from science and industry point of view. Although polymer materials are ideal for forming fibrous materials expeditiously and easily, their mechanical, electrical, thermal, rheological and optical properties need improvement.

Nowadays the fastest, easiest and cheapest method for production of polymeric fibrous materials is electrospinning [1]. Electrospinning is the most efficient way of fiber production in nano- and submicron range compared to standard mechanical fiber-spinning technologies as drawing, template synthesis, phase separation and self-assembly [2]. Nowadays fibers for different applications can be produced by electrospinning like biomedicine [3, 4], engineering, pharmacology, filtering and composite materials etc. Potential applications of polymeric nanofibers are in next fields: industry, military protective clothing, nano-sensors, cosmetic products etc.

For special applications in military, industry or sensor fields mechanical, thermal and electrical properties of fibrous membranes need improvement and CNTs are widely used for this purpose. There are several problems in CNTs functionalization and processing in electrospinning. For example, manipulation of multi-walled CNTs (MWCNTs) is limited by aggregation, insolubility and poor dispersion in polymer matrix. Also weak interfacial adhesion between MWCNT and polymer matrix, inefficient load transfer between matrix and MWCNT and consequently decrease of mechanical properties should be overecome to produce composite material with enhanced properties.

According to the literature polymer grafting on CNTs gives the best result in transducing their excellent properties to polymer matrix in final product. Therefore, there have been many researches dedicated in finding the best solution for functionalization of CNTs [5, 6]. For example, functionalization of CNTs can be conducted with non-covalent bonding and with covalent bonding of polymer molecules on CNTs. With covalent chemical bonding (grafting) are established stronger bonds compared to non-covalent modification and is improved CNTs dispersion in solvents and in polymers [7]. Literature review showed that there are two widely used methods of covalent bonding between SAN and the CNTs: covalent functionalization by reactive melt blending [8] and surface initiated atom transfer radical polymerization [6].

In addition, a literature review showed efficient utilization of CNTs with the help of ILs [9]. Our previous research [10, 11] showed a positive impact of [Bmim]Cl (1-butyl-3-methylimidazolium chloride) addition to the polymer solution on the electrospinning process and the morphology of produced fibers. It was found that the distance between the top of the needle and the collector could be increased and process stability improved. Fiber morphology was improved with addition of IL: beads free fibers were obtained with average diameter lower for more than seven times (up to 275 nm). It was also found that IL can be effectively used as dispersing agent for MWCNTs. Based on previous research 20% of SAN polymer, 20% of [Bmim]Cl and 1% of different MWCNTs by weight of SAN were chosen as optimum concentrations for current study.

In this study reactive melt blending was chosen due to the methods simplicity and speed. During this research melt blending method was supplemented and one-step method for grafting CNTs onto SAN was developed. Motivated by creation of reinforced conductive SAN membranes prepared SANm-g-CNTs were used in combination with [Bmim]Cl to produce semi conductive reinforced SAN membrane.

2. Experimental

2.1. Materials

Styrene-co-acrylonitrile polymer was purchased from Polimeri Europa SRL (Italy), $Zn(Ac)_2{\cdot}2H_2O$ (zinc acetate dihydrate) from EMSURE® (Germany), AE (2-aminoethanol) from Merck Millipore (Germany) and MWCNT-COOHs from Cheap Tubes Inc. (USA). The MWCNT-COOHs have average diameter of 8-15 nm, average length of 0.5-2.0 µm, 2.56 wt% content of –COOH functional groups and 95 wt% purity. All CNTs used in this study are multi-walled CNTs and will be considered as CNTs. THF (tetrahydrofuran) and methanol were purchased from Honeywell Riedel-de Haen and used as received.

Chlorobutan, 1-methylimidazole and ethyl acetate were purchased by Merck Millipore (Germany) and used as received. DMSO (dimethyl sulfoxide) was supplied by Merck KGaA (Germany) and used as received. CNTs with an average diameter of 9.5 nm, average length of 1.5 µm and 95 wt% purity were purchased from Nanocyl S.A. (Belgium).

2.2. Preparation of oxazoline modified SAN and SAN grafted CNTs

First to dissolve and achieve better homogenization of $Zn(Ac)_2{\cdot}2H_2O$ in AE the mixture in ratio 1:83 was ultrasonically mixed [12] using Sonoplus HD 2070 sonicator with MS73 smaller nozzle (BANDELIN electronic GmbH & Co. KG) for 10 minutes. SAN was modified using the procedure partially reported in [8]:

1) SAN (4.5 g) was first melted in HAAKE™ MiniCTW Micro-Conical Twin Screw Compounder using rotational speed 20 rpm at 150°C

2) a mixture of AE and $Zn(Ac)_2{\cdot}2H_2O$ (455.4 mg) was then quickly added to the SAN and mixed with polymer at 150°C for 10 min using a rotation speed of 80 rpm

3) next, the temperature was increased up to 200°C and the blending was continued for next 20 min

4) the oxazoline modified SAN (SANm) was then extruded from the compounder

5) SANm was diluted in 45 ml of THF and mechanically mixed for 45 min, and then precipitated in 1350 ml of methanol. Obtained mixture was filtered with 0.45 µm pore size PTFE filters (Sartonus Stedim Biotech Gmbh, Germany). Process was repeated several times to ensure complete removing of $Zn(Ac)_2$ residue and AE. The resulting SANm was dried in a vacuum oven at room temperature for 24 h. The yield of this process was 79%. Obtained material was characterized by FT-IR and TGA.

For nanotube grafting with SANm the steps 1-3 were repeated, CNT-COOHs in weight ratio of 1/20 to SANm were then added, and melt blended at a rotating speed of 80 rpm at 200°C for another 30 min. Finally, the resulting material was dissolved in THF and centrifuged (EBA 21, Hettich Centrifugen, Germany) at 6000 rpm for 30 min in 50 ml falcon tubes. Centrifugate was removed. The washing procedure in THF was repeated several times until transparent centrifugate was obtained to ensure complete removal of $Zn(Ac)_2$ residue, ungrafted SANm and AE. Solid precipitate was dried in vacuum oven for 24h at 80°C to remove THF. The yield of this process was 55%. Obtained material was characterized by ^1H NMR and TGA.

2.3. Preparation of [Bmim]Cl

[Bmim]Cl was synthesized using the procedure reported in [13]. In standard preparation method, 1.5 mole of chlorobutan and 1.0 mole of 1-methylimidazole are mixed in a round-bottomed flask fitted with a reflux condenser and stirred for 3 days at 80°C. After the two phases formed, the top phase containing the reagents was removed by washing several times with ethyl acetate. The yellowish IL product of [Bmim]Cl was further heated up to 50°C under vacuum to remove ethyl acetate. Only one ionic liquid, [Bmim]Cl, was used in this study and through the paper it is considered as IL.

2.4. Preparation and electrospinning of solutions

Four series of SAN solutions with IL and different CNTs for the electrospinning experiments were prepared by mechanical and ultrasonical mixing techniques (see table. 1). The concentration of IL and CNTs was calculated by weight to SAN mass and remained constant during experiments, 20% and 1% respectively. SANm-g-CNTs are considered as special type of CNTs in this study. Viscosity and electrical conductivity of electrospinning solutions were measured for each solution.

All solutions were electrospun from a 2.5 ml syringe with a medical needle of an inner diameter 0.1 mm. A MK Series power supply (GLASSMAN EUROPE Limited, UK) was used to generate a voltage of 20 kV. Fibers were collected to the rotating drum of a diameter 7.5 cm covered with aluminum foil. The distance between the tip of the needle and the collector was constantly 20 cm and pumping rate was 0.6 ml/h., NE-1000 Single Syringe Pump (New Era Pump Systems, Inc.) was used for pumping the electrospinning solutions. Mechanical, electrical properties and morphology were investigated for each electrospun membrane.

2.5. Characterization

FT-IR spectra were recorded on an Interspec 200-X FTIR spectrometer, with 16 scans averaged at resolution of 1 cm^{-1} for SAN and SANm.

TGA experiments with a Setaram LabsysEvo 1600 thermoanalyzer were carried out under non-isothermal conditions by heating up to 800ºC at the heating rate of 10°C/min in argon atmosphere. Standard 0.1 ml alumina crucibles were used, the mass of the samples was 4-5 mg and the gas flow was 60 ml/min.

^{1}H NMR spectrum was recorded with a Bruker Avance III spectrometer operating at 500 MHz for protons. Sample (7 mg/ml) was first dispersed in d6-DMSO by keeping it at 50°C overnight followed by vortex mixing for several minutes. The spectrum was collected at room temperature with 32 scans.

Viscosity of electrospinning solutions was measured by Physica MCR 501 rheometer (Anton Paar, Austria) at rate 100/s using cone-plate geometry (cone angle 2° and diameter 2.5 cm) at 23^{o}C.

The electrical conductivity of the solutions was measured with SevenCompact Conductivity S230 electrical conductivity meter (Mettler Toledo, Switzerland) at room temperature.

The electrical conductance of the electrospun membranes was measured with High Resistance Meter Model HR2 (AlphaLab, Inc., USA) at room temperature. The thickness of each sample was measured from five different points and the average was calculated. After that, each sample was placed into 10 mm width and 10 mm length cell between electrodes and values detected. Finally, conductance was calculated into conductivity considering thickness of the samples.

Mechanical properties of the electrospun membranes were measured at 23°C and relative humidity 65% using a tensile testing instrumentation Instron 5866 (Instron Corporation, UK). The samples were cut in a rectangular shape, width of 1 mm and length of 10 mm. The thickness of each sample was measured by digital thickness gauge (INSIZE CO., LTD.). A 2.5 N load cell was used for tensile testing procedures applying a constant strain rate of 10 mm/min. Collected data was analyzed and parameters as tensile stress at maximum load and modulus were calculated using Bluehill^{TM} 2 Version 2.17 software.

The morphology of the electrospun fibers was analyzed using SEM microscope Gemini Zeiss Ultra 55 (Germany). Pictures of various magnification from 500 to 100000 were done for all samples. Average fiber diameter was calculated for each sample. TEM measurements for SANm-g-CNTs were done with FEI Titan Themis 200 working at 80 kV.

3. Results and discussion

3.1. Characterization of SANm and SANm-g-CNTs

Oxazolines can be prepared in different ways by utilization of amino alcohols. The simplest and cost-efficient method usually involves reaction of amino alcohol and carboxylic acid [14]. At temperatures below 200°C, the rate of linking reaction is insufficient [15]. Decomposition temperature of SAN, 375°C, makes it perfect polymer for grafting reaction on CNT in a compounder at high temperature.

In this research firstly SAN cyano groups reacted with AE in presence of $Zn(Ac)_2$ catalyst to form SANm or oxazoline-modified polymer. CNT-COOH were added after this modification reaction and grafting reaction between oxazoline group of SANm and carboxilic group of nanotubes took place to form covalent bonding and cover CNTs with polymer molecules (see fig. 1).

FT-IR spectra of SAN and SANm were recordered and compared in order to confirm formation of oxazoline group during modification reaction of SAN. From fig. 2 it can be seen that both SAN and SANm spectra have peaks at 1601 cm^{-1} and 2237 cm^{-1} which correspond respectively to mono-substituted C=C bond of the aromatic ring of styrene and C≡N bond of acrylonitrile functional group [12]. SANm spectra have additional strong peak at 1664 cm^{-1}, corresponding to expected oxazoline functional group (vibration of N=C bond) which confirms formation of new bonds in SAN molecule [8].

To confirm the reaction between SANm oxazoline group and carboxylic group on the surface of carbon nanotubes ^1H NMR was performed for SAN-g-MWCNTs. From the spectrum (fig. 3) the styrene aromatic protons between 6.84 and 7.17 ppm are clearly identifiable. Unfortunately the solvent peaks are overlapping the acrylonitrile peaks around 2.0-3.5 ppm.

Regardless, the signal from styrene units shows after extensive purification steps that grafting reaction took place and MWCNTs surface is covalently coated with SAN.

TGA was used to determine the amount of polymer grafted onto CNT and characterize the thermal behavior of SAN, SANm, CNT-COOH and SANm-g-CNTs (see fig. 4). CNT-COOH TG curve shows a continuous decomposition with the increase of temperature. The same is true for SANm-g-CNTs decomposition at temperatures above 445°C. This can be explained by decomposition of unreacted –COOH groups on the CNTs and impurities that CNT-COOH sample contained. SAN starts to decompose at 375°C and loses its weight completely at 445°C, the same result report Ma Y., Pang *et al* [15]. Although SANm curve is similar to SAN curve, SANm starts to decompose at 360°C and loses weight completely at the same temperature as SAN does. SAN modification reaction into SANm induced polymer to decompose at a lower temperature and changed the degradation pathway. In case of SANm-g-CNT weight loss starts at 360°C, which is attributed to the grafted SANm onto the CNTs. The SAN polymer content on the CNTs is about 35 wt% as estimated by TGA.

TEM microscopy showed that after CNTs grafting with SANm their structure take core and shell form where inside layer is nanotube and outside layer is modified polymer. From fig. 5 graphite sheet structure can be clearly observed. Polymer layer thickness on CNT is near 8 nm.

3.2. Effect of polymer grafting of CNTs on properties of the electrospinning solutions

Now the solutions electrical conductivity dependence on addition of different CNTs and solution preparation method will be discussed (see fig. 6). In case of mechanically mixed solutions, the electrical conductivity increases with addition of nanotubes almost twice compared to pure polymer solutions. CNTs have excellent electrical properties and therefore improve electrical conductivity of polymer solutions. There is a difference of electrical conductivity between SAN solutions with added CNT, CNT-COOH and SANm-g-CNT. This is because electrical properties are sensitive to the degree of functionalization and to the chemical nature of the functional group [16]. If CNTs are modified with carboxyl groups, the dispersion in polar solvents enhance due to the combination of polar–polar affinity and electrostatic repulsion. This results in better conductivity of solutions with CNT-COOH compared to the solution with pristine CNTs and SANm-g-CNTs. Electrical conductivity of solution with added SANm-g-CNT is slightly smaller comparing to solutions with ungrafted CNT and CNT-COOH because SANm-g-CNT are covered with non-conductive SANm polymer.

For improving the dispersion of CNTs into polymer solution, the ultrasonic irradiation was used. Fig. 6 shows the increase of electrical conductivity with application of ultrasonic treatment. Ultrasonication reduces the size and amount of nanotube agglomerates thus helping to transduce their electrical properties into polymer solution [17].

Our previous research [10] showed positive impact of addition of IL on the dispersion of CNTs into electrospinning solutions. IL acted as a dispersive agent for CNTs, it reduced the size and amount of CNTs agglomerates. For this reason, the IL was added and same series of solutions prepared. With an addition of IL, the electrical conductivity of all solutions increases for three orders of magnitude (see fig. 6) compared to IL-free solutions. This phenomenon is caused by the nature of IL molecules. [Bmim]Cl is a liquid salt at room temperature that consists of large $[\text{Bmim}]^+$ cations and small Cl^- anions. With an addition of IL into the SAN polymer solution, the ionic pairs dissociate in DMSO and increase the amount of charge carriers. Similar results were observed in our previous research [10].

The decrease of the electrical conductivity of IL containing solutions after ultrasonic irradiation can be explained by the decrease of electrical conductivity of IL itself during ultrasonication. Initial electrical conductivity of IL was 78.3 and after 3h of ultrasonication it reduced to 71.1 μS/cm. Decrease of electrical conductivity of IL is caused by oxidative degradation of IL under ultrasonication, which is discussed below [18].

It is well known that morphology and consequently mechanical properties of electrospun membrane strongly depend on rheological properties of the electrospinning solutions, especially on viscosity. The viscosity of all electrospinning solutions was measured at 100/s shear rate to evaluate the influence of CNTs grafting with polymer on solutions viscosity (see table. 2).

The impact of IL on the viscosity of the solution is different depending on solution preparation technique. With the addition of IL into mechanically mixed solutions, the decrease of solutions viscosity was observed, the exception is SAN in DMSO + SANm-g-CNTs. The same phenomenon was observed in our previous study [10]. This phenomenon can be explained by few reasons. It is known from the literature, that imidazolium ILs can be used to exfoliate or re-bundle the CNTs agglomerates. S.Bellayer *et al* showed experimentally, that “cation-π” interaction between imidazolium ions and a large π-electronic surface of CNTs causes the exfoliation of CNTs agglomerates [19]. The π-π interaction shielding model for dispersion process of CNTs in imidazole ILs was proposed by J.Y. Wang *et al* [20]. By this theory, CNTs agglomerates gradually exfoliate by shearing force into smaller bundles and detached separate CNTs are surrounded by ILs immediately. During this process, strong π-π interaction of CNTs is shielded due to a large dielectric constant of imidazole ILs and prevent re-bundeled nanotubes and smaller agglomerates from aggregation. The viscosity is known as a fluid's resistance to flow. Viscosity of pure IL is lower compared to the viscosity of SAN in DMSO solution. For this reason, it acts as a lubricant in solutions.

As the dispersion of CNTs into polymer solution was improved with the addition of IL the viscosity of mechanically mixed solutions decreased. Z.Fan and S.G.Advani found the same phenomenon while study of rheology of MWCNT suspensions [21]. Also, the decrease of solutions viscosity with the addition of IL is related to the decrease of intermolecular interactions resulting from IL dilution in DMSO [22]. The increase of the viscosity of SAN in DMSO + SANm-g-CNTs mechanically mixed solution can be explained by covalent grafting of CNTs by the polymer. In this research, it was found that IL has bad compatibility with SAN and SANm: pure SAN and SANm do not dissolve in pure IL. This means that in solutions with SANm-g-CNTs IL ions can reach only the ungrafted surface of CNT. As a consequence IL cannot play the role of dispersant SANm-g-CNTs. Figure 7 presents the scheme of discussed above theory. Unfortunately, no relevant literature was found for better explanation of interactions between SAN and SANm, SAN and IL, or SANm and IL. More precise rheological research is needed to explain this effect.

Now the effect of ultrasonic treatment on electrospinning solutions viscosity will be discussed. It was found, that the viscosity of solutions with IL increases after ultrasonic treatment. This can be explained by the increase of viscosity of IL during ultrasonication. The viscosity of pure IL before and after ultrasonication was measured and values are 0.97 and 1.38 Pa·s respectively. During the oxidative degradation under ultrasonication, some ions are degraded and as a consequence not degraded ions have lower mobility in solution [18]. This causes the decrease of the electrical conductivity and increase of the viscosity of IL-containing solutions under ultrasonic treatment.

The viscosity of all IL-free solutions decreases with the application of ultrasonic treatment. With application of ultrasound, bigger amount of energy was transduced to solutions thus increasing the dispersion level of IL, SAN and CNTs into DMSO and consequently the decrease of viscosity value was observed. The similar results were observed in the study of Y.

Y. Huang *et al* [23]. It was found, that with application of high-energy ultrasound during mixing the CNTs disperse better into polymer matrix and as a result, viscosity reduces.

3.3. Effect of CNTs grafting with polymer on electrospun membrane properties

Fig. 8 represent membrane electrical conductivity. Electrospinning of mechanically mixed SAN in DMSO+CNT+IL solution was not stable; no continuous fibers were produced for evaluation of membrane mechanical and electrical properties. Due to this reason, this membrane is excluded from the further discussion.

It was found that all membranes without IL are non-conductive. Addition of IL increases electrical conductivity of membranes up to semiconductor level. By applying of ultrasound membrane electrical conductivity decrease was observed in pure SAN+IL and SAN+CNT-COOH+IL membranes. This can be caused by decrease of electrical conductivity of IL itself during ultrasonication. In SANm-g-CNT containing membranes the opposite effect was observed.

The electrical conductivity of mechanically mixed SAN+IL and SAN+SANm-g-CNT+IL is nearly the same. Surprisingly after ultrasonic treatment, membranes of higher electrical conductivity can be obtained in case of SAN+SANm-g-CNTs+IL. The grafting of SANm on CNTs causes this. After ultrasonic treatment grafted CNTs disperse easily compared to ungrafted thus transducing their extraordinary high electrical conductivity into polymer matrix overcoming the observed decrease in conductivity of IL itself.

Fig. 9 and fig. 10 represent mechanical properties of all obtained membranes. Comparing IL-free membranes electrospun from mechanically mixed solutions, it can be seen that SAN membrane has lowest tensile stress at maximum load and modulus. With addition of different CNTs tensile stress and modulus of SAN membranes increase from 0.18 and 5.21 MPa up to 0.43 and 9.72 MPa for SAN+CNTs, up to 1.31 and 41 MPa for SAN+CNT-COOHs, and up to 2.91 and 72 MPa for SAN+SANm-g-CNTs, respectively. Membranes with CNTs have higher tensile stress than membranes spun from pure polymer solution due to outstanding mechanical properties of CNTs [24]. CNT-COOHs and SANm-g-CNTs show higher impact on mechanical properties compared to unmodified CNT. According to the literature, all CNTs with functional groups provide higher strength than CNT. This is due to the better dispersion of functionalized CNTs [25] in a certain matrix.

The effect of ultrasonic treatment on mechanical properties of obtained membranes is also shown in fig. 9 and fig. 10. It is clearly seen that with application of ultrasound to solution the tensile stress at maximum load and modulus of membrane increase drastically. With ultrasonic mixing higher amount of energy is transfered to polymer solution with filler inside thus providing better dispersion of CNTs into polymer matrix. Due to that better load transfer to the filled network is achieved, resulting in more uniform stress distribution, which in turn enhance the mechanical properties of the composite polymer membrane [8, 26].

The behavior of SAN+SANm-g-CNT+IL system is different to other ones and the ultrasonic treatment caused opposite effect: tensile stress and modulus of electrospun membrane decrease. This phenomenon can be explained by covalent bonding of SANm to CNTs. In case of ungrafted nanotubes, IL can easily cover the CNTs. Application of ultrasound enhance dispersion of ungrafted CNTs and CNT-COOH and IL is connected to CNTs surface. Nevertheless, in case of polymer-grafted CNTs separate nanotubes are coated fully or partially with the polymer, IL cannot reach the CNTs surface (see fig.5 and fig.7). As it was discussed before IL does not mix with SAN and SANm. By this reason, the opposite effect appears during ultrasonic mixing in SAN+SANm-g-CNT+IL system and the decrease of mechanical properties is observed. For example, during fiber formation when the solvent is evaporated, in dry SAN+CNT+IL and SAN+CNT-COOH+IL membranes IL is distributed on the surface of CNT and connected by “cation-π” interaction discussed above. But in case of

SAN+SANm-g-CNT+IL the system with two polymers, which are very close but not identical, that do not mix with IL is formed. During ultrasonication, more homogeneous distribution of SAN, IL, and SANm-g-CNTs is achieved in solution. Which means, that in dry fiber IL is distributed better compared to the mechanically mixed system. But as IL cannot stay on the surface of SANm-g-CNT more stress location sites can appear in fiber after ultrasonication of the electrospinning solution. This can cause the decrease of SAN+SANm-g-CNT+IL membrane mechanical properties after ultrasonication of electrospinning solution. Unfortunately, no relevant literature about SAN(SANm)/IL fiber structure after mechanical stress was found to prove this theory. A deeper study of SAN(SANm)/IL membranes behavior and structure under mechanical stress is needed to confirm experimentally this theory.

The effect of added IL on mechanical properties of membranes was also studied. As can be seen from fig. 9 and fig.10 in both preparation methods, mechanical and ultrasonic mixing, the improvement of mechanical properties was observed with addition of IL. For example, SAN+SANm-g-CNT membrane modulus increased from 72 up to 420 MPa in case of mechanically mixed solution. In the same system but ultrasonically mixed increase of membrane modulus was from 110 up to 139 MPa. This is indirectly related to increase of electrical conductivity of electrospinning solutions. With increased electrical conductivity of solution, the higher stretching force is applied to the electrospinning jet at the same variables. At higher stretching force, thinner fibers and as a result stronger membranes are produced [27]. The same result was observed in our previous research [10].

Finally, we can conclude, that the best results of mechanical and electrical properties were found for polymer membrane with SANm-g-CNTs and IL. The increase of mechanical properties was in two orders of magnitude compared to SAN membranes and in average twice higher than membranes with unmodified CNTs and CNT-COOH. Both together IL and

SANm-g-CNTs enhance electrical conductivity of electrospinning solution. From another point of view, covalent bonding of SANm to CNTs provides better dispersion of CNTs into polymer matrix and uniform load transfer in final product is reached thus enhancing material strength properties.

The morphology of obtained fibers was studied by SEM (see fig. 11 and fig. 12). In case of pure SAN membranes there can be seen several beads along the fibers. These are solvent beads, which have stretched shape. Fig. 13 represents dependence of fiber average diameter on addition of different CNTs, IL and application of different mixing techniques. In IL-free membranes with application of ultrasound smoother fibers of lower average diameter can be produced due to increased electrical conductivity of solutions. In case of IL containing solutions, as evident from fig. 13 no significant effect of ultrasonic treatment was observed on fiber average diameter. Comparing membranes with and without IL it is clearly seen that addition of IL decreases fiber average diameter. This phenomenon can be also explained by increased solution electrical conductivity with dissociation of $[\mathrm{Bmim}]^{+}\mathrm{Cl}^{-}$ pair into ions.

Conclusions

Reactive melt blending method for CNT grafting with SAN polymer was successfully modified and simplified. 35% content of SAN polymer in SANm-g-CNT sample was achieved with process yield of 55%.

Four parallels of mechanically and ultrasonically mixed solutions with addition of different CNTs and IL were prepared and solution properties investigated. It was found that SANm-g-CNTs have the same impact on solution properties as CNT and CNT-COOHs in mechanically mixed solutions. However, with application of ultrasonic irradiation SANm-g-CNTs increase solution electrical conductivity more than other CNTs. In case of IL-containing solutions, no difference was found between effect of CNTs, CNT-COOHs and SANm-g-CNTs on solution electrical conductivity. IL increased in average for three orders solution electrical conductivity. With application of ultrasonic irradiation to IL containing solutions, the electrical conductivity of all solutions decreased.

Viscosity was measured for all electrospinning solutions. It was found that ultrasonication has the different effect on the viscosity of solutions with and without IL. Application of ultrasonic treatment to IL-free solutions decreased the viscosity in all solutions because of better dispersion of different CNTs and SAN into DMSO. However, with the addition of IL different effect of ultrasonic treatment was observed. The viscosity of solutions with IL increased after ultrasonication because of oxidative degradation of IL under ultrasonication.

The best result in mechanical test was observed in composite membranes with SANm-g-CNTs. 16 times higher tensile stress at maximum load and 14 times higher modulus was achieved with addition of SANm-g-CNTs into elctrospinning solution comparing with pure SAN membrane. This is also 7 times higher comparing to membranes reinforced with ungrafted CNTs and CNT-COOH. In combination of grafting method, ultrasonic treatment and IL application the mechanical properties of SAN membrane can be increased even more, in two orders of magnitude comparing to pure SAN membrane, which is very promising result.

It was also discovered that the electrical conductivity of fibers cannot be increased only by addition of different CNTs. IL is needed to produce membranes with electrical conductivity of semiconductor level. The highest electrical conductivity was achieved by addition of IL and SANm-g-CNTs; and ultrasonic treatment.

Acknowledgements

The Archimedes Foundation Implementing Agency of Structural Support is acknowledged for its support under grant “CNT Reinforced Electrospun Nano-fibers and Yarns”, no. 3.2.1101.12-0018.

List of abbreviations:

AE	*2-aminoethanol*
[Bmim]Cl	*1-butyl-3-methylimidazolium chloride*
CNT	*Carbon nanotubes*
DMSO	*Dimethyl sulfoxide*
FT-IR	*Fourier transform infrared spectroscopy*
^{1}H *NMR*	*Nuclear magnetic resonance*
IL	*Ionic liquid*
MWCNT	*Multi-walled carbon nanotubes*
MWCNT-COOH	*Multi-walled carbon nanotubes with carboxyl groups*
SAN	*Poly(styrene-co-acrylonitrile)*
SANm-g-MWCNT	*Multiwalled carbon nanotube grafted with modified poly(styrene-co-acrylonitrile)*
SANm	*Modified poly(styrene-co-acrylonitrile)*
$Zn(Ac)_2{\cdot}2H_2O$	*Zinc acetate dihydrate*
TEM	*Transmission electron microscopy*
TGA	*Thermogravimetric analyses*
THF	*Tetrahydrofuran*

References

1. Ramakrishna, S. (2005) *Introduction to electrospining and nanofibers,* Singapore.
2. Li, Z., Wang, C. (2013) *One-dimentional nanostructures. Electrospinning technique and unique nanofibers,* Netherlands.
3. Sill, T. J., von Recum, H. A. (2008) Electrospinning: applications in drug delivery and tissue engineering, *Biomaterials,* 29: 1989-2006. doi: 10.1016/j.biomaterials.2008.01.011.
4. Agarwal, S., Wendorff, J. H., Greiner, A. (2008) Use of electrospinning technique for biomedical applications, *Polymer,* 49: 5603-5621. doi: 10.1016/j.polymer.2008.09.014.
5. Plackett, D. (2011) *Biopolymers – New materials for sustainable films and coatings,* United Kingdom.
6. Choi, W. S., Ryu, S.H. (2010) Enhancement of Dispersion of Carbon Nanotube and Physical Properties of Poly(styrene-co-acrylonitrile)/ Multiwalled Carbon Nanotube Nanocomposite via Surface Initiated ATRP, *J APPL POLYM SCI* , 116: 2930–2936.
7. Liu, P. (2005) Modifications of carbon nanotubes with polymers, *EUR POLYM J*, 45: 2693–2703.
8. Shi, J.-H., Yang B.X., Goh, S.H. (2009) Covalent functionalization of multiwalled carbon nanotubes with poly(styrene-co-acrylonitrile) by reactive melt blending, *EUR POLYM J*, 45: 1002-1008.
9. Yonghui, L., Li, Y., Shaohua, Z., Jie, Y., Lijuan, S., Liqiang, Z. (2010) Dispersion of multiwalled carbon nanotubes by ionic liquid-type Gemini imidazolium surfactants in aqueous solution, *COLLOID SURFACE A*, 359: 66-70. doi:10.1016/j.colsurfa.2010.01.065.

10. Gudkova, V., Krumme, A., Märtson, T., Rikko, M., Tarasova, E., Savest, N., Viirsalu, M. (2015) 1-butyl-3-methylimidazolium chloride assisted electrospinning of SAN/MWCNTs conductive reinforced composite membranes, *J ELECTROSTAT*, 78: 11-16.
11. Gudkova, V., Krumme, A., Märtson, T., Rikko, M., Tarasova, E., Savest, N., Viirsalu, M. (2014) The impact of 1-butyl-3-methylimidazolium chloride on electrospinning process of SAN polymer solutions and electrospun fibre morphology, *J ELECTROSTAT*, 72: 433–436.
12. Hu, G.-H., Scaffaro, R. & La Mantia, F. (1998) Chemical Modification of Nitrile to Oxazoline Functionality on a Styrene-Acrylonitrile Copolymer in the Melt, Journal of Macromolecular Science, *J MACROMOL SCI A,* 35: 457-474.
13. Rogers, R., Heather, D., Huddleston, J., Reichert, W., Visser, A., Broker, G. (2001) Characterization and comparison of hydrophilic andhydrophobic room temperature ionic liquids incorporating theimidazolium cation, *GREEN CHEM*, , 3: 156–164.
14. Frump, J.A. (1971) Oxazolines. Their preparation, reactions, and applications, *CHEM REV*, 71: 5.
15. Ma, Y., Pang, Y. (2015) Mechanism Study on Char Formation of Zinc Acetylacetonate on ABS Resin, *CHINESE J POLYM SCI*, 33: 772-782.
16. Lee, J., Kim, M., Hong, C.K., Shim, S.E. (2007) Measurement of the dispersion stability of pristine and surface-modified multiwalled carbon nanotubes in various nonpolar and polar solvents, *MEAS SCI TECHNOL*, 18: 3707–3712.
17. Xie, X.-L., Mai, Y.-W., Zhou, X.-P. (2005) Dispersion and alignment of carbon nanotubes in polymer matrix: A review, *MAT SCI ENG R*, 49: 89–112.

18. Ewa, M.S., Malgorzata, C., Stolte, S., Stepnowski, P. (2011) Stability of Ionic Liquids in Application Conditions, *Curr Org Chem*, 15: 1974-1991. doi:10.2174/138527211795703630.

19. Bellayer, S., Gilman, J.W., Eidelman, N., Bourbigot, S., Flambard, X., Fox, D.M. and de Long, H.C., Trulove, P.C. (2005) Preparation of homogeneously dispersed multiwalled carbon nanotube/polystyrene nanocomposites via melt extrusion using trialkyl imidazolium compatibilizer, *Adv. Funct. Mater*, 15: 910-916.

20. Wang, J.Y., Chu, H.B., Li, Y. (2008) Why single-walled carbon nanotubes can be dispersed in imidazolium-based ionic liquids, *ACS Nano*, 2: 2540–2546.

21. Fan, Z., Advani, S.G. (2007) Rheology of multiwall carbon nanotube suspensions, *J. Rheol.* 51: 585-604.

22. G. Yanfang, W. Tengfang, Y. Dahong, P. Changjun, L. Honglai, H. Ying, *CHINESE J CHEM ENG,* 16, 2 (2008).

23. Y. Y. Huang, S. V. Ahir, and E. M. Terentjev, *PHYS REV*, 73 (2006).

24. Z. Spitalsky, D. Tasis,K. Papagelis, C. Galliotis, *PROG POLYM SCI*, 5 (2009).

25. O. Eren, N. Ucar, A. Onen, I. Karacan, N. Kizildag, N. Demirsoy, O. Vurur, I. Borazan, *INDIAN J FIBRE TEXT,* 41 (2016).

26. M. Bhattacharya, *MATERIALS*, 9, 4 (2016).

27. D. Papkov, Y. Zou, M. N. Andalib, A. Goponenko, S. Z. D. Cheng, Y. A. Dzenis, *ACSNano*, 7, 4 (2013).

List of figures:

Fig. 1. Scheme of CNT grafting reaction with SAN

Fig. 2. FT-IR spectra of SAN (solid line) and SANm (dotted line)

Fig. 3. 1H NMR spectrum of SANm-g-CNT in d6-DMSO

Fig. 4. TG curves for SAN, SANm, CNT-COOH and SANm-g-CNT

Fig. 5. TEM micrographs of SANm-g-CNTs

Fig. 6. Solutions electrical conductivity dependence on addition of different CNTs, IL, and solution preparation method

Fig. 7. Scheme of IL interaction with CNT and SANm-g-CNT

Fig. 8. Membrane electrical conductivity dependence on addition of different CNTs, IL and solution preparation method

Fig. 9. Membrane tensile stress dependence on addition of different CNTs, IL and solution preparation method

Fig. 10. Modulus of membrane dependence on addition of different CNTs, IL and solution preparation method

Fig. 11. SEM micrographs of SAN fibers with different CNTs electrospun from mechanically (A-D) and ultrasonically (E-H) mixed solutions

Fig. 12. SEM micrographs of SAN fibers with IL and different CNTs electrospun from mechanically (A-D) and ultrasonically (E-H) mixed solutions

Fig. 13. Fiber average diameter dependence on addition of different CNTs, IL and solution preparation method

Table.1. Composition and preparation of electrospinning solutions

Solution	Preparation of mechanically mixed solutions	Preparation of ultrasonically mixed solutions
SAN in DMSO	First a SAN in DMSO solution was mixed by mechanical stirring at 60ºC for 24 h. After that, IL and CNTs were added and stirred for another 24 h at 60ºC.	First SAN in DMSO solution was mixed by mechanical stirring at 60ºC for 24 h. After that, IL and CNTs were added and stirred for another 24 h at 60ºC. At last solutions were ultrasonically treated for 3 h.
SAN in DMSO+CNT		
SAN in DMSO+CNT-COOH		
SAN in DMSO+SANm-g-CNT		
SAN in DMSO+IL		
SAN in DMSO+CNT+IL		
SAN in DMSO+CNT-COOH+IL		
SAN in DMSO+SANm-g-CNT+IL		

Table. 2. Viscosity of solutions

	Mechanically mixed	Ultrasonically mixed
SAN in DMSO	2.26	2.12
SAN in DMSO+CNT	2.91	2.90
SAN in DMSO+CNT-COOH	2.31	1.90
SAN in DMSO+SANm-g-CNT	2.50	1.91
SAN in DMSO+IL	0.79	3.58
SAN in DMSO+CNT+IL	2.81	4.93
SAN in DMSO+CNT-COOH+IL	0.87	3.86
SAN in DMSO+SANm-g-CNT+IL	5.80	3.23

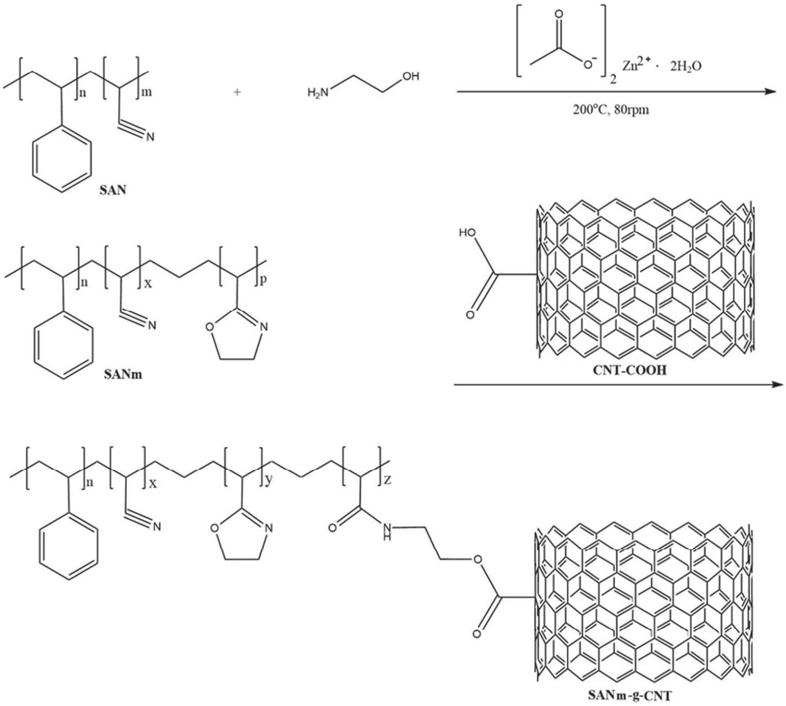

Fig. 1. Scheme of CNT grafting reaction with SAN

36x33mm (600 x 600 DPI)

Fig. 2. FT-IR spectra of SAN (solid line) and SANm (dotted line)

18x7mm (600 x 600 DPI)

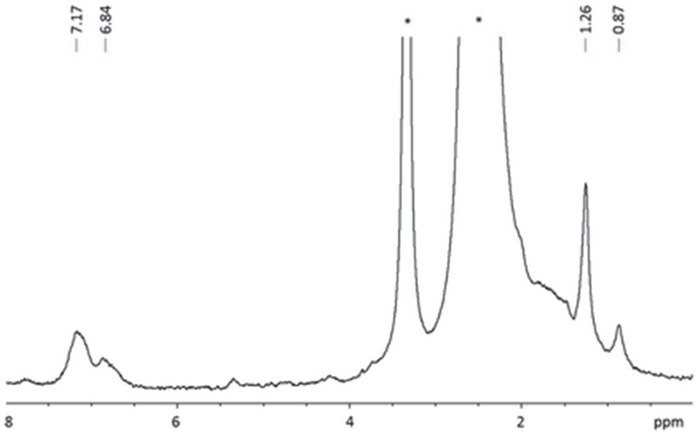

Fig. 3. 1H NMR spectrum of SANm-g-CNT in d6-DMSO

18x11mm (600 x 600 DPI)

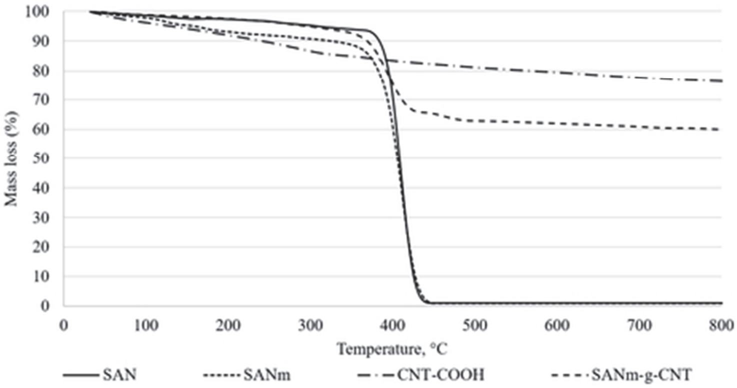

Fig. 4. TG curves for SAN, SANm, CNT-COOH and SANm-g-CNT

19x10mm (600 x 600 DPI)

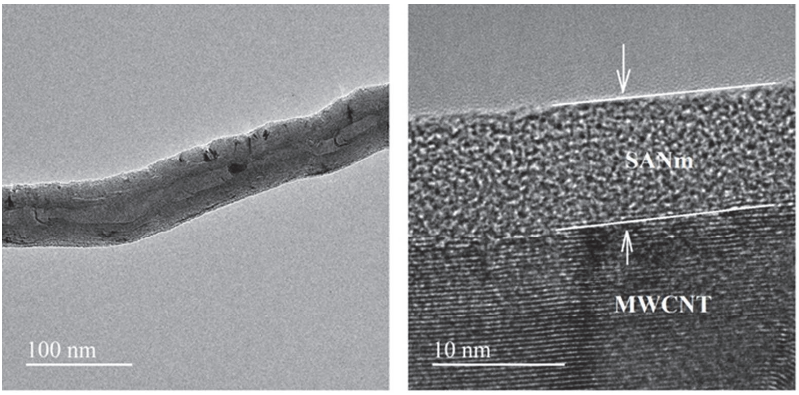

Fig. 5. TEM micrographs of SANm-g-CNTs

29x14mm (600 x 600 DPI)

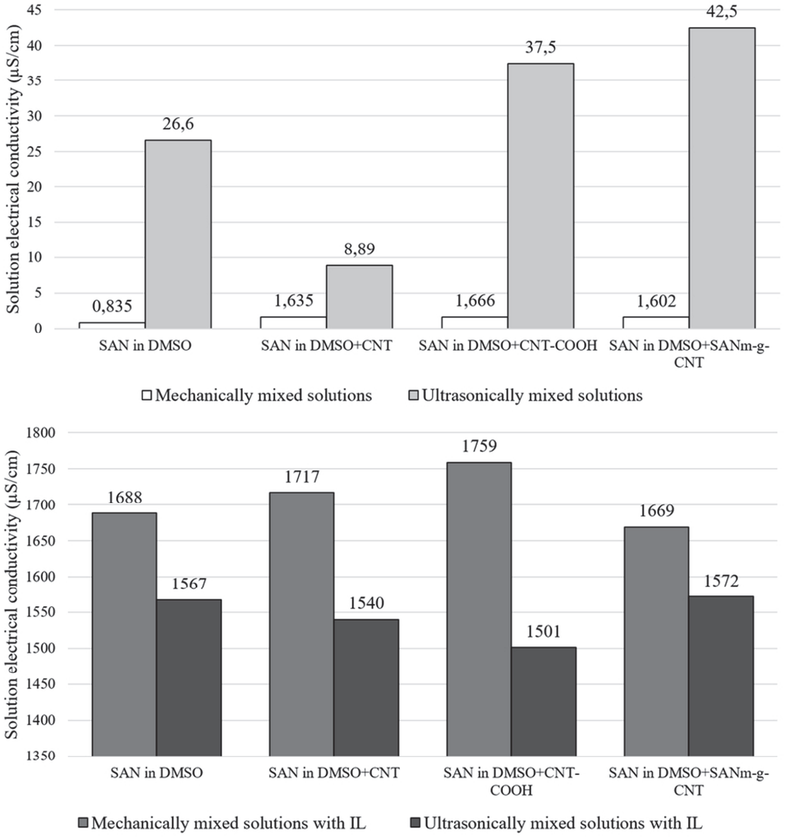

Fig. 6. Solutions electrical conductivity dependence on addition of different CNTs, IL, and solution preparation method

42x45mm (600 x 600 DPI)

Fig. 7. Scheme of IL interaction with CNT and SANm-g-CNT

11x2mm (600 x 600 DPI)

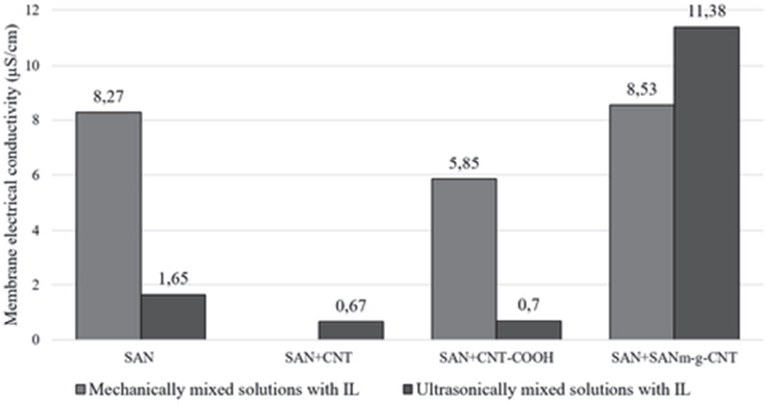

Fig. 8. Membrane electrical conductivity dependence on addition of different CNTs, IL and solution preparation method

20x10mm (600 x 600 DPI)

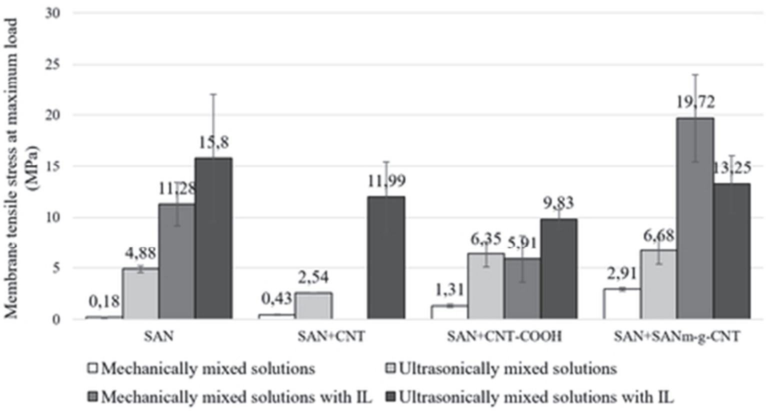

Fig. 9. Membrane tensile stress dependence on addition of different CNTs, IL and solution preparation method

20x10mm (600 x 600 DPI)

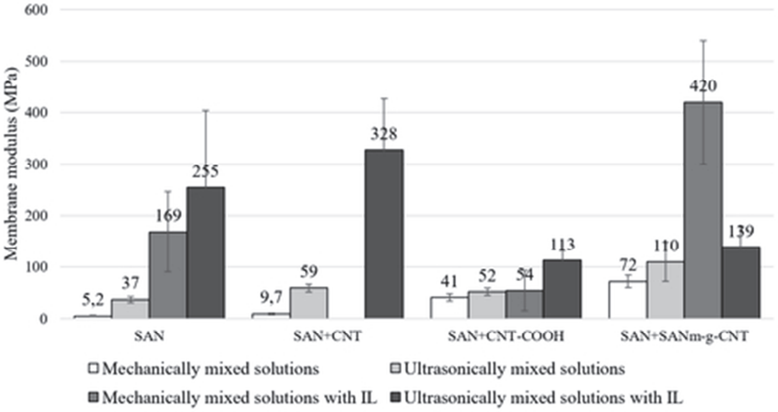

Fig. 10. Modulus of membrane dependence on addition of different CNTs, IL and solution preparation method

21x11mm (600 x 600 DPI)

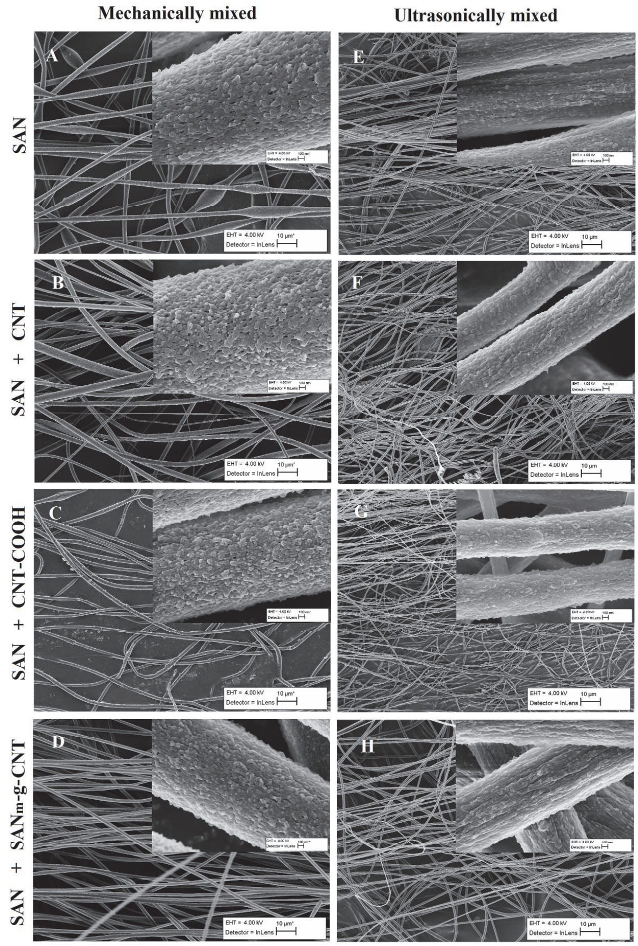

Fig. 11. SEM micrographs of SAN fibers with different CNTs electrospun from mechanically (A-D) and ultrasonically (E-H) mixed solutions

92x138mm (600 x 600 DPI)

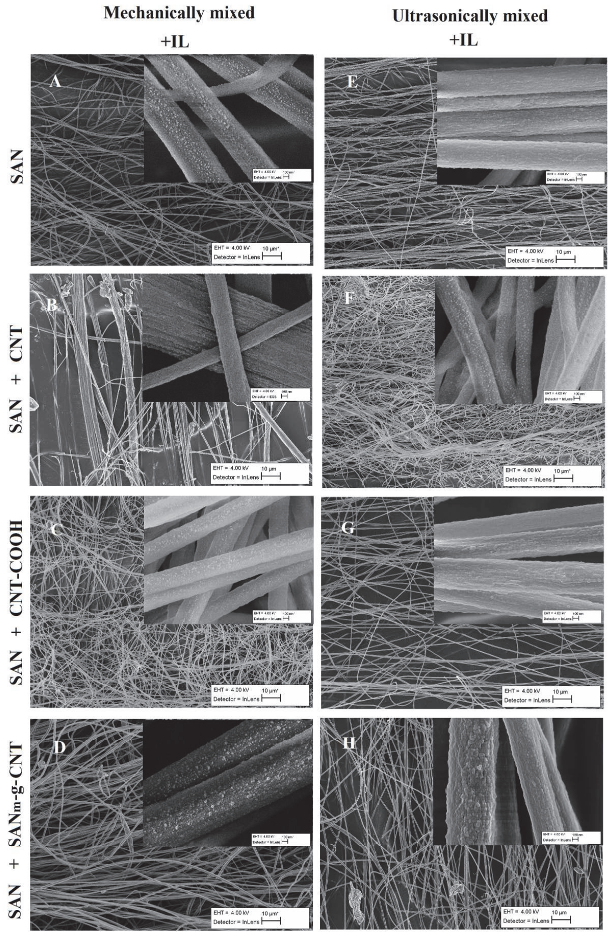

Fig. 12. SEM micrographs of SAN fibers with IL and different CNTs electrospun from mechanically (A-D) and ultrasonically (E-H) mixed solutions

97x149mm (600 x 600 DPI)

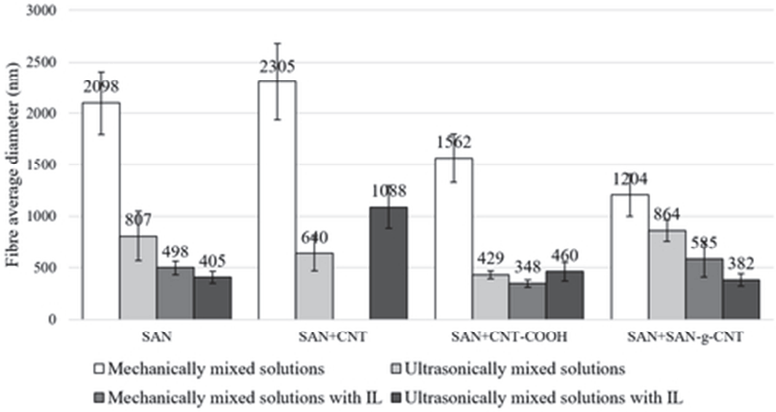

Fig. 13. Fiber average diameter dependence on addition of different CNTs, IL and solution preparation method

20x11mm (600 x 600 DPI)

APPENDIX B

Properties of 1,2-DCE and DMSO [109]

	1,2-DCE	**DMSO**
Name	1,2-Dichloroethane	Dimethylsulphoxide
Physical properties		
Molecular weight	99	78
Empirical formula	$C_2H_4Cl_2$	$C_2H_6O_1S_1$
Boiling point (°C)	83.5	189
Freezing point (°C)	-36	+18.5
Specific gravity (20/4)	1.253	1.101
Surface tension (20°C dyn/cm)	32.2	43.7
Absolute viscosity (25°C cP)	0.9	2.0
Fire hazards		
Flash point (closed cup °C)	13	95
Autoignition temperature (°C)	413	255
Electrical conductivity	$4x10^{-11}$	$2x10^{-9}$
Lower explosive limit (ppm)	62000	30000
Upper explosive limit (ppm)	169000	420000
Solvent properties		
Solubility parameter	9.8	13.0
Dielectric constant (20°C)	10.45	46.6
Polarity (water 100)	32.7	44.4
Evaporationt time (ether = 1)	2.7	1500
Solubility in water (25°C %w/w)	0.81	Total
Solubility of water in (25°C %w/w)	0.15	Total

APPENDIX C

Curriculum vitae

1. Personal data

Name	Viktoria Vassiljeva (maiden name Gudkova)
Date and place of birth	08.05.1985, Tallinn, Estonia
Citizenship	Estonian
E-mail address	viktoria.vassiljeva@ttu.ee

2. Education

Educational institution	Graduation year	Education(field of study/degree)
Tallinn University of Technology	2012	Chemical and Materials Technology/ Master's Degree
Tallinn University of Technology	2007	Applied Chemistry and Biotechnology/ Bachelor’s degree
Tallinn Läänemere Secondary School	2004	Secondary education

3. Language competence/skills (fluent, average, basic skills)

Language	Level
russian	native
estonian	fluent
english	fluent

4. Special courses

October 2017: Presentation skills training course, Graduate school of functional materials and technologies (FMTDK)

20.09.2017 – 22.09.2017: 17th Baltic Polymer Symposium co-organized by Tallinn University of Technology and COST action CA15107. Participation with oral presentation on topic “Electrospinning of conductive reinforced membrane”

19.04.2017 – 21.04.2017: Electrospinning COST Action MP1206 on the topic “Electrospinning: From Design and Processing to Advanced Nanomaterials and Applications”. Participated with poster presentation on topic “Electrospinning of SAN conductive reinforced membranes”

07.04.2017 – 08.04.2017: Graduate school of functional materials and technologies – conference. Participation with oral presentation on topic “1-butyl-3-methylimidazolium chloride assisted electrospinning of SAN/MWCNTS conductive reinforced composite membranes”

26.09.2016 – 27.09.2016: Electrospinning COST Action MP1206 on the topic “Electrospinning: From Design and Processing to Advanced Nanomaterials and Applications”. Participated with poster presentation on topic “Ionic liquid assisted coaxial electrospinning of core-sheath polymer fibers”

18.09.2013 – 21.09.2013: 13th International Conference Baltic Polymer Symposium 2013. Participated with poster presentation on topic “The effect of addition of ionic liquid on the electrospinning conditions of san solutions and the morphology of obtained nanofibers”

07.03.2013 – 08.03.2013: Graduate school of functional materials and technologies – conference. Participated with poster presentation on topic “Influence of addition of MWCNT on PA6 solubility in formic acid and solution viscosity properties”

5. Professional employment

Period	Organisation	Position
2017 - …	Tallinn University of Technology	Engineer
2015 - 2016	Tallinn University of Technology	Learning service provision
2012 - 2015	Tallinn University of Technology	Early stage researcher
2008 - 2012	Krimelte OÜ	R&D Chemist
2007 - 2008	North Estonia Medical Blood Centre	Blood group laboratory assistant

6. Research activity, including honours and thesis supervised

Projects:

10.01.2017 – …:

“Fully electrospun durable electrode and electrochemical double-layer capacitor for high frequency applications”, Tallinn University of Technology, Contract No. 4000119258/16/NL/CBi.

15.02.2017 – 27.10.2017:

“Nordic E-pavement research and development”, Tallinn University of Technology, Contract No. 17-00120/003

16.03.2012 − 30.06.2015:

AR12135 "Carbon Nanotube Reinforced Electrospun Nano-fibres and Yarns", Andres Krumme, Tallinn University of Technology, Faculty of Chemical and Materials Technology, Department of Polymer Materials, Chair of Polymer Technology.

Supervised thesises:

Kaia-Kristiina Kirikal, Master's Degree, 2017. “One-step carbon nanotube grafting with polymer by reactive melt blending for electrospinning of reinforced composite membranes”, Tallinn University of Technology, Department of Materials and Environmental Technology, Laboratory of Polymers and Textile Technology.

Kaia-Kristiina Kirikal, Bachelor’s degree, 2015. “1-Butyl-3-methylimidazolium chloride assisted coaxial electrospinning of styrene-acrylonitrile copolymer”, Tallinn University of Technology, Faculty of Chemical and Materials Technology, Department of Polymer Materials, Chair of Polymer Technology.

Merit Rikko, Master's Degree, 2015. “The impact of carbon nanotubes and ionic liquid on the properties of electrospinning solutions and obtained membranes”, Tallinn University of Technology, Faculty of Chemical and Materials Technology, Department of Polymer Materials, Chair of Polymer Technology.

Nadezda Vitkovski, Master's Degree, 2014. “The impact of cell openers and their concentrations on the properties of one component polyurethane foam”, Tallinn University of Technology, Faculty of Chemical and Materials Technology, Department of Polymer Materials, Chair of Polymer Technology.

Anni Blumkvist, Bachelor’s degree, 2013. “The utilization of oil shale ash as a filler in neutral silicone sealant”, Tallinn University of Technology, Faculty of

Chemical and Materials Technology, Department of Polymer Materials, Chair of Polymer Technology.

Maiu Tiismus, Bachelor’s degree, 2013. “The effect of addition of ionic liquid and alumina nanofiber on viscosity of poly(styrene-co-acrylonitrile) solution”, Tallinn University of Technology, Faculty of Chemical and Materials Technology, Department of Polymer Materials, Chair of Polymer Technology.

Merit Rikko, Bachelor’s degree, 2013. “The effect of addition of ionic liquid and alumina nanofiber on viscosity of poly(styrene-co-acrylonitrile) solution”, Tallinn University of Technology, Faculty of Chemical and Materials Technology, Department of Polymer Materials, Chair of Polymer Technology.

Elulookirjeldus

1. Isikuandmed

Ees- ja perekonnanimi	Viktoria Vassiljeva (end. Gudkova)
Sünniaeg ja -koht	08.05.1985, Tallinn, Eesti
Kodakondsus	Eesti
E-posti aadress	viktoria.vassiljeva@ttu.ee

2. Hariduskäik

Õppeasutus (nimetus lõpetamise ajal)	Lõpetamise aeg	Haridus (eriala/kraad)
Tallinna Tehnikaülikool	2012	Keemia ja materjalitehnoloogia/ magistrikraad
Tallinna Tehnikaülikool	2007	Rakenduskeemia ja biotehnoloogia/ bakalaureusekraad
Tallinna Läänemere Gümnaasium	2004	Keskharidus

3. Keelteoskus (alg-, kesk- või kõrgtase)

Keel	Tase
vene keel	emakeel
eesti keel	kõrgtase
inglise keel	kõrgtase

4. Täiendusõpe

Octoober, 2017: Esnemisoskuste koolitus, Funktsionaalsete Materjalide ja Tehnoloogiate Doktorikool (FMTDK)

20.09.2017 – 22.09.2017: 17th Baltic Polymer Symposium, korraldatud Tallinna Tehnikaülikooli ja COST koostööprogrammi CA15107 poolt. Osalemine suulise ettekannega teemal "Electrospinning of conductive reinforced membrane"

19.04.2017 – 21.04.2017: Elektroketruse COST koostööprogramm MP1206 teemal "Electrospinning: From Design and Processing to Advanced Nanomaterials and Applications". Osalemine stendiettekannega teemal "Electrospinning of SAN conductive reinforced membranes"

07.04.2017 – 08.04.2017: Funktsionaalsete Materjalide ja Tehnoloogiate Doktorikool – konverents. Osalemine suulise ettekannega teemal "1-butyl-3-methylimidazolium chloride assisted electrospinning of SAN/MWCNTS conductive reinforced composite membranes"

26.09.2016 – 27.09.2016: Elektroketruse COST koostööprogramm MP1206 teemal "Electrospinning: From Design and Processing to Advanced Nanomaterials and Applications". Osalemine stendiettekannega teemal "Ionic liquid assisted coaxial electrospinning of core-sheath polymer fibers"

18.09.2013 – 21.09.2013: 13th International Conference Baltic Polymer Symposium 2013. Osalemine stendiettekannega teemal "The effect of addition of ionic liquid on the electrospinning conditions of san solutions and the morphology of obtained nanofibers"

07.03.2013 – 08.03.2013: Funktsionaalsete Materjalide ja Tehnoloogiate Doktorikool – konverents. Osalemine stendiettekannega teemal "Influence of addition of MWCNT on PA6 solubility in formic acid and solution viscosity properties"

5. Teenistuskäik

Töötamise aeg	Tööandja nimetus	Ametikoht
2017 - …	Tallinna Tehnikaülikool	Insener
2015 - 2016	Tallinna Tehnikaülikool	Õppeteenuse osutamine
2012 - 2015	Tallinna Tehnikaülikool	Nooremteadur
2008 - 2012	Krimelte OÜ	Arenduskeemik
2007 - 2008	Põhja-Eesti Regionaalhaigla verekeskus	Veregrupi labori laborant

6. Teadustegevus, sh tunnustused ja juhendatud lõputööd

Projektid:

10.01.2017 – …:

“Fully electrospun durable electrode and electrochemical double-layer capacitor for high frequency applications”, Tallinna Tehnikaülikool, töövõtuleping nr. 4000119258/16/NL/CBi.

15.02.2017 – 27.10.2017:

“Nordic E-pavement teadus- ja arendusprojekt”, Tallinna Tehnikaülikool, töövõtuleping nr. 17-00120/003

16.03.2012 − 30.06.2015:

AR12135 "Elektroketruse teel valmistatud ja süsinik-nanotorudega armeeritud nanokiud ning lõngad (16.03.2012−30.06.2015)", Andres Krumme, Tallinna Tehnikaülikool, Tallinna Tehnikaülikool, Keemia ja materjalitehnoloogia teaduskond, Polümeermaterjalide instituut, Polümeeride tehnoloogia õppetool.

Supervised thesises:

Kaia-Kristiina Kirikal, Magistrikraad, 2017. “Süsiniknanotorude katmine polümeeriga üheastmelisel kompaundimismeetodil tugevdatud komposiitmembraanide elektroketruseks”, Tallinna Tehnikaülikool, Materjali- ja keskkonnatehnoloogia instituut, Polümeeride ja tekstiilitehnoloogia labor.

Kaia-Kristiina Kirikal, Bakalaureusekraad, 2015. “Ioonvedeliku kasutamine kahekihilise kiu valmistamisel koaksiaalse elektroketruse meetodil”, Tallinna Tehnikaülikool, Keemia ja materjalitehnoloogia teaduskond, Polümeermaterjalide instituut, Polümeeride tehnoloogia õppetool.

Merit Rikko, Magistrikraad, 2015. “Süsiniknanotorude ja ioonvedeliku mõju elektrokedratavate lahuste ja saadud membraanide omadustele”, Tallinna Tehnikaülikool, Keemia ja materjalitehnoloogia teaduskond, Polümeermaterjalide instituut, Polümeeride tehnoloogia õppetool.

Nadezda Vitkovski, Magistrikraad, 2014. “Pooriavajate ja nende kontsentratsioonide mõju ühekomponentse polüuretaanvahu omadustele”, Tallinna Tehnikaülikool, Keemia ja materjalitehnoloogia teaduskond, Polümeermaterjalide instituut, Polümeeride tehnoloogia õppetool.

Anni Blumkvist, Bakalaureusekraad, 2013. “Põlevkivituha kasutamine neutraalse silikoonhermeetiku täiteainena”, Tallinna Tehnikaülikool, Keemia ja materjalitehnoloogia teaduskond, Polümeermaterjalide instituut, Polümeeride tehnoloogia õppetool.

Maiu Tiismus, Bakalaureusekraad, 2013. “Ioonvedeliku ja alumiiniumoksiidi nanokiudude lisamise mõju polü(stüreen-ko-akrüülnitriili) lahuse”, Tallinna Tehnikaülikool, Keemia ja materjalitehnoloogia teaduskond, Polümeermaterjalide instituut, Polümeeride tehnoloogia õppetool.

Merit Rikko, Bakalaureusekraad, 2013. “Ioonvedeliku lisamise mõju elektrokedratavate SAN lahuste elektroketrustingimustele ja saadavate nanokiudude morfoloogiale”, Tallinna Tehnikaülikool, Keemia ja materjalitehnoloogia teaduskond, Polümeermaterjalide instituut, Polümeeride tehnoloogia õppetool.

LIST OF OTHER PUBLICATIONS

1. Savest, N., Plamus, T., Tarasova, E., Viirsalu, M., Krasnou, I., Gudkova, V., Küppar, K.-A., Krumme, A. 2016. “The effect of ionic liquids on the conductivity of electrospun polyacrylonitrile membranes”. *Journal of Electrostatics*, 83: 63−68. (10.1016/j.elstat.2016.07.006)

2. Tarasova, E., Byzova, A., Savest, N., Viirsalu, M., Gudkova, V., Märtson, T., Krumme, A. 2015. “Influence of preparation process on morphology and conductivity of carbon black based electrospun nanofibers.” *Fullerenes, Nanotubes and Carbon Nanostructures*, 23: 695−700. (http://dx.doi.org/10.1080/1536383X.2014.974090)

3. Tarasova, E., Tamberg, K.-G., Viirsalu, M., Savest, N., Gudkova, V., Krasnou, I., Krumme, A. 2015. “Formation of uniform PVDF fibers under ultrasound exposure in presence of anionic surfactant”. Journal of Electrostatics, 76: 39−47. (https://doi.org/10.1016/j.elstat.2015.05.004)

4. Sardar, J., Mäeorg, U., Krasnou, I., Baddam, V., Gudkova, V., Krumme, A., Savest, N., Tarasova, E., Viirsalu, M. 2016. “Synthesis of Polymerizable Ionic Liquid Monomer and Its Characterizations.” *IOP Conf. Series: Materials Science and Engineering,* 111: 012021. (doi:10.1088/1757-899X/111/1/012021)

DISSERTATIONS DEFENDED AT TALLINN UNIVERSITY OF TECHNOLOGY ON *NATURAL AND EXACT SCIENCES*

1. **Olav Kongas**. Nonlinear Dynamics in Modeling Cardiac Arrhytmias. 1998.
2. **Kalju Vanatalu**. Optimization of Processes of Microbial Biosynthesis of Isotopically Labeled Biomolecules and Their Complexes. 1999.
3. **Ahto Buldas**. An Algebraic Approach to the Structure of Graphs. 1999.
4. **Monika Drews**. A Metabolic Study of Insect Cells in Batch and Continuous Culture: Application of Chemostat and Turbidostat to the Production of Recombinant Proteins. 1999.
5. **Eola Valdre**. Endothelial-Specific Regulation of Vessel Formation: Role of Receptor Tyrosine Kinases. 2000.
6. **Kalju Lott**. Doping and Defect Thermodynamic Equilibrium in ZnS. 2000.
7. **Reet Koljak**. Novel Fatty Acid Dioxygenases from the Corals *Plexaura homomalla* and *Gersemia fruticosa*. 2001.
8. **Anne Paju**. Asymmetric oxidation of Prochiral and Racemic Ketones by Using Sharpless Catalyst. 2001.
9. **Marko Vendelin**. Cardiac Mechanoenergetics *in silico*. 2001.
10. **Pearu Peterson**. Multi-Soliton Interactions and the Inverse Problem of Wave Crest. 2001.
11. **Anne Menert**. Microcalorimetry of Anaerobic Digestion. 2001.
12. **Toomas Tiivel**. The Role of the Mitochondrial Outer Membrane in *in vivo* Regulation of Respiration in Normal Heart and Skeletal Muscle Cell. 2002.
13. **Olle Hints**. Ordovician Scolecodonts of Estonia and Neighbouring Areas: Taxonomy, Distribution, Palaeoecology, and Application. 2002.
14. **Jaak Nõlvak**. Chitinozoan Biostratigrapy in the Ordovician of Baltoscandia. 2002.
15. **Liivi Kluge**. On Algebraic Structure of Pre-Operad. 2002.
16. **Jaanus Lass**. Biosignal Interpretation: Study of Cardiac Arrhytmias and Electromagnetic Field Effects on Human Nervous System. 2002.
17. **Janek Peterson**. Synthesis, Structural Characterization and Modification of PAMAM Dendrimers. 2002.
18. **Merike Vaher**. Room Temperature Ionic Liquids as Background Electrolyte Additives in Capillary Electrophoresis. 2002.
19. **Valdek Mikli**. Electron Microscopy and Image Analysis Study of Powdered Hardmetal Materials and Optoelectronic Thin Films. 2003.
20. **Mart Viljus**. The Microstructure and Properties of Fine-Grained Cermets. 2003.
21. **Signe Kask**. Identification and Characterization of Dairy-Related *Lactobacillus*. 2003.
22. **Tiiu-Mai Laht**. Influence of Microstructure of the Curd on Enzymatic and Microbiological Processes in Swiss-Type Cheese. 2003.
23. **Anne Kuusksalu**. 2–5A Synthetase in the Marine Sponge *Geodia cydonium*. 2003.

24. **Sergei Bereznev**. Solar Cells Based on Polycristalline Copper-Indium Chalcogenides and Conductive Polymers. 2003.
25. **Kadri Kriis**. Asymmetric Synthesis of C_2-Symmetric Bimorpholines and Their Application as Chiral Ligands in the Transfer Hydrogenation of Aromatic Ketones. 2004.
26. **Jekaterina Reut**. Polypyrrole Coatings on Conducting and Insulating Substracts. 2004.
27. **Sven Nõmm**. Realization and Identification of Discrete-Time Nonlinear Systems. 2004.
28. **Olga Kijatkina**. Deposition of Copper Indium Disulphide Films by Chemical Spray Pyrolysis. 2004.
29. **Gert Tamberg**. On Sampling Operators Defined by Rogosinski, Hann and Blackman Windows. 2004.
30. **Monika Übner**. Interaction of Humic Substances with Metal Cations. 2004.
31. **Kaarel Adamberg**. Growth Characteristics of Non-Starter Lactic Acid Bacteria from Cheese. 2004.
32. **Imre Vallikivi**. Lipase-Catalysed Reactions of Prostaglandins. 2004.
33. **Merike Peld**. Substituted Apatites as Sorbents for Heavy Metals. 2005.
34. **Vitali Syritski**. Study of Synthesis and Redox Switching of Polypyrrole and Poly(3,4-ethylenedioxythiophene) by Using *in-situ* Techniques. 2004.
35. **Lee Põllumaa**. Evaluation of Ecotoxicological Effects Related to Oil Shale Industry. 2004.
36. **Riina Aav**. Synthesis of 9,11-Secosterols Intermediates. 2005.
37. **Andres Braunbrück**. Wave Interaction in Weakly Inhomogeneous Materials. 2005.
38. **Robert Kitt**. Generalised Scale-Invariance in Financial Time Series. 2005.
39. **Juss Pavelson**. Mesoscale Physical Processes and the Related Impact on the Summer Nutrient Fields and Phytoplankton Blooms in the Western Gulf of Finland. 2005.
40. **Olari Ilison**. Solitons and Solitary Waves in Media with Higher Order Dispersive and Nonlinear Effects. 2005.
41. **Maksim Säkki**. Intermittency and Long-Range Structurization of Heart Rate. 2005.
42. **Enli Kiipli**. Modelling Seawater Chemistry of the East Baltic Basin in the Late Ordovician–Early Silurian. 2005.
43. **Igor Golovtsov**. Modification of Conductive Properties and Processability of Polyparaphenylene, Polypyrrole and polyaniline. 2005.
44. **Katrin Laos**. Interaction Between Furcellaran and the Globular Proteins (Bovine Serum Albumin β-Lactoglobulin). 2005.
45. **Arvo Mere**. Structural and Electrical Properties of Spray Deposited Copper Indium Disulphide Films for Solar Cells. 2006.
46. **Sille Ehala**. Development and Application of Various On- and Off-Line Analytical Methods for the Analysis of Bioactive Compounds. 2006.
47. **Maria Kulp**. Capillary Electrophoretic Monitoring of Biochemical Reaction Kinetics. 2006.

48. **Anu Aaspõllu.** Proteinases from *Vipera lebetina* Snake Venom Affecting Hemostasis. 2006.
49. **Lyudmila Chekulayeva**. Photosensitized Inactivation of Tumor Cells by Porphyrins and Chlorins. 2006.
50. **Merle Uudsemaa**. Quantum-Chemical Modeling of Solvated First Row Transition Metal Ions. 2006.
51. **Tagli Pitsi**. Nutrition Situation of Pre-School Children in Estonia from 1995 to 2004. 2006.
52. **Angela Ivask**. Luminescent Recombinant Sensor Bacteria for the Analysis of Bioavailable Heavy Metals. 2006.
53. **Tiina Lõugas**. Study on Physico-Chemical Properties and Some Bioactive Compounds of Sea Buckthorn (*Hippophae rhamnoides* L.). 2006.
54. **Kaja Kasemets**. Effect of Changing Environmental Conditions on the Fermentative Growth of *Saccharomyces cerevisae* S288C: Auxo-accelerostat Study. 2006.
55. **Ildar Nisamedtinov**. Application of ^{13}C and Fluorescence Labeling in Metabolic Studies of *Saccharomyces* spp. 2006.
56. **Alar Leibak**. On Additive Generalisation of Voronoï's Theory of Perfect Forms over Algebraic Number Fields. 2006.
57. **Andri Jagomägi**. Photoluminescence of Chalcopyrite Tellurides. 2006.
58. **Tõnu Martma**. Application of Carbon Isotopes to the Study of the Ordovician and Silurian of the Baltic. 2006.
59. **Marit Kauk**. Chemical Composition of $CuInSe_2$ Monograin Powders for Solar Cell Application. 2006.
60. **Julia Kois**. Electrochemical Deposition of $CuInSe_2$ Thin Films for Photovoltaic Applications. 2006.
61. **Ilona Oja Açik**. Sol-Gel Deposition of Titanium Dioxide Films. 2007.
62. **Tiia Anmann**. Integrated and Organized Cellular Bioenergetic Systems in Heart and Brain. 2007.
63. **Katrin Trummal**. Purification, Characterization and Specificity Studies of Metalloproteinases from *Vipera lebetina* Snake Venom. 2007.
64. **Gennadi Lessin**. Biochemical Definition of Coastal Zone Using Numerical Modeling and Measurement Data. 2007.
65. **Enno Pais**. Inverse problems to determine non-homogeneous degenerate memory kernels in heat flow. 2007.
66. **Maria Borissova**. Capillary Electrophoresis on Alkylimidazolium Salts. 2007.
67. **Karin Valmsen**. Prostaglandin Synthesis in the Coral *Plexaura homomalla*: Control of Prostaglandin Stereochemistry at Carbon 15 by Cyclooxygenases. 2007.
68. **Kristjan Piirimäe**. Long-Term Changes of Nutrient Fluxes in the Drainage Basin of the Gulf of Finland – Application of the PolFlow Model. 2007.
69. **Tatjana Dedova**. Chemical Spray Pyrolysis Deposition of Zinc Sulfide Thin Films and Zinc Oxide Nanostructured Layers. 2007.

70. **Katrin Tomson**. Production of Labelled Recombinant Proteins in Fed-Batch Systems in *Escherichia coli*. 2007.
71. **Cecilia Sarmiento**. Suppressors of RNA Silencing in Plants. 2008.
72. **Vilja Mardla**. Inhibition of Platelet Aggregation with Combination of Antiplatelet Agents. 2008.
73. **Maie Bachmann**. Effect of Modulated Microwave Radiation on Human Resting Electroencephalographic Signal. 2008.
74. **Dan Hüvonen**. Terahertz Spectroscopy of Low-Dimensional Spin Systems. 2008.
75. **Ly Villo**. Stereoselective Chemoenzymatic Synthesis of Deoxy Sugar Esters Involving *Candida antarctica* Lipase B. 2008.
76. **Johan Anton**. Technology of Integrated Photoelasticity for Residual Stress Measurement in Glass Articles of Axisymmetric Shape. 2008.
77. **Olga Volobujeva**. SEM Study of Selenization of Different Thin Metallic Films. 2008.
78. **Artur Jõgi**. Synthesis of 4'-Substituted 2,3'-dideoxynucleoside Analogues. 2008.
79. **Mario Kadastik**. Doubly Charged Higgs Boson Decays and Implications on Neutrino Physics. 2008.
80. **Fernando Pérez-Caballero**. Carbon Aerogels from 5-Methylresorcinol-Formaldehyde Gels. 2008.
81. **Sirje Vaask**. The Comparability, Reproducibility and Validity of Estonian Food Consumption Surveys. 2008.
82. **Anna Menaker**. Electrosynthesized Conducting Polymers, Polypyrrole and Poly(3,4-ethylenedioxythiophene), for Molecular Imprinting. 2009.
83. **Lauri Ilison**. Solitons and Solitary Waves in Hierarchical Korteweg-de Vries Type Systems. 2009.
84. **Kaia Ernits**. Study of In_2S_3 and ZnS Thin Films Deposited by Ultrasonic Spray Pyrolysis and Chemical Deposition. 2009.
85. **Veljo Sinivee**. Portable Spectrometer for Ionizing Radiation "Gammamapper". 2009.
86. **Jüri Virkepu**. On Lagrange Formalism for Lie Theory and Operadic Harmonic Oscillator in Low Dimensions. 2009.
87. **Marko Piirsoo**. Deciphering Molecular Basis of Schwann Cell Development. 2009.
88. **Kati Helmja**. Determination of Phenolic Compounds and Their Antioxidative Capability in Plant Extracts. 2010.
89. **Merike Sõmera**. Sobemoviruses: Genomic Organization, Potential for Recombination and Necessity of P1 in Systemic Infection. 2010.
90. **Kristjan Laes**. Preparation and Impedance Spectroscopy of Hybrid Structures Based on $CuIn_3Se_5$ Photoabsorber. 2010.
91. **Kristin Lippur**. Asymmetric Synthesis of 2,2'-Bimorpholine and its 5,5'-Substituted Derivatives. 2010.
92. **Merike Luman**. Dialysis Dose and Nutrition Assessment by an Optical Method. 2010.

93. **Mihhail Berezovski**. Numerical Simulation of Wave Propagation in Heterogeneous and Microstructured Materials. 2010.
94. **Tamara Aid-Pavlidis**. Structure and Regulation of BDNF Gene. 2010.
95. **Olga Bragina**. The Role of Sonic Hedgehog Pathway in Neuro- and Tumorigenesis. 2010.
96. **Merle Randrüüt**. Wave Propagation in Microstructured Solids: Solitary and Periodic Waves. 2010.
97. **Marju Laars**. Asymmetric Organocatalytic Michael and Aldol Reactions Mediated by Cyclic Amines. 2010.
98. **Maarja Grossberg**. Optical Properties of Multinary Semiconductor Compounds for Photovoltaic Applications. 2010.
99. **Alla Maloverjan**. Vertebrate Homologues of Drosophila Fused Kinase and Their Role in Sonic Hedgehog Signalling Pathway. 2010.
100. **Priit Pruunsild**. Neuronal Activity-Dependent Transcription Factors and Regulation of Human *BDNF* Gene. 2010.
101. **Tatjana Knjazeva**. New Approaches in Capillary Electrophoresis for Separation and Study of Proteins. 2011.
102. **Atanas Katerski**. Chemical Composition of Sprayed Copper Indium Disulfide Films for Nanostructured Solar Cells. 2011.
103. **Kristi Timmo.** Formation of Properties of $CuInSe_2$ and $Cu_2ZnSn(S,Se)_4$ Monograin Powders Synthesized in Molten KI. 2011.
104. **Kert Tamm**. Wave Propagation and Interaction in Mindlin-Type Microstructured Solids: Numerical Simulation. 2011.
105. **Adrian Popp**. Ordovician Proetid Trilobites in Baltoscandia and Germany. 2011.
106. **Ove Pärn**. Sea Ice Deformation Events in the Gulf of Finland and This Impact on Shipping. 2011.
107. **Germo Väli**. Numerical Experiments on Matter Transport in the Baltic Sea. 2011.
108. **Andrus Seiman**. Point-of-Care Analyser Based on Capillary Electrophoresis. 2011.
109. **Olga Katargina**. Tick-Borne Pathogens Circulating in Estonia (Tick-Borne Encephalitis Virus, *Anaplasma phagocytophilum*, *Babesia* Species): Their Prevalence and Genetic Characterization. 2011.
110. **Ingrid Sumeri**. The Study of Probiotic Bacteria in Human Gastrointestinal Tract Simulator. 2011.
111. **Kairit Zovo**. Functional Characterization of Cellular Copper Proteome. 2011.
112. **Natalja Makarytsheva**. Analysis of Organic Species in Sediments and Soil by High Performance Separation Methods. 2011.
113. **Monika Mortimer**. Evaluation of the Biological Effects of Engineered Nanoparticles on Unicellular Pro- and Eukaryotic Organisms. 2011.
114. **Kersti Tepp**. Molecular System Bioenergetics of Cardiac Cells: Quantitative Analysis of Structure-Function Relationship. 2011.

115. **Anna-Liisa Peikolainen**. Organic Aerogels Based on 5-Methylresorcinol. 2011.
116. **Leeli Amon**. Palaeoecological Reconstruction of Late-Glacial Vegetation Dynamics in Eastern Baltic Area: A View Based on Plant Macrofossil Analysis. 2011.
117. **Tanel Peets**. Dispersion Analysis of Wave Motion in Microstructured Solids. 2011.
118. **Liina Kaupmees**. Selenization of Molybdenum as Contact Material in Solar Cells. 2011.
119. **Allan Olspert**. Properties of VPg and Coat Protein of Sobemoviruses. 2011.
120. **Kadri Koppel**. Food Category Appraisal Using Sensory Methods. 2011.
121. **Jelena Gorbatšova**. Development of Methods for CE Analysis of Plant Phenolics and Vitamins. 2011.
122. **Karin Viipsi**. Impact of EDTA and Humic Substances on the Removal of Cd and Zn from Aqueous Solutions by Apatite. 2012.
123. **David Schryer**. Metabolic Flux Analysis of Compartmentalized Systems Using Dynamic Isotopologue Modeling. 2012.
124. **Ardo Illaste**. Analysis of Molecular Movements in Cardiac Myocytes. 2012.
125. **Indrek Reile**. 3-Alkylcyclopentane-1,2-Diones in Asymmetric Oxidation and Alkylation Reactions. 2012.
126. **Tatjana Tamberg**. Some Classes of Finite 2-Groups and Their Endomorphism Semigroups. 2012.
127. **Taavi Liblik**. Variability of Thermohaline Structure in the Gulf of Finland in Summer. 2012.
128. **Priidik Lagemaa**. Operational Forecasting in Estonian Marine Waters. 2012.
129. **Andrei Errapart**. Photoelastic Tomography in Linear and Non-linear Approximation. 2012.
130. **Külliki Krabbi**. Biochemical Diagnosis of Classical Galactosemia and Mucopolysaccharidoses in Estonia. 2012.
131. **Kristel Kaseleht**. Identification of Aroma Compounds in Food using SPME-GC/MS and GC-Olfactometry. 2012.
132. **Kristel Kodar**. Immunoglobulin G Glycosylation Profiling in Patients with Gastric Cancer. 2012.
133. **Kai Rosin**. Solar Radiation and Wind as Agents of the Formation of the Radiation Regime in Water Bodies. 2012.
134. **Ann Tiiman**. Interactions of Alzheimer’s Amyloid-Beta Peptides with Zn(II) and Cu(II) Ions. 2012.
135. **Olga Gavrilova**. Application and Elaboration of Accounting Approaches for Sustainable Development. 2012.
136. **Olesja Bondarenko**. Development of Bacterial Biosensors and Human Stem Cell-Based *In Vitro* Assays for the Toxicological Profiling of Synthetic Nanoparticles. 2012.

137. **Katri Muska**. Study of Composition and Thermal Treatments of Quaternary Compounds for Monograin Layer Solar Cells. 2012.
138. **Ranno Nahku**. Validation of Critical Factors for the Quantitative Characterization of Bacterial Physiology in Accelerostat Cultures. 2012.
139. **Petri-Jaan Lahtvee**. Quantitative Omics-level Analysis of Growth Rate Dependent Energy Metabolism in *Lactococcus lactis*. 2012.
140. **Kerti Orumets**. Molecular Mechanisms Controlling Intracellular Glutathione Levels in Baker's Yeast *Saccharomyces cerevisiae* and its Random Mutagenized Glutathione Over-Accumulating Isolate. 2012.
141. **Loreida Timberg**. Spice-Cured Sprats Ripening, Sensory Parameters Development, and Quality Indicators. 2012.
142. **Anna Mihhalevski**. Rye Sourdough Fermentation and Bread Stability. 2012.
143. **Liisa Arike**. Quantitative Proteomics of *Escherichia coli*: From Relative to Absolute Scale. 2012.
144. **Kairi Otto**. Deposition of In_2S_3 Thin Films by Chemical Spray Pyrolysis. 2012.
145. **Mari Sepp**. Functions of the Basic Helix-Loop-Helix Transcription Factor TCF4 in Health and Disease. 2012.
146. **Anna Suhhova**. Detection of the Effect of Weak Stressors on Human Resting Electroencephalographic Signal. 2012.
147. **Aram Kazarjan**. Development and Production of Extruded Food and Feed Products Containing Probiotic Microorganisms. 2012.
148. **Rivo Uiboupin**. Application of Remote Sensing Methods for the Investigation of Spatio-Temporal Variability of Sea Surface Temperature and Chlorophyll Fields in the Gulf of Finland. 2013.
149. **Tiina Kriščiunaite**. A Study of Milk Coagulability. 2013.
150. **Tuuli Levandi**. Comparative Study of Cereal Varieties by Analytical Separation Methods and Chemometrics. 2013.
151. **Natalja Kabanova**. Development of a Microcalorimetric Method for the Study of Fermentation Processes. 2013.
152. **Himani Khanduri**. Magnetic Properties of Functional Oxides. 2013.
153. **Julia Smirnova**. Investigation of Properties and Reaction Mechanisms of Redox-Active Proteins by ESI MS. 2013.
154. **Mervi Sepp**. Estimation of Diffusion Restrictions in Cardiomyocytes Using Kinetic Measurements. 2013.
155. **Kersti Jääger**. Differentiation and Heterogeneity of Mesenchymal Stem Cells. 2013.
156. **Victor Alari**. Multi-Scale Wind Wave Modeling in the Baltic Sea. 2013.
157. **Taavi Päll**. Studies of CD44 Hyaluronan Binding Domain as Novel Angiogenesis Inhibitor. 2013.
158. **Allan Niidu**. Synthesis of Cyclopentane and Tetrahydrofuran Derivatives. 2013.
159. **Julia Geller**. Detection and Genetic Characterization of *Borrelia* Species Circulating in Tick Population in Estonia. 2013.

160. **Irina Stulova**. The Effects of Milk Composition and Treatment on the Growth of Lactic Acid Bacteria. 2013.
161. **Jana Holmar**. Optical Method for Uric Acid Removal Assessment During Dialysis. 2013.
162. **Kerti Ausmees**. Synthesis of Heterobicyclo[3.2.0]heptane Derivatives *via* Multicomponent Cascade Reaction. 2013.
163. **Minna Varikmaa**. Structural and Functional Studies of Mitochondrial Respiration Regulation in Muscle Cells. 2013.
164. **Indrek Koppel**. Transcriptional Mechanisms of BDNF Gene Regulation. 2014.
165. **Kristjan Pilt**. Optical Pulse Wave Signal Analysis for Determination of Early Arterial Ageing in Diabetic Patients. 2014.
166. **Andres Anier**. Estimation of the Complexity of the Electroencephalogram for Brain Monitoring in Intensive Care. 2014.
167. **Toivo Kallaste**. Pyroclastic Sanidine in the Lower Palaeozoic Bentonites – A Tool for Regional Geological Correlations. 2014.
168. **Erki Kärber**. Properties of ZnO-nanorod/In_2S_3/$CuInS_2$ Solar Cell and the Constituent Layers Deposited by Chemical Spray Method. 2014.
169. **Julia Lehner**. Formation of Cu_2ZnSnS_4 and $Cu_2ZnSnSe_4$ by Chalcogenisation of Electrochemically Deposited Precursor Layers. 2014.
170. **Peep Pitk**. Protein- and Lipid-rich Solid Slaughterhouse Waste Anaerobic Co-digestion: Resource Analysis and Process Optimization. 2014.
171. **Kaspar Valgepea**. Absolute Quantitative Multi-omics Characterization of Specific Growth Rate-dependent Metabolism of *Escherichia coli*. 2014.
172. **Artur Noole**. Asymmetric Organocatalytic Synthesis of 3,3'-Disubstituted Oxindoles. 2014.
173. **Robert Tsanev**. Identification and Structure-Functional Characterisation of the Gene Transcriptional Repressor Domain of Human Gli Proteins. 2014.
174. **Dmitri Kartofelev**. Nonlinear Sound Generation Mechanisms in Musical Acoustic. 2014.
175. **Sigrid Hade**. GIS Applications in the Studies of the Palaeozoic Graptolite Argillite and Landscape Change. 2014.
176. **Agne Velthut-Meikas**. Ovarian Follicle as the Environment of Oocyte Maturation: The Role of Granulosa Cells and Follicular Fluid at Pre-Ovulatory Development. 2014.
177. **Kristel Hälvin**. Determination of B-group Vitamins in Food Using an LC-MS Stable Isotope Dilution Assay. 2014.
178. **Mailis Päri**. Characterization of the Oligoadenylate Synthetase Subgroup from Phylum Porifera. 2014.
179. **Jekaterina Kazantseva**. Alternative Splicing of *TAF4*: A Dynamic Switch between Distinct Cell Functions. 2014.
180. **Jaanus Suurväli**. Regulator of G Protein Signalling 16 (RGS16): Functions in Immunity and Genomic Location in an Ancient MHC-Related Evolutionarily Conserved Synteny Group. 2014.

181. **Ene Viiard**. Diversity and Stability of Lactic Acid Bacteria During Rye Sourdough Propagation. 2014.
182. **Kristella Hansen**. Prostaglandin Synthesis in Marine Arthropods and Red Algae. 2014.
183. **Helike Lõhelaid**. Allene Oxide Synthase-lipoxygenase Pathway in Coral Stress Response. 2015.
184. **Normunds Stivrinš**. Postglacial Environmental Conditions, Vegetation Succession and Human Impact in Latvia. 2015.
185. **Mary-Liis Kütt**. Identification and Characterization of Bioactive Peptides with Antimicrobial and Immunoregulating Properties Derived from Bovine Colostrum and Milk. 2015.
186. **Kazbulat Šogenov**. Petrophysical Models of the CO_2 Plume at Prospective Storage Sites in the Baltic Basin. 2015.
187. **Taavi Raadik**. Application of Modulation Spectroscopy Methods in Photovoltaic Materials Research. 2015.
188. **Reio Põder**. Study of Oxygen Vacancy Dynamics in Sc-doped Ceria with NMR Techniques. 2015.
189. **Sven Siir**. Internal Geochemical Stratification of Bentonites (Altered Volcanic Ash Beds) and its Interpretation. 2015.
190. **Kaur Jaanson**. Novel Transgenic Models Based on Bacterial Artificial Chromosomes for Studying BDNF Gene Regulation. 2015.
191. **Niina Karro**. Analysis of ADP Compartmentation in Cardiomyocytes and Its Role in Protection Against Mitochondrial Permeability Transition Pore Opening. 2015.
192. **Piret Laht**. B-plexins Regulate the Maturation of Neurons Through Microtubule Dynamics. 2015.
193. **Sergei Žari**. Organocatalytic Asymmetric Addition to Unsaturated 1,4-Dicarbonyl Compounds. 2015.
194. **Natalja Buhhalko**. Processes Influencing the Spatio-temporal Dynamics of Nutrients and Phytoplankton in Summer in the Gulf of Finland, Baltic Sea. 2015.
195. **Natalia Maticiuc**. Mechanism of Changes in the Properties of Chemically Deposited CdS Thin Films Induced by Thermal Annealing. 2015.
196. **Mario Öeren**. Computational Study of Cyclohexylhemicucurbiturils. 2015.
197. **Mari Kalda**. Mechanoenergetics of a Single Cardiomyocyte. 2015.
198. **Ieva Grudzinska**. Diatom Stratigraphy and Relative Sea Level Changes of the Eastern Baltic Sea over the Holocene. 2015.
199. **Anna Kazantseva**. Alternative Splicing in Health and Disease. 2015.
200. **Jana Kazarjan**. Investigation of Endogenous Antioxidants and Their Synthetic Analogues by Capillary Electrophoresis. 2016.
201. **Maria Safonova**. SnS Thin Films Deposition by Chemical Solution Method and Characterization. 2016.
202. **Jekaterina Mazina**. Detection of Psycho- and Bioactive Drugs in Different Sample Matrices by Fluorescence Spectroscopy and Capillary Electrophoresis. 2016.

203. **Karin Rosenstein**. Genes Regulated by Estrogen and Progesterone in Human Endometrium. 2016.
204. **Aleksei Tretjakov**. A Macromolecular Imprinting Approach to Design Synthetic Receptors for Label-Free Biosensing Applications. 2016.
205. **Mati Danilson**. Temperature Dependent Electrical Properties of Kesterite Monograin Layer Solar Cells. 2016.
206. **Kaspar Kevvai**. Applications of ^{15}N-labeled Yeast Hydrolysates in Metabolic Studies of *Lactococcus lactis* and *Saccharomyces Cerevisiae*. 2016.
207. **Kadri Aller**. Development and Applications of Chemically Defined Media for Lactic Acid Bacteria. 2016.
208. **Gert Preegel**. Cyclopentane-1,2-dione and Cyclopent-2-en-1-one in Asymmetric Organocatalytic Reactions. 2016.
209. **Jekaterina Služenikina**. Applications of Marine Scatterometer Winds and Quality Aspects of their Assimilation into Numerical Weather Prediction Model HIRLAM. 2016.
210. **Erkki Kask**. Study of Kesterite Solar Cell Absorbers by Capacitance Spectroscopy Methods. 2016.
211. **Jürgen Arund**. Major Chromophores and Fluorophores in the Spent Dialysate as Cornerstones for Optical Monitoring of Kidney Replacement Therapy. 2016.
212. **Andrei Šamarin**. Hybrid PET/MR Imaging of Bone Metabolism and Morphology. 2016.
213. **Kairi Kasemets**. Inverse Problems for Parabolic Integro-Differential Equations with Instant and Integral Conditions. 2016.
214. **Edith Soosaar**. An Evolution of Freshwater Bulge in Laboratory Scale Experiments and Natural Conditions. 2016.
215. **Peeter Laas**. Spatiotemporal Niche-Partitioning of Bacterioplankton Community across Environmental Gradients in the Baltic Sea. 2016.
216. **Margus Voolma**. Geochemistry of Organic-Rich Metalliferous Oil Shale/Black Shale of Jordan and Estonia. 2016.
217. **Karin Ojamäe**. The Ecology and Photobiology of Mixotrophic Alveolates in the Baltic Sea. 2016.
218. **Anne Pink**. The Role of CD44 in the Control of Endothelial Cell Proliferation and Angiogenesis. 2016.
219. **Kristiina Kreek**. Metal-Doped Aerogels Based on Resorcinol Derivatives. 2016.
220. **Kaia Kukk**. Expression of Human Prostaglandin H Synthases in the Yeast Pichia pastoris. 2016.
221. **Martin Laasmaa**. Revealing Aspects of Cardiac Function from Fluorescence and Electrophysiological Recordings. 2016.
222. **Eeva-Gerda Kobrin**. Development of Point of Care Applications for Capillary Electrophoresis. 2016.
223. **Villu Kikas**. Physical Processes Controlling the Surface Layer Dynamics in the Stratified Gulf of Finland: An Application of Ferrybox Technology. 2016.

224. **Maris Skudra**. Features of Thermohaline Structure and Circulation in the Gulf of Riga. 2017.
225. **Sirje Sildever**. Influence of Physical-Chemical Factors on Community and Populations of the Baltic Sea Spring Bloom Microalgae. 2017.
226. **Nicolae Spalatu**. Development of CdTe Absorber Layer for Thin-Film Solar Cells. 2017.
227. **Kristi Luberg**. Human Tropomyosin-Related Kinase A and B: from Transcript Diversity to Novel Inhibitors. 2017.
228. **Andrus Kaldma**. Metabolic Remodeling of Human Colorectal Cancer: Alterations in Energy Fluxes. 2017.
229. **Irina Osadchuk**. Structures and Catalytic Properties of Titanium and Iridium Based Complexes. 2017.
230. **Roman Boroznjak**. A Computational Approach for Rational Monomer Selection in Molecularly Imprinted Plolymer Synthesis. 2017.
231. **Sten Erm**. Use of Mother-Daughter Multi-Bioreactor Systems for Studies of Steady State Microbial Growth Space. 2017.
232. **Merike Kriisa**. Study of ZnO:In, Zn(O,S) and Sb_2S_3 Thin Films Deposited by Aerosol Methods. 2017.
233. **Marianna Surženko**. Selection of Functional Starter Bacteria for Type I Sourdough Process. 2017.
234. **Nkwusi God'swill Chimezie**. Formation and Growth of Cu_2ZnSnS_4 Monograin Powder in Molten CdI_2. 2017.
235. **Ruth Tomson**. Urea- and Creatinine-Based Parameters in the Optical Monitoring of Dialysis: The Case of Lean Body Mass and Urea Rebound Assessment. 2017.
236. **Natalja Jepihhina**. Heterogeneity of Diffusion Restrictions in Cardiomyocytes. 2017.
237. **Sophie Maria Teresa Marinucci de Reguardati**. High-Accuracy Reference Standards for Quantitative Two-Photon Absorption Spectroscopy. 2017.
238. **Martin Lints**. Optimised Signal Processing for Nonlinear Ultrasonic Nondestructive testing of Complex Materials and Biological Tissues. 2017.
239. **Maris Pilvet**. Study of $Cu_2(Zn,Cd)SnS_4$ Absorber Materials for Monograin Layer Solar Cells. 2017.
240. **Sirli Rosenvald**. Application of Gas Chromatography-Olfactometry (GC-O) and Correlation with Sensory Analysis. 2017.
241. **Jelena Maricheva**. Electrodeposition of Cadmium Chalcogenide Films for Hybrid Solar Cells. 2017.